CASE FILE COPY

NATIONAL ADVISORY COMMITTEE FOR AERONAUTICS

TECHNICAL NOTE 2221

EQUATIONS AND CHARTS FOR THE RAPID ESTIMATION OF
HINGE-MOMENT AND EFFECTIVENESS PARAMETERS FOR
TRAILING-EDGE CONTROLS HAVING LEADING AND
TRAILING EDGES SWEPT AHEAD OF

THE MACH LINES

By Kennith L. Goin

Langley Aeronautical Laboratory Langley Air Force Base, Va.



Washington November 1950

NATIONAL ADVISORY COMMITTEE FOR AERONAUTICS

TECHNICAL NOTE 2221

EQUATIONS AND CHARTS FOR THE RAPID ESTIMATION OF
HINGE-MOMENT AND EFFECTIVENESS PARAMETERS FOR
TRAILING-EDGE CONTROLS HAVING LEADING AND
TRAILING EDGES SWEPT AHEAD OF

THE MACH LINES

By Kennith L. Goin

SUMMARY

Existing conical-flow solutions have been used to calculate the hinge-moment and effectiveness parameters of trailing-edge controls having leading and trailing edges swept ahead of the Mach lines and having streamwise root and tip chords. Equations and detailed charts are presented for the rapid estimation of these parameters. Also included is an approximate method by which these parameters may be corrected for airfoil-section thickness.

Deflected controls are assumed to be located either at the wing tip or far enough inboard to prevent the outermost Mach lines from the controls from crossing the wing tip. For either of these locations, the innermost Mach lines are assumed not to cross the wing root chord. The method for determining control hinge moment resulting from wing angle-of-attack loading is valid for wing plan forms having the leading edges swept ahead of the Mach lines and having streamwise tips. The only additional restrictions are that the controls must not be influenced by the tip conical flow from the opposite wing panel or by the interaction of the wing-root Mach cone with the wing tip.

INTRODUCTION

Linearized theory, though neglecting viscosity and second-order effects existing in practice, is the most practical method now available for estimating the characteristics of control surfaces at supersonic speeds. A general application of this theory to control surfaces having edges swept either ahead of or behind the Mach lines is presented in reference 1. (Edges swept ahead of or behind the Mach lines are

2 NACA TN 2221

subsequently referred to as supersonic or subsonic edges.) Conical-flow solutions for various deflected control configurations are presented in reference 2. Such solutions were used in reference 3 to evaluate the characteristics of a restricted family of trailing-edge control surfaces.

In the present paper a general analysis based on existing conical-flow solutions has been made which will apply to a broad range of trailing-edge control configurations having supersonic edges and will provide for a comprehensive coverage of control location, aspect ratio, taper ratio, and sweep. Equations and detailed charts are presented from which lift, pitching-moment, rolling-moment, and hinge-moment coefficients due to control deflection, and hinge-moment coefficients due to control deflection, and hinge-moment coefficient due to wing angle of attack, as predicted by linearized theory, may be determined in an estimated 5 percent of the time required without the use of such equations and charts. Also included is an approximate method by which these hinge-moment and effectiveness parameters may be corrected for airfoil-section thickness.

The equations and charts presented are applicable to control-surface plan forms that vary throughout the range in which the leading and trailing edges are supersonic and the root and tip chords are in a streamwise direction. Deflected controls are assumed to be located either at the wing tip or far enough inboard to prevent the outermost Mach lines from the controls from crossing the wing tip. For either of these locations, the innermost Mach lines are assumed not to cross the wing root chord. The method for calculating the hinge-moment coefficient due to wing angle of attack is valid for wing plan forms having straight supersonic edges and streamwise tips. This method is restricted only in that the controls must not lie in a region influenced by the tip conical flow from the opposite wing panel or by the interaction of the wing-root Mach cone with the wing tip.

SYMBOLS

М	free-stream Mach number
$\beta = \sqrt{M^2 - 1}$	
c ₁ , c ₂	functions of Mach number used in calculating two-dimensional-flow characteristics
Λ	angle of sweep of wing leading edge, positive when swept back
$V_{ m HL}$	angle of sweep of control hinge line, positive when swept back

$\Lambda_{ ext{TE}}$.	angle of sweep of wing trailing edge, positive when swept back
${\tt b_f}$	span of control surface
c _{fr}	root chord of control surface
$^{\mathrm{c}}\mathtt{f_{t}}$	tip chord of control surface
$\lambda_{\mathbf{f}}$	control-surface taper ratio (c_{f_t}/c_{f_r})
$\mathtt{S}_{\mathtt{f}}$	area of control surface
Af	aspect ratio of control surface (b_f^2/S_f)
$A_{f}^{\dagger} = \beta A_{f}$	
Ma	area moment of control surface about hinge axis
$s_\mathtt{L}$	area of a loaded region
s_{L_o}	area of part of deflected control surface lying in two- dimensional-flow region less area lying in region of overlap of conical-flow fields
$\mathbf{m}_{\mathbf{O}}$	moment of S_{L_0} about hinge axis
ı _o	moment of S_{L_0} about control root chord
$\overline{\mathbf{x}}$	distance of center of loading from control hinge axis measured normal to hinge axis
ÿ	spanwise distance of center of loading from control root chord
θ	slope of airfoil-section contour
t/2c	one-half airfoil-thickness ratio measured in plane normal to control hinge axis
(t/c) _{max}	maximum airfoil-thickness ratio measured in plane normal to control hinge axis
x/c	chordwise position measured in plane normal to control hinge axis

 x_h/c chordwise location of control hinge axis measured in plane normal to control hinge axis (t/2c), (x/c)dimensions measured in plane normal to wing leading edge $\mathbf{x}_{\mathbf{f}}$ distance of leading edge of control root chord behind wing axis of pitch distance of root chord of control from root chord of y_f wing ъ wing span c_r wing root chord wing tip chord c_{t.} \overline{c} mean aerodynamic chord of wing area of semispan wing $g = \frac{\tan \Lambda}{\beta}$ $a = \frac{\tan \Lambda_{HL}}{\beta}$ $d = \frac{\tan \Lambda_{TE}}{8}$ wing angle of attack, degrees α δ angle of control-surface deflection measured in streamwise direction, degrees free-stream dynamic pressure 'q Lift induced by deflected control qS_f Moment about control root chord induced by deflected control Cm = Moment about hinge axis induced by deflected control

$$C_h = \frac{\text{Hinge moment}}{2qM_a}$$

$$\mathtt{C_L} \; = \; \frac{\mathtt{Lift \; induced \; by \; deflected \; control}}{\mathtt{qS}}$$

$$C_{l} = \frac{\text{Rolling moment about wing root chord}}{2qbS}$$

$$C_{m} = \frac{Pitching moment about wing axis of pitch}{qS\overline{c}}$$

$$F_1$$
 thickness correction factor for $C_{L_{\delta}}$ and $C_{l_{\delta}}$

F₂ thickness correction factor for
$$C_{h_{\delta}}$$
 and $C_{m_{\delta}}$

$$F_3$$
 thickness correction factor for $C_{h_{\alpha}}$

$$C_{n}$$
 pressure coefficient $(\Delta p/q)$

two-dimensional pressure coefficient
$$\left(\frac{2\delta}{57.3\beta\sqrt{1-a^2}}\right)$$
 or $\left(\frac{2\alpha}{57.3\beta\sqrt{1-g^2}}\right)$

P' local pressure ratio
$$(C_p/C_{p_o})$$

P average value of pressure ratio P' over conical-flow
$$\frac{\left(\int_{S_L} P^* dS_L\right)}{S_L}$$

$$\tau^{\dagger} = \tau + \Lambda_{min}$$

$$t = \beta \tan \tau$$

 $t^{\dagger} = \beta \tan \tau^{\dagger}$

 $r = \frac{1}{t}$

n, r^t nondimensional coordinates used in integration of wing

root and tip conical pressures

η angle of sweep of line intersecting conical-flow regions

of wing at angle of attack

Subscripts:

δ, α denote partial derivative of force and moment coeffi-

cients with respect to δ or α

cp denotes center-of-pressure ray location

Superscript:

indicates that parameters P, PS_L, PS_L \overline{x} , PS_L \overline{y} , t_{cp}, and r_{cp} refer to loss of loading from two-dimensional

value rather than to actual loading

ANALYSIS

Characteristics Due to Deflection of Control Surfaces

Scope. - Existing solutions of the linearized equations of fluid motion have been used as a basis for calculating the characteristics due to deflection of trailing-edge control surfaces on wings in steady flight at supersonic speeds. These solutions, as presented in reference 2, are applicable to configurations for which the leading and trailing edges of the control are supersonic and the root and tip chords are streamwise. Two control-surface locations are considered. The control is assumed to be located either at the wing tip or far enough inboard to prevent the outermost Mach line from the control from crossing the wing tip. For either of these locations, the innermost Mach lines are assumed not to cross the wing root chord. For these locations, deflected control-surface characteristics are functions only of Mach number and control-surface plan (The parameter $C_{h_{\delta}}$ depends on control-surface location only when the control is located inboard from the wing tip and lies in the region influenced by the interaction of the control-tip Mach cone with the wing tip.) If the limitations previously mentioned are considered, the analysis

is valid for all controls except those located at the wing tip and having

the inboard conical-flow regions intersecting the tip. In such cases, the conical pressures on the control, as given in reference 2, are not applicable in the region influenced by the interaction of the Mach cone with the wing tip. Necessary corrections for this region can be determined by the method described in reference 4. Such corrections are not considered in the present paper because of the prohibitive amount of computation involved. Results not including these corrections are presented, however, because they should be very useful as an indication of trends and should in many cases closely approximate the corrected result.

Method. - In order to determine control-surface characteristics, the two-dimensional region and the triangular segments of the conical-flow regions (fig. 1) are considered independently. The characteristics are obtained by summing the products of pressure ratio and nondimensionalarea and moment-arm parameters for all parts (table I). The nature of conical flow is such that the pressure is constant along any ray from the origin of the flow field. Any infinitesimal triangle having the origin of the flow field as an apex, therefore, has its center of pressure located at two-thirds of the distance from the apex to the base. It follows that the summation of the loading of such infinitesimal triangles results in a finite triangle having its center of pressure lying on a line parallel to the base and located at two-thirds of the distance from the apex to the base. The center-of-pressure location and, consequently, the desired moment arms, can therefore be determined from the location of the ray on which the center of pressure lies. General equations for the average pressure ratio and center-of-pressure ray location for each conical segment (tables II(a) and II(b)) were obtained by integrating the pressure equations of reference 2. (See appendix A.) Table II(c) presents equations for the nondimensional-area and moment-arm parameters (in terms of center-of-pressure ray location) for each conical segment. Equations pertaining to the two-dimensional region were obtained by treating this region as a simple geometric area and are also included in table II(c). Results obtained by evaluating the general equations of table II when they become indeterminate at taper ratios of 1.0 are presented in table III.

For regions in which the two conical-flow fields overlap, the method of superposition must be used wherein the losses in pressure ratio from the two-dimensional value ($P^* = 1.0$) in the two conical-flow regions are additive; that is,

$$P' = 1.0 - (1.0 - P_{mc_1}') - (1.0 - P_{mc_2}')$$

= -1.0 + $P_{mc_1}' + P_{mc_2}'$

NACA TN 2221

(Subscripts mc1 and mc2 refer to inboard and outboard conical-flow regions.) The net effects of the pressure distribution in this region are obtained by adding the effects of the two conical-flow regions as though the flow regions did not overlap and subtracting the effects of a two-dimensional pressure distribution. This subtraction is accomplished by use of the equations for the two-dimensional region (tables II(c) and In calculating control hinge moments it was convenient to calculate the effects of regions I and II or III (fig. 1) and then subtract the effects of the parts of these regions lying off the control. For controls located at the wing tip and having the inboard Mach cone intersecting the tip, a similar procedure was also used to reduce to zero the lift, pitching moment, and rolling moment contributed by the triangular part of the inboard conical-flow region lying beyond the tip. As previously mentioned for this case, a rigid application of linearized theory would require a correction, as described in reference 4, to the loading assumed in the region influenced by the interaction of the root Mach cone with the free edge. It should be pointed out that the areas influenced by such interactions become appreciable for extreme conditions and approximate results for such configurations should be used with caution.

Hinge Moment Due to Wing Angle-of-Attack Change

Scope. - Conical-flow solutions for swept wings at supersonic speeds, as presented in reference 5, are used as a basis for the analysis. These solutions are applicable to wing plan forms having straight supersonic edges and streamwise tips.

As in the analysis for deflected control surfaces, only control surfaces having supersonic edges and streamwise root and tip chords are considered. The only restrictions regarding control location are that the control must not lie in a region influenced by the tip conical flow from the opposite wing panel or by the interaction of the wing-root Mach cone with the wing tip.

Method. The method consists essentially of determining the hingemoment parameter $PS_L\overline{x}$ for the flap by assuming two-dimensional loading and then subtracting the losses resulting from the wing-root and wing-tip conical flows. The conical-flow losses are obtained by dividing the conical regions into a series of triangular segments, each having its apex at the origin of the Mach cone, and summing the hinge-moment parameters $\left(PS_L\overline{x}\right)^*$ for these segments as illustrated in figure 2. In determining $\left(PS_L\overline{x}\right)^*$ for the triangular segments, integrations of the loading are necessary for obtaining P^* and \overline{x} . As has been previously explained for this type of conical-flow segment, it is sufficient to determine P^*

NACA TN 2221 9

and t_{cp} because the moment arm \overline{x} can be determined from t_{cp} . method for obtaining P^* and $t_{\rm cp}$ is illustrated in figure 3 and involves integrating the pressure losses along the bases of the segments. From integrations of the pressure losses between 0 and n_1 (or 0 and r_1 , values of P^* and n_{cp} (or r_{cp}) are obtained. Values of P^* and values of tcp, corresponding to ncp (or rcp'), obtained in this manner are applicable to the triangular segment bounded by the Mach line, the ray $\tau = \tau_1$, and the section intersecting the Mach cone. Results have been obtained by numerical integration using Simpson's rule (reference 6) except in regions where the slopes of the pressure curves become infinite (fig. 3). In these regions, integrating coefficients, as presented in reference 7, have been used. Forms by which the integrations were made are presented in tables IV to VII. The upper part of these forms are used for computing the pressure distributions (1 - P') along the sections intersecting the Mach cones (fig. 3). In the lower part of the form, the areas and area moments about $n (or r^{\dagger}) = 0$ of the curves of $(l - P^{\dagger})$ plotted against n (or r^{\dagger}) are determined and are used to obtain P^{\star} and t_{CD} for the corresponding triangular segmen and top for the corresponding triangular segments. Tables IV to VII can be used directly for calculating the loading distribution for intermediate cases or cases not included in the present paper.

Method for Approximately Correcting Results Obtained

from Use of Linearized Theory for Airfoil-Section Thickness

Scope. The method for approximately correcting the theoretical results for airfoil-section thickness is based on the assumption that, at any chordwise position on an airfoil having finite thickness, the ratio of conical to two-dimensional pressure is the same as that predicted by linearized theory for an infinitely thin flat plate. (This method is a variation of the method presented in reference 8.) The method can be logically applied only to configurations having similar sections at all spanwise positions affected. The method is expected to give most accurate results at moderate and high Mach numbers for thin controls located inboard from the wing tip and having relatively large areas over which the flow is two-dimensional.

Method. - On the basis of the preceding assumption, the method requires the determination of the following three factors:

$$F_{1} = \frac{C_{L}! \text{(Two-dimensional with thickness)}}{C_{L}! \text{(Two-dimensional flat plate)}}$$

$$= \frac{C_{l}! \text{(Two-dimensional with thickness)}}{C_{l}! \text{(Two-dimensional flat plate)}} \tag{1}$$

$$F_2 = \frac{C_m'(\text{Two-dimensional with thickness})}{C_m'(\text{Two-dimensional flat plate})}$$

$$= \frac{C_{h}(\text{Two-dimensional with thickness})}{C_{h}(\text{Two-dimensional flat plate})}$$
 (2)

$$F_{3} = \frac{C_{h}(\text{Two-dimensional with thickness})}{C_{h}(\text{Two-dimensional flat plate})}$$
 (3)

(The coefficients in equations (1) and (2) are for deflected controls, and the coefficients in equation (3) are those resulting from wing angle-of-attack loading.) Corrected values of ${}^{C}_{L_{\delta}}$, ${}^{C}_{l_{\delta}}$, ${}^{C}_{m_{\delta}}$, ${}^{C}_{n_{\delta}}$, and ${}^{C}_{h_{\alpha}}$ are obtained by multiplying the results obtained by use of the linearized theory for three-dimensional flat plates by the appropriate factors.

The factors are determined, as described in appendix B, by using the Busemann second-order approximation to determine the coefficients for sections having thickness. This approximation gives results which are generally in good agreement with results obtained by use of the more involved exact theories. The theory is not considered accurate, however, at Mach numbers for which the shocks become detached or at Mach numbers below about 1.3 (reference 9). For the general group of airfoil sections that are symmetrical about the chord plane, equations for the correction factors as derived in appendix B are:

$$F_{1} = \frac{1}{\left(1 - \frac{x_{h}}{c}\right)} \int_{x_{h}/c}^{1.0} \left(1 + 2 \frac{c_{2}}{c_{1}} \frac{d}{d} \frac{t}{2c}\right) d \frac{x}{c}$$
 (4)

$$F_{2} = \frac{2}{\left(1 - \frac{x_{h}}{c}\right)^{2}} \int_{x_{h}/c}^{1.0} \left(\frac{x}{c} - \frac{x_{h}}{c}\right) \left(1 + 2\frac{c_{2}}{c_{1}} \frac{d\frac{t}{2c}}{d\frac{x}{c}}\right) d\frac{x}{c}$$
 (5)

$$F_{3} = \frac{2}{\left(1 - \frac{x_{h}}{c}\right)^{2}} \int_{x_{h}/c}^{1.0} \left(\frac{x}{c} - \frac{x_{h}}{c}\right) \left[1 + 2\frac{c_{2}}{c_{1}} \frac{d\left(\frac{t}{2c}\right)^{i}}{d\left(\frac{x}{c}\right)^{i}}\right] d\frac{x}{c}$$
 (6)

CHARTS

Presentation

Aside from the restrictions regarding location, the characteristics of deflected control surfaces are functions only of control plan form and Mach number. The effects of plan form and Mach number are determined from solutions to equations (tables I to III) involving the vari-

ables $\frac{\tan \Lambda_{\rm HL}}{\beta}$, $\frac{\tan \Lambda_{\rm TE}}{\beta}$, and $\lambda_{\rm f}$. (For untapered controls the varia-

bles are $\frac{\tan \Lambda_{HL}}{\beta}$ and βA_f) Figure 4 presents βC_{L_δ} , βC_{l_δ} , βC_{m_δ} , and βC_{h_δ} as functions of these variables for controls located at the wing tip. Each chart of figure 4 presents the characteristics of a series of plan forms having a fixed hinge-line sweep angle (if the Mach number is considered to be fixed) and varying trailing-edge sweep angles and taper ratios. The solid-line curves present the effects of varying taper ratio for plan forms having fixed hinge line and trailing-edge sweep angles. The characteristics of controls having constant aspect ratios are indicated in the charts for βC_{h_δ} by dashed lines. Constant-

aspect-ratio curves are not included in the charts for the other characteristics because, in many cases, they would be quite confusing. If desired, such curves can be drawn by simply determining the taper ratio at which the curve will intersect each of the curves of constant d from the following relation:

$$\lambda_{f} = \frac{2 - A_{f}!(a - d)}{2 + A_{f}!(a - d)}$$

12 NACA TN 2221

For inversely tapered controls, the parameter $1/\lambda_{\hat{\mathbf{f}}}$ is used as a coordinate to avoid elongation of the curves. Calculations were made at values of $\lambda_{\hat{\mathbf{f}}}$ and $\frac{1}{\lambda_{\hat{\mathbf{f}}}}$ = 0, 0.20, 0.40, 0.60, 0.80, and 0.95 and at values of $A_{\hat{\mathbf{f}}}$ ' = 0.8, 2.0, 4.0, 6.0, 8.0, and 10.0 for untapered controls. Calculated results not included in the charts are presented in table VIII. The results not included in the charts are mainly for configurations

having values of $\frac{\tan \Lambda_{TE}}{\beta}$ near |1.0| and, consequently, having extremely large areas of induced loading on the wing. Results for such configurations are of little practical value because if these large areas are to lie entirely on the wing, as has been assumed, the wing must have a very large span or the control must have a very small chord.

Charts presenting the characteristics of deflected controls located inboard from the wing tip are presented in figures 5 and 6. These charts vary somewhat from those for controls located at the wing tip. Equations for $\beta C_{L_{\delta}}{}^{\bullet}$ and $\beta C_{m_{\delta}}{}^{\bullet}$ were simplified and found to be dependent only on

$$\frac{\tan \Lambda_{HL}}{\beta}$$
 and $\frac{\tan \Lambda_{TE}}{\beta}$. These equations, with results in chart form, are

presented in figure 5. Charts for $\beta C_{h_{\delta}}$ and $\beta C_{l_{\delta}}$! (fig. 6) are presented only for normal taper ratios because the characteristics of inversely tapered controls can be obtained by entering the charts at

$$\frac{-\tan \Lambda_{\rm HL}}{\beta}$$
, $\frac{-\tan \Lambda_{\rm TE}}{\beta}$, and $1/\lambda_{\rm f}$.

The computing form for $C_{h_{\alpha}}$ is presented in table IX and is self-explanatory. Supplementary charts for determining the loading distribution (P* and t_{cp}) for the various triangular segments of the conicalflow regions are presented in figures 7 to 10. It should be pointed out that figures 8 and 10 can easily be used for determining the spanwise and chordwise loading of the wings considered in this paper and will therefore be of value in making loads analyses.

Use

In order to use the charts for determining the characteristics of deflected controls, values of $\frac{\tan \Lambda_{HL}}{\beta}$, $\frac{\tan \Lambda_{TE}}{\beta}$, and λ_f for the configuration being considered must be determined. These values are then

NACA TN 2221

used for entry into the charts, figures 4 or 5 and 6, depending on control location. The coefficients obtained from the charts have been made non-dimensional by use of control geometric parameters. For determining the coefficients based on the usual wing parameters, the following equations are given (approximate thickness correction factors are included but can be neglected by letting the factors equal 1.0):

$$(C_{L_{\delta}})_{c} = F_{1}C_{L_{\delta}}, \frac{S_{f}}{S}$$
 (7)

$$\left(^{C}_{h_{\delta}}\right)_{c} = F_{2}^{C}_{h_{\delta}} \tag{10}$$

(The subscript c indicates that the approximate thickness correction factors have been included.)

For determining the control hinge moment due to wing angle of attack, preliminary calculations are first made on the computing form of table IX. Results of these computations indicate positions in the charts (figs. 7 to 10) from which P^* and $t_{\rm cp}$ are to be obtained. Values from the charts are then inserted in table IX and the operations indicated in the computing form are completed. The approximate thickness correction factor can be applied by use of the following equation:

$$\left(\mathbf{C}_{\mathbf{h}_{\alpha}}\right)_{\mathbf{c}} = \mathbf{F}_{\mathbf{3}}\mathbf{C}_{\mathbf{h}_{\alpha}} \tag{11}$$

Illustrative Example

As an example of the use of the charts, the control-surface characteristics are determined for the configuration shown in figure 11. The wing is assumed to have 5-percent-thick symmetrical parabolic sections in planes normal to the control hinge line.

Lift and pitching-moment coefficients are obtained by entering the charts of figure 5 at values of $\frac{\tan \Lambda_{HL}}{\beta}=0.40$ and $\frac{\tan \Lambda_{TE}}{\beta}=0.35$. Hinge-moment and rolling-moment coefficients are obtained by entering the charts of figure 6(g) at values of $\frac{\tan \Lambda_{TE}}{\beta}=0.35$ and $\lambda_f=0.713$. Coefficients obtained from the charts are $\beta C_{L_8}'=0.0748$, $\beta C_{m_8}'=-0.0365$, $\beta C_{l_8}'=0.0372$, and $\beta C_{h_8}=-0.0345$. The calculation of C_{h_α} for the example is presented in table IX. Preliminary calculations are made in table IX(a) and in column (1) of table IX(b). Values of n and recalculated in column (1) are used to enter the charts (figs. 7 to 10). Values of P* and t_{cp} obtained from the computations are completed. The theoretical value of C_{h_α} is -0.0194.

The equation for the section contour in a plane normal to the control hinge axis is

$$\frac{t}{2c} = 2\left(\frac{t}{c}\right)_{max} \left[\frac{x}{c} - \left(\frac{x}{c}\right)^{2}\right]$$
 (12)

The slope in this plane at any point along the airfoil is

$$\frac{d}{d} \frac{\frac{t}{2c}}{\frac{x}{c}} = 2\left(\frac{t}{c}\right)_{\max} \left(1 - 2\frac{x}{c}\right) \tag{13}$$

Substitution of equation (13) in equations (4) and (5) yields the following equations for F_1 and F_2 :

$$F_1 = 1 - 4 \frac{C_2}{C_1} \left(\frac{t}{c}\right)_{max} \frac{x_h}{c}$$
 (14)

$$F_2 = 1 - \frac{\mu}{3} \frac{C_2}{C_1} \left(\frac{t}{c}\right)_{max} \left(1 + 2 \frac{x_h}{c}\right)$$
 (15)

For determining F_3 , the equation for the section contour in a plane normal to the wing leading edge is written as

$$\left(\frac{t}{2c}\right)' = \frac{2\left(\frac{t}{c}\right)_{\text{max}}}{\cos(\Lambda - \Lambda_{\text{HL}})} \left[\frac{\left(\frac{x}{c}\right)' - \left(\frac{x}{c}\right)'^2}{1 + K\left(\frac{x}{c}\right)'}\right]$$
(16)

where

$$K = \tan(\Lambda - \Lambda_{HL})\tan(\Lambda - \Lambda_{TE})$$

The slope of the airfoil contour in this plane is

$$\frac{d\left(\frac{t}{2c}\right)'}{d\left(\frac{x}{c}\right)'} = \frac{2\left(\frac{t}{c}\right)_{\max}}{\cos\left(\Lambda - \Lambda_{HL}\right)} \left\{ \frac{1 - 2\left(\frac{x}{c}\right)' - K\left(\frac{x}{c}\right)'^{2}}{\left[1 + K\left(\frac{x}{c}\right)'\right]^{2}} \right\}$$
(17a)

or in terms of x/c

$$\frac{d\left(\frac{t}{2c}\right)}{d\left(\frac{x}{c}\right)^{*}} = \frac{2\left(\frac{t}{c}\right)_{\max}}{\cos\left(\Lambda - \Lambda_{\text{HL}}\right)} \left[1 - 2\frac{x}{c} + \frac{K}{1 + K}\left(\frac{x}{c}\right)^{2}\right]$$
(17b)

Substitution of equation (17b) in equation (6) yields the following equation for F_3 :

$$F_{3} = 1 - \frac{2C_{2}(\frac{t}{c})_{max}}{3C_{1}(1 + K)\cos(\Lambda - \Lambda_{HL})} \left[2\left(1 + 2\frac{x_{h}}{c}\right) - K\left(1 - \frac{x_{h}}{c}\right) \right]$$
 (18)

From equations (14), (15), and (18), the following correction factors are obtained for the sample configuration: $F_1 = 0.8077$, $F_2 = 0.7889$, and $F_3 = 0.7355$. It is of interest to note that these values indicate appreciable losses in loading due to airfoil-section thickness, and it might be pointed out that greater losses would be obtained for thicker airfoil sections.

The coefficients obtained from the charts and the preceding correction factors are then substituted in equations (4) to (8). The results obtained are:

$$(c_{L_\delta})_c = 0.00411$$

$$\left(C_{m_{\delta}}\right)_{c} = -0.00318$$

$$\left(c_{l_{\delta}}\right)_{c} = 0.000619$$

$$\left(c_{h_{\delta}}\right)_{c} = -0.0182$$

$$\binom{C_{h_{\alpha}}}{c} = -0.0143$$

Langley Aeronautical Laboratory
National Advisory Committee for Aeronautics
Langley Air Force Base, Va., September 8, 1950

APPENDIX A

METHOD OF INTEGRATING PRESSURES OVER CONICAL

REGIONS OF DEFLECTED CONTROLS

The pressure distributions in the conical-flow regions shown in figure 12 are given in reference 2. With suitable changes in notation these are:

For region I,

$$P^{\dagger} = \frac{1}{\pi} \cos^{-1} \frac{a - t}{1 - at}$$
 (A1)

For region III,

$$P' = \frac{1}{\pi} \cos^{-1} \frac{1 - (2 + a)t}{1 + at}$$
 (A2)

Because the flow is conical in regions I and III, integrations of the pressures along the trailing edge within these regions are representative of integrations over corresponding triangular segments having the Mach cone origin as apexes. For such integrations, a coordinate for distance along the trailing edge must be introduced. The nondimensional coordinate chosen was $t' = \beta \tan \tau'$ (fig. 12 and reference 2). The integrations required for determining average pressure ratio and center-of-pressure ray location for any segment are

$$P = \frac{\int_{t_{1}^{i}}^{t_{2}^{i}} P^{i} dt^{i}}{\int_{t_{1}^{i}}^{t_{2}^{i}} dt^{i}}$$
(A3)

and

$$t_{cp'} = \frac{\int_{t_1'}^{t_2'} t'P' dt'}{\int_{t_1'}^{t_2'} P' dt'}$$
(A4)

(Subscripts 1 and 2 indicate values of t' corresponding to the end points of the part of t' over which integrations were made.)

A Mach number of $\sqrt{2}$ was assumed for convenience ($\beta=1$) in making the integrations of equations (A3) and (A4). This assumption is valid because any case of Mach number greater than 1 can readily be reduced to an equivalent case at $M=\sqrt{2}$ by an affine transformation corresponding to the Prandtl-Glauert transformation for the subsonic case (reference 5). An example of this transformation is shown in figure 13. The equivalent plan form is obtained by dividing all streamwise dimensions by β and leaving lateral dimensions unchanged; consequently, values of a, d, and t (for equivalent points) are the same. From equations (A1) and (A2), it can readily be seen that values of P' for equivalent points are the same. It follows that summation of P' over equivalent regions results in equal values of P and $t_{\rm CP}$. It is apparent from figure 13, however, that values of $t_{\rm CP}$ are different. This difference is of no consequence because values of $t_{\rm CP}$ for the equivalent wing (obtained from $t_{\rm CP}$ and geometric relations) are the same as values of $t_{\rm CP}$ for the initial wing.

The procedures followed in the integrations of equations (A3) and (A4) are the same for regions I and III and are only shown for region I. If the Mach number is assumed to equal $\sqrt{2}$, where $\beta = 1$, equation (A1) may be written in terms of t' as follows:

$$P' = \frac{1}{\pi} \cos^{-1} \frac{(a+d) - (1-ad)t'}{(1+ad) - (a-d)t'}$$

If y is substituted for $\cos \pi P^{1}$, equations (A3) and (A4) become

$$P = \frac{\frac{-(1-a^2)(1+d^2)}{\pi} \int_{y_1}^{y_2} \frac{\cos^{-1}y}{\left[(1-ad)-(a-d)y\right]^2} dy}{-(1-a^2)(1+d^2) \int_{y_1}^{y_2} \frac{dy}{\left[(1-ad)-(a-d)y\right]^2}}$$
(A5)

$$t_{cp'} = \frac{\frac{-(1-a^2)(1+d^2)}{\pi} \int_{y_1}^{y_2} \frac{(a+d)-(1+ad)y}{\sqrt{[1-ad)-(a-d)y}} \cos^{-1}y \, dy}{\frac{-(1-a^2)(1+d^2)}{\pi} \int_{y_1}^{y_2} \frac{\cos^{-1}y}{\sqrt{[1-ad)-(a-d)y}} \, dy}$$
(A6)

Integration by parts was then employed in the solutions of equations (A5) and (A6).

For cases in which the conical-flow region overlaps the opposite parting line, the average pressure loss and center-of-pressure ray location are required for regions I_a and \bar{I}_b (fig. 1). Equations (A3) and (A4) may be used in obtaining the solutions for region I_a by a slight modification requiring no additional integration. Thus,

$$P^* = \frac{\int_{t_1!}^{t_2!} (1 - P!) dt!}{\int_{t_1!}^{t_2!} dt!} = 1 - \frac{\int_{t_1!}^{t_2!} P! dt!}{\int_{t_1!}^{t_2!} dt!}$$
(A7)

$$t_{cp'} = \frac{\int_{t_1'}^{t_2'} t'(1 - P')dt'}{\int_{t_1'}^{t_2'} (1 - P')dt'} = \frac{\left[\frac{t'2}{2}\right]_{t_1'}^{t_2'} - \int_{t_1'}^{t_2'} t'P' dt'}{\left[t'\right]_{t_1'}^{t_2'} - \int_{t_1'}^{t_2'} P' dt'}$$
(A8)

In obtaining the solutions for region I_b (fig. 1), essentially the same procedure as previously outlined was used. The parameter $r=\frac{1}{t}$ was used to represent distance along the parting line nondimensionally. Values of P^* and r_{cp} were obtained by making integrations similar to those in equations (A7) and (A8) (before simplifications).

Results of integrations over all regions shown in figure 1 are presented in tables II(a) and II(b). Results of evaluating these equations at taper ratios of 1.0, where they become indeterminate, are presented in table III(a).

APPENDIX B

METHOD FOR DETERMINING THICKNESS CORRECTION FACTORS

The pressure coefficient at any point on a two-dimensional surface as given by the Busemann second-order approximation (reference 8, with suitable changes in notation) is

$$C_{p} = C_{1}(\delta + \theta) + C_{2}(\delta + \theta)^{2}$$
(B1)

(The angle δ is considered positive when calculating C_p for lower surface and negative when calculating C_p for upper surface. Throughout appendix B, δ is considered to be in radians.) The constants C_1 and C_2 are functions only of Mach number. Equations for these constants and tabulated values are presented in reference 10.

The lifting pressure coefficient at any chordwise position is simply the difference between the pressure coefficients on the lower and upper surfaces. The net lift coefficient is obtained by integrating the local lifting pressure coefficients between the hinge line $\left(\frac{x}{c} = \frac{x_h}{c}\right)$ and the trailing edge $\left(\frac{x}{c} = 1.0\right)$. (See fig. 14.) Thus,

$$C_{L'}_{\text{thickness}(\delta)} = \frac{1}{1 - \frac{x_h}{c}} \int_{x_h/c}^{1.0} \left[\left(C_p \right)_L - \left(C_p \right)_U \right] d \frac{x}{c}$$
 (B2)

(The subscripts L and U denote lower and upper surfaces.) Similarly, the hinge-moment coefficient is obtained by integrating the products of local lifting pressure coefficient and moment arm between the hinge line and the trailing edge. Thus,

$$C_{h_{\text{thickness}}(\delta)} = \frac{-1}{\left(1 - \frac{x_h}{c}\right)^2} \int_{\mathbf{x}_h/c}^{1.0} \left(\frac{x}{c} - \frac{x_h}{c}\right) \left[\left(C_p\right)_L - \left(C_p\right)_{\underline{U}}\right] d\frac{x}{c}$$
 (B3)

NACA TN 2221 21

An application of sweepback theory, as explained in reference 9, must be used for determining $^{\rm C}_{\rm P_L}$ - $^{\rm C}_{\rm P_U}$. It is important to note that, for deflected controls, this theory requires the use of the Mach number component and the airfoil section in a plane normal to the control hinge axis. Values of $^{\rm C}_{\rm L}$ and $^{\rm C}_{\rm h}$ thus obtained are based on the dynamic-pressure component normal to the hinge line and the deflection angle measured in a plane normal to the hinge line. Values of $^{\rm C}_{\rm L}$ and $^{\rm C}_{\rm h}$ for a two-dimensional flat-plate control, based on the same q and $^{\rm S}_{\rm h}$ are obtained by considering the Mach number normal to the hinge line in

determining values of C1. Equations for these coefficients are

$$C_{L}^{\dagger}$$
 = $2C_{1}\delta$ (B4)

$$C_{h_{flat plate}} = -C_{1}\delta$$
 (B5)

The following correction factors are then determined by dividing equations (B2) and (B3) by equations (B4) and (B5), respectively:

$$F_{1} = \frac{1}{2C_{1}\delta\left(1 - \frac{x_{h}}{c}\right)} \int_{x_{h}/c}^{1.0} \left[\left(C_{p}\right)_{L} - \left(C_{p}\right)_{U}\right] d\frac{x}{c}$$
(B6)

$$F_2 = \frac{1}{c_1 \delta \left(1 - \frac{x_h}{c}\right)^2} \int_{x_h/c}^{1.0} \left(\frac{x}{c} - \frac{x_h}{c}\right) \left[\left(c_p\right)_L - \left(c_p\right)_U\right] d\frac{x}{c}$$
 (B7)

If the sections are assumed to be symmetrical about the chord plane, equations (B7) and (B8) can be simplified because

$$(C_p)_L - (C_p)_U = 2\delta \left(C_1 + 2C_2 \frac{d \frac{t}{2c}}{d \frac{x}{c}} \right)$$
 (B8)

Equations (B6) and (b7) then become

$$F_{1} = \frac{1}{1 - \frac{x_{h}}{c}} \int_{x_{h}/c}^{1.0} \left(1 + 2 \frac{c_{2}}{c_{1}} \frac{d \frac{t}{2c}}{d \frac{x}{c}} \right) d \frac{x}{c}$$
 (B9)

$$F_{2} = \frac{2}{\left(1 - \frac{x_{h}}{c}\right)^{2}} \int_{x_{h}/c}^{1.0} \left(\frac{x}{c} - \frac{x_{h}}{c}\right) \left(1 + 2\frac{c_{2}}{c_{1}}\frac{d\frac{t}{2c}}{d\frac{x}{c}}\right) d\frac{x}{c}$$
 (B10)

The equation for F_3 may be written as equation (B7) for F_2 (substituting α for δ)

$$F_{3} = \frac{1}{c_{1}\alpha \left(1 - \frac{x_{h}}{c}\right)^{2}} \int_{x_{h}/c}^{1.0} \left(\frac{x}{c} - \frac{x_{h}}{c}\right) \left[c_{p}\right]_{L} - \left(c_{p}\right)_{U} d\frac{x}{c}$$
(B11)

In this case, however, the airfoil section and Mach number component in a plane normal to the wing leading edge must be used in determining values of c_1 and $c_p_L - c_p_U$.

For symmetrical sections, the equation for F_3 may be simplified in the same manner as the equivalent equation for F_2 . Thus,

$$F_{3} = \frac{2}{\left(1 - \frac{x_{h}}{c}\right)^{2}} \int_{x_{h}/c}^{1.0} \left(\frac{x}{c} - \frac{x_{h}}{c}\right) \left[1 + 2\frac{c_{2}}{c_{1}} \frac{d\left(\frac{t}{2c}\right)^{t}}{d\left(\frac{x}{c}\right)^{t}}\right] d\frac{x}{c}$$
 (B12)

Equation (Bl2) will in some cases become somewhat involved because $\frac{d(t/c)^{\,t}}{d(x/c)^{\,t}}$ must be determined from the equation for the airfoil section in

a plane normal to the wing leading edge and must then be written in terms of x/c (unless the surfaces are plane). It should be pointed out that suitable approximations for most symmetrical biconvex airfoils (which in general require involved expressions for defining the contour) may be obtained by assuming the sections to have parabolic contours. General equations for the thickness correction factors for symmetrical sections having parabolic contours have been derived in the illustrative example of the present paper.

REFERENCES

- 1. Frick, Charles W., Jr.: Application of the Linearized Theory of Supersonic Flow to the Estimation of Control-Surface Characteristics. NACA TN 1554, 1948.
- 2. Lagerstrom, P. A., and Graham, Martha E.: Linearized Theory of Supersonic Control Surfaces. Rep. No. SM-13060, Douglas Aircraft Co., Inc., July 24, 1947.
- Kainer, Julian H., and Marte, Jack E.: Theoretical Supersonic Characteristics of Inboard Trailing-Edge Flaps Having Arbitrary Sweep and Taper. Mach Lines behind Flap Leading and Trailing Edges. NACA TN 2205, 1950.
- 4. Cohen, Doris: The Theoretical Lift of Flat Swept-Back Wings at Supersonic Speeds. NACA TN 1555, 1948.
- 5. Lagerstrom, P. A., Wall, D., and Graham, M. E.: Formulas in Three-Dimensional Wing Theory. Rep. No. SM-11901, Douglas Aircraft Co., Inc., July 8, 1946.
- 6. Sokolnikoff, Ivan S., and Sokolnikoff, Elizabeth S.: Higher Mathematics for Engineers and Physicists. Second ed., McGraw-Hill Book Co., Inc., 1941.
- 7. Lock, C. N. H., and Knowler, A. E.: Integrating Coefficients for Airscrew Analysis. R. & M. No. 2043, British A.R.C., 1941.
- 8. Bonney, E. Arthur: Aerodynamic Characteristics of Rectangular Wings at Supersonic Speeds. Jour. Aero. Sci., vol. 14, no. 2, Feb. 1947, pp. 110-116.
- 9. Laitone, Edmund V.: Exact and Approximate Solutions of Two-Dimensional Oblique Shock Flow. Jour. Aero. Sci., vol. 14, no. 1, Jan. 1947, pp. 25-41.
- 10. The Staff of the Ames 1- by 3-Foot Supersonic Wind-Tunnel Section: Notes and Tables for Use in the Analysis of Supersonic Flow. NACA TN 1428, 1947.

Table I.- General equations used for determining characteristics of deflected controls [Subscripts I, I_a , I_b , I_c , II, II_a , II_b , II_c , III, III_a , and III_b refer to regions defined in fig. 1]

(a) Configuration Having Control Located Inboard from the Wing Tip.

Parameter	Formula
c _{L8} '	$\frac{2C_{p_0}}{\delta} \left[\frac{S_{L_0}}{S_f} + \left(P \frac{S_L}{S_f} \right)_I + \left(P \frac{S_L}{S_f} \right)_{II} \right]$
C _{m8} ⁴	$\frac{-2C_{p_0}}{\delta} \left[\frac{m_0}{2M_a} + \left(P \frac{S_L \overline{x}}{2M_a} \right)_I + \left(P \frac{S_L \overline{x}}{2M_a} \right)_{II} \right]$
с ₁₈ •	$\frac{2c_{p_0}}{\delta} \left[\frac{\iota_0}{b_f S_f} + \left(P \frac{S_L \overline{y}}{b_f S_f} \right)_I + \left(P \frac{S_L \overline{y}}{b_f S_f} \right)_{II} \right]$
$c_{h_{\delta}}$	$\frac{-2C_{p_{0}}}{\delta}\left[\frac{m_{0}}{2M_{a}} + \left(P\frac{S_{L}\vec{x}}{2M_{a}}\right)_{I_{c}} + \left(P\frac{S_{L}\vec{x}}{2M_{a}}\right)_{I_{a}} - \left(P\frac{S_{L}\vec{x}}{2M_{a}}\right)_{I_{b}}^{*} + \left(P\frac{S_{L}\vec{x}}{2M_{a}}\right)_{II_{c}} + \left(P\frac{S_{L}\vec{x}}{2M_{a}}\right)_{II_{a}}^{*} - \left(P\frac{S_{L}\vec{x}}{2M_{a}}\right)_{II_{b}}^{*}\right]$

(b) Configuration Having Control Located at the Wing Tip.

Parameter	Formula
c _{L8} '	$\frac{2C_{P_{O}}}{\delta} \left[\frac{S_{L_{O}}}{S_{f}} + \left(P \frac{S_{\underline{L}}}{S_{f}} \right)_{\underline{I}} + \left(P \frac{S_{\underline{L}}}{S_{f}} \right)_{\underline{I}_{\underline{a}}}^{*} - \left(P \frac{S_{\underline{L}}}{S_{f}} \right)_{\underline{I}_{\underline{b}}}^{*} + \left(P \frac{S_{\underline{L}}}{S_{f}} \right)_{\underline{I}\underline{I}\underline{I}} \right]$
C _{m6}	$\frac{-2C_{p_{o}}}{\delta}\left[\frac{m_{o}}{2M_{a}} + \left(P \frac{S_{L}\overline{x}}{2M_{a}}\right)_{I} + \left(P \frac{S_{L}\overline{x}}{2M_{a}}\right)_{I_{a}}^{*} - \left(P \frac{S_{L}\overline{x}}{2M_{a}}\right)_{I_{b}}^{*} + \left(P \frac{S_{L}\overline{x}}{2M_{a}}\right)_{III}\right]$
c _{l8} '	$\frac{2C_{p_0}}{\delta} \left[\frac{l_0}{b_f S_f} + \left(P \frac{S_L \overline{y}}{b_f S_f} \right)_I + \left(P \frac{S_L \overline{y}}{b_f S_f} \right)_{I_a}^* - \left(P \frac{S_L \overline{y}}{b_f S_f} \right)_{I_b}^* + \left(P \frac{S_L \overline{y}}{b_f S_f} \right)_{III} \right]$
c _{h8}	$\frac{-2C_{p_{o}}}{\delta}\left[\frac{m_{o}}{2M_{a}} + \left(P\frac{S_{L}\overline{x}}{2M_{a}}\right)_{I_{c}} + \left(P\frac{S_{L}\overline{x}}{2M_{a}}\right)_{I_{a}}^{*} - \left(P\frac{S_{L}\overline{x}}{2M_{a}}\right)_{I_{b}}^{*} + \left(P\frac{S_{L}\overline{x}}{2M_{a}}\right)_{III} + \left(P\frac{S_{L}\overline{x}}{2M_{a}}\right)_{III_{a}}^{*} - \left(P\frac{S_{L}\overline{x}}{2M_{a}}\right)_{III_{b}}^{*}\right]$

NACA

OF DEFLECTED CONTROLS HAVING TAPERED PLAN FORMS

(a) Average Pressure Ratio

[Values of P for regions II, IIa, IIb, and IIc are obtained by substituting -a, -d, and $1/\lambda_f$ for a, d, and λ_f in equations for regions I, Ia, Ib, and Ic, respectively. In cases where plus and minus signs are together (±), the upper sign must be used when values of a and d substituted are such that a - d is negative and the lower sign must be used when values of a and d substituted are such that a - d is positive.]

Region (fig. 1)	Average pressure ratio
I	$P = \frac{\sqrt{(1 - a^2)(1 - d^2)} - (1 - a)(1 + d)}}{2(a - d)}$
Ia	$P^* = \frac{1-d}{\lambda_f(1-d) - (1-a)} \left\{ \frac{\lambda_f}{\pi} \cos^{-1} \left[\frac{(1-a^2) - \lambda_f(1-ad)}{\lambda_f(a-d)} \right] - \frac{1}{\pi} \sqrt{\frac{1-a^2}{1-d^2}} \cos^{-1} \left[\frac{(1-ad) - \lambda_f(1-d^2)}{(a-d)} \right] \right\}$
I _b `	$P^* = \frac{1}{\lambda_f(1-d) - (1-a)} \left\{ \frac{\lambda_f}{\pi} (a - d) \cos^{-1} \left[\frac{(1-a^2) - \lambda_f(1-ad)}{\lambda_f(a-d)} \right] + \frac{(1-\lambda_f)\sqrt{1-a^2}}{\pi} \log_e \left[\frac{(a-\lambda_f d) \pm \sqrt{2\lambda_f(1-ad) - \lambda_f^2(1-d^2) - (1-a^2)}}{1-\lambda_f} \right] \right\}$
ı _c	$P = \frac{1 - d}{a - d} \sqrt{\frac{1 - a^2}{1 - d^2}} \left(1 - \frac{1}{\pi} \cos^{-1} d\right) + \frac{1}{\pi} \cos^{-1} a - \frac{1 - a}{1 - d}$
111	$P = \frac{(1 + a) - \sqrt{(1 + a)(1 + d)}}{a - d}$
III _e	$P^* = \frac{1}{(1+d) - \lambda_f(1+a)} \left\{ \frac{1+d}{\pi} \cos^{-1} \left[\frac{(2+a+d) - 2\lambda_f(1+a)}{(a-d)} \right] - \frac{\lambda_f \sqrt{(1+a)(1+d)}}{\pi} \cos^{-1} \left[\frac{2(1+d) - \lambda_f(2+a+d)}{\lambda_f(a-d)} \right] \right\}$
IIIP	$P^* = \frac{1}{\lambda_f(1+a) - (1+d)} \left\{ \frac{a-d}{\pi} \cos^{-1} \left[\frac{(2+a+d) - 2\lambda_f(1+a)}{(a-d)} \right] \mp \frac{2}{\pi} \sqrt{(1+a)(1-\lambda_f) \left[\frac{\lambda_f}{\Lambda_f}(1+a) - (1+d) \right]} \right\}$

NACA

OF DEFLECTED CONTROLS HAVING TAPERED PLAN FORMS - Continued

(b) Center-of-Pressure Ray Location.

[Values of t_{cp} ' (or r_{cp}) for regions II, II_a, II_b, and II_c are obtained by substituting -a, -d, and $1/\lambda_f$ for a, d, and λ_f in equations for regions I, Ia, Ib, and Ic, respectively. In cases where plus and minus signs are together (±), the upper sign must be used when values of a and d substituted are such that a - d is negative and the lower sign must be used when values of a and d substituted are such that a - d is positive.]

Region (fig. 1)	Center-of-pressure ray location (t _{cp} ^t or r _{cp})
I	$t_{cp}' = \frac{1}{4P(a-d)^2} \left\{ \sqrt{\frac{1-a^2}{1-d^2}} \left(1 + 3ad - 3d^2 - ad^3\right) - \frac{1+d}{1-d} \left[(1-a^2)(1-d^2) - 2d(1-a)^2 \right] \right\}$
	$t_{cp}^{**} = \frac{1}{2P^{*}(a-d)(1+d)[\lambda_{f}(1-d)-(1-a)]} \left\{ \frac{\left(1-d^{2}\right)}{\pi} \left[2\lambda_{f}(1+ad) - \lambda_{f}^{2}(1+d^{2})\right] \cos^{-1} \left[\frac{(1-a^{2}) - \lambda_{f}(1-ad)}{\lambda_{f}(a-d)}\right] - \frac{1}{2P^{*}(a-d)(1+d)[\lambda_{f}(1-d)-(1-a)]} \right\}$
Ia	$\frac{1}{\pi} \sqrt{\frac{1-a^2}{1-a^2}} (1 + 3ad - 3d^2 - ad^3) \cos^{-1} \left[\frac{(1-ad) - \lambda_f (1-d^2)}{a-d} \right] \pm \frac{1}{\pi} \sqrt{\frac{1-a^2}{1-a^2}} $
	$\frac{(1+d^2)}{\pi} \sqrt{(1-a^2) \left[2\lambda_f (1-ad) - \lambda_f^2 (1-d^2) - (1-a^2) \right]} $
	$r_{cp}^* = \frac{1}{2p^* \left[\lambda_f (1-d) - (1-a) \right]} \left\{ \frac{\lambda_f (a-d) \left[2a - \lambda_f (a+d) \right]}{\pi (1-\lambda_f)} \cos^{-1} \left[\frac{(1-a^2) - \lambda_f (1-ad)}{\lambda_f (a-d)} \right] \pm \frac{1}{2p^* \left[\lambda_f (a-d) - (1-a) \right]} \right\}$
Ib	$\frac{\sqrt{(1-a^2)[2\lambda_f(1-ad)-\lambda_f^2(1-d^2)-(1-a^2)]}}{\pi} +$
	$\frac{a(1-\lambda_f)\sqrt{1-a^2}}{\pi}\log_e\left \frac{(a-\lambda_f d)\pm\sqrt{2\lambda_f(1-ad)-\lambda_f^2(1-d^2)-(1-a^2)}}{1-\lambda_f}\right \right\}$
	$t_{cp}' = \frac{1}{2P(1+d)(a-d)^2} \left\{ \sqrt{\frac{1-a^2}{1-d^2}} (1+3ad-3d^2-ad^3) \left(1-\frac{1}{\pi}\cos^{-1}d\right) + \frac{(a-d)(1+d^2)\sqrt{1-a^2}}{\pi} - \frac{1}{\pi} \cos^{-1}d\right\} + \frac{(a-d)(1+d^2)\sqrt{1-a^2}}{\pi} - \frac{1}{\pi} \cos^{-1}d + $
I _c	$\frac{1+d}{1-d}\left[(1-a^2)(1-d^2)-2d(1-a)^2\right]+\frac{(1-d^2)(1+2ad-d^2)}{\pi}\cos^{-1}a$
·	$t_{cp'} = \frac{1}{4P(1+d)(a-d)^2} \left\{ \sqrt{(1+a)(1+d)\left[(2-a+d)(1-d^2)+2ad(1+d)+2d(1+a)\right]} - \frac{1}{4P(1+d)(a-d)^2} \right\}$
	$2\left[(1-a^2)(1-a^2)+2d(1+a)^2\right]$
	$t_{cp}^{**} = \frac{1}{4p^{*}(a-d)\left[\lambda_{f}(1+a)-(1+d)\right]} \left\{ \frac{2(1+d)\left[2\lambda_{f}(1+ad)+(1+d^{2})\right]\cos^{-1}\left[\frac{(2+a+d)-2\lambda_{f}(1+a)}{a-d}\right] \pm \frac{1}{(2+a)^{2}} \left[\frac{(2+a+d)^{2}}{a-d}\right] \pm \frac{1}{(2+a)^{2}} \left[\frac{(2+a)^{2}}{a-d}\right] \pm \frac{1}{(2+a)^{2}} \left[\frac{(2+a)^{2}}{a-d}\right] \pm \frac{1}{(2+a)^{2}} \left[\frac{(2+a)^{2}}{a-d}\right] \pm \frac{1}{(2+a)^{2}} \left[\frac{(2+a)^{2}}{a-d}\right] \pm \frac{1}{(2+a)^{2}} \left[\frac{(2+a)^{2}}{a-$
111 _a	$\frac{2(1+d^2)}{\pi}\sqrt{(1+a)\left[\lambda_f(2+a+d)-\lambda_f^2(1+a)-(1+d)\right]}-$
	$\frac{\lambda_{f}}{\pi} \sqrt{\frac{1+a}{1+d}} \left[(2-a+d)(1-d^{2}) + 2ad(1+d) + 2d(1+a) \right] \cos^{-1} \left[\frac{2(1+d) - \lambda_{f}(2+a+d)}{\lambda_{f}(a-d)} \right]$
-	$r_{cp}^* = \frac{1}{6p^*(1 - \lambda_f)[\lambda_f(1 + a) - (1 + d)]} \left\{ \frac{3(a - d)[2a\lambda_f - (a + d)]}{\pi} cos^{-1} \left[\frac{(2 + a + d) - 2\lambda_f(1 + a)}{a - d} \right] \pm \frac{1}{(a - d)[2a\lambda_f - (a + d)]} \right\}$
III	$\frac{2\left[2\lambda_{f}(1-2a)-(2-3a-d)\right]}{\pi}\sqrt{(1+a)\left[\lambda_{f}(2+a+d)-\lambda_{f}^{2}(1+a)-(1+d)\right]}\right\}$
	J

~_NACA_

OF DEFLECTED CONTROLS HAVING TAPERED PLAN FORMS - Concluded

(c) Geometric Parameters.

$$S_{\mathbf{f}} = \frac{\beta b_{\mathbf{f}}^2(a - d)(1 + \lambda_{\mathbf{f}})}{2(1 - \lambda_{\mathbf{f}})}$$

$$2M_{a} = \frac{\beta^{2}b_{f}^{3}(a-d)^{2}(1-\lambda_{f}^{3})}{3(1-\lambda_{f}^{3})\sqrt{1+\beta^{2}a^{2}}}$$

Region (fig. 1)	s _L /s _f	s _L ⊽/b _f s _f	S _L ∓/2M _B
. 1	$\frac{2(a-d)}{(1-\lambda_f^2)(1-d^2)}$	$\frac{s_L}{s_f} \frac{2(a-d)(t_{cp}'-d)}{3(1-\lambda_f)(1+d^2)}$	$\frac{s_L}{s_f} \frac{1 - \lambda_f^2}{1 - \lambda_f^3} \left[\frac{(1 + ad) - (a - d)t_{cp}}{1 + d^2} \right]$
Ia	$\frac{\lambda_{\mathbf{f}}(1-d)-(1-a)}{(1-\lambda_{\mathbf{f}}^2)(1-d)}$	$\frac{s_L}{s_f} \frac{2(a-d)(t_{cp'}-d)}{3(1-\lambda_f)(1+d^2)}$	$\frac{s_{L}}{s_{f}^{2}} \frac{1 - \lambda_{f}^{2}}{1 - \lambda_{f}^{3}} \left[\frac{(1 + ad) - (a - d)t_{cp}}{1 + d^{2}} \right]$
Ib	$\frac{\lambda_{f}(1-d) - (1-a)}{(1+\lambda_{f})(a-d)}$	<u>e</u> s <u>t</u> 3 s _f	$\frac{s_L}{s_f} \frac{1 - \lambda_f^2}{1 - \lambda_f^3} \frac{\left[(1 - \lambda_f)(r_{cp} - a) \right]}{a - d}$
. I _c		· ·	$\frac{(a-d)[(1+ad)-(a-d)t_{cp}]}{(1-\lambda_f^2)(1-d)(1+d^2)}$
, II	$\frac{2\lambda_{f}^{2}(a-d)}{(1-\lambda_{f}^{2})(1-d^{2})}$	$\frac{s_L}{s_f} \left[1 - \frac{2\lambda_f(a-d)(t_{cp}'+d)}{3(1-\lambda_f)(1+d^2)} \right]$	$\frac{s_L}{s_f} \lambda_f \frac{1 - \lambda_f^2}{1 - \lambda_f^3} \left[\frac{(1 + ad) + (a - d)t_{cp}}{1 + d^2} \right]$
II _a			$\frac{\lambda_{f}^{2} \left[\lambda_{f} (1+a) - (1+d) \right] \left[(1+ad) + (a-d) t_{cD} \right]}{(1-\lambda_{f}^{3})(1+d)(1+d^{2})}$
11p			$\frac{(1-\lambda_f)^2 \left[\lambda_f (1+a) - (1+d) \right] (r_{cp}+a)}{(1-\lambda_f^3)(a-d)^2}$
II,			$\frac{\lambda_f^{3}(a-d)[(1+ad)+(a-d)t_{cp}]}{(1-\lambda_f^{3})(1+d)(1+d^2)}$
III	$\frac{\lambda_f^2(a-d)}{(1-\lambda_f^2)(1+d)}$	$\frac{s_{L}}{s_{f}} \left[1 - \frac{2\lambda_{f}(a-d)(t_{cp}'+d)}{3(1-\lambda_{f})(1+d^{2})} \right]$	$\frac{\lambda_{f}^{3}(a-d)\left[(1+ad)+(a-d)t_{cp}^{-1}\right]}{(1-\lambda_{f}^{3})(1+d)(1+d^{2})}$
III _a			$\frac{\lambda_{f}^{2}\left[\dot{\lambda}_{f}(1+a)-(1+d)\right]\left[(1+ad)+(a-d)t_{cp}\right]}{(1-\lambda_{f}^{3})(1+d)(1+d^{2})}$
. III _p			$\frac{(1-\lambda_{f})^{2} \left[\lambda_{f}(1+a)-(1+d)\right] (r_{cp}+a)}{(1-\lambda_{f}^{3})(a-d)^{2}}$
Two-dimensional	$\frac{\left(\frac{1-a}{1-d}\right)-\lambda_f^2\left(\frac{1+a}{1+d}\right)}{(1-\lambda_f^2)}$	$ \begin{cases} (1+a)(1-\lambda_f) - \frac{(a-d)^3}{(1-\lambda_f)^2(1-d)^2} - \\ & \underbrace{\left[(1+d) - \lambda_f(1+a) \right]^3}_{(1-\lambda_f)^2(1+d)^2} \\ & \underbrace{3(a-d)(1+\lambda_f)} \end{cases} $	$\frac{\left(\frac{1-a}{1-d}\right)^2 - \lambda_f^3 \left(\frac{1+a}{1+d}\right)^2}{2(1-\lambda_f^3)}$

TABLE III.- COMPONENT PARTS OF EQUATIONS USED IN CALCULATING CHARACTERISTICS

OF DEFLECTED CONTROLS BAVING UNTAFERED FLAN FORMS
(a) Average Pressure Ratio and Center-Of-Pressure Ray Location.

ą	
[Values of P and $t_{\rm cp}$ ' (or $r_{ m cp}$) for regions II, IIs, $i_{ m Ib}$, and II $_{ m c}$ are obtained by substituting $-i_{ m cp}$	for a in equations for regions I, Ig, Ib, and Ic, respectively.
ت	

13 $ P^{*} = \frac{1}{2} $ 14 $ P^{*} = \frac{1}{2} $ 15 $ P^{*} = \frac{1}{2} $ 16 $ P^{*} = \frac{1}{2} $ 17 $ P^{*} = \frac{1}{2} $ 18 $ P^{*} = \frac{1}{2} $ 19 $ P^{*} = \frac{1}{2} $ 19 $ P^{*} = \frac{1}{2} $ 19 $ P^{*} = \frac{1}{2} $ 10 $ P^{*} = \frac{1}{2} $ 10 $ P^{*} = \frac{1}{2} $ 11 $ P^{*} = \frac{1}{2} $	Region (fig. 1)	Average pressure ratio	Center-of-pressure ray location (tcp' or rcp)
$ \frac{1}{(1+a)[1-(1-a)Ar]} \left\{ \frac{\sqrt{(1-a^2)} \left[\frac{1}{2} + 2aAr^{1} - (1-a^2)Ar^{12}\right]}{x} - \frac{1}{c_D} \right\} $ $ \frac{1}{a} \frac{1}{$		~¶Qi Ⅱ Q.	$t_{\rm CP}' = \frac{8a + (1 + a^2)}{k(1 - a^2)}$
$= \frac{1}{1 - (1 - a)A_{L}^{1}} \left\{ \frac{1}{\pi} \cos^{-1} \left[(1 - a^{2})A_{L}^{1} - a \right] + \frac{1}{4} - (1 - a^{2})A_{L}^{1} - a \right] + \frac{A_{L}^{1} \sqrt{1 - a^{2}}}{\pi} \log_{e} \left[\frac{1 + aA_{L}^{1} - \sqrt{1 + 2aA_{L}^{1} - (1 - a^{2})A_{L}^{1}}}{A_{L}^{1}} \right] \right\}$ $= \frac{1}{(1 + a)} \left\{ \frac{1 + a}{\pi} \cos^{-1} a - \frac{\sqrt{1 - a^{2}}}{\pi} \right\}$ $= \frac{2A_{L}^{1} (1 + a) - 3}{\pi} \left\{ \frac{2\sqrt{A_{L}^{1} (1 + a) \left[\frac{1}{L} - A_{L}^{1} (1 + a) \right]}}{\pi} - \frac{2A_{L}^{1} (1 + a) - 3}{\pi} \right\}$ $= \frac{2A_{L}^{1} (1 + a) - 3}{\pi} \cos^{-1} \left[\frac{1}{2}A_{L}^{1} (1 + a) - 1 \right] - \frac{1}{\pi} \right\}$ $= \frac{1}{1 - (1 + a)A_{L}^{1}} \left\{ \frac{1}{\pi} \cos^{-1} \left[\frac{1}{2}A_{L}^{1} (1 + a) - 1 \right] - \frac{1}{\pi} \right\}$ $= \frac{2\sqrt{A_{L}^{1} (1 + a)}A_{L}^{1}} \left\{ \frac{1}{\pi} \cos^{-1} \left[\frac{1}{2}A_{L}^{1} (1 + a) - 1 \right] - \frac{1}{\pi} \right\}$		$\left\{ \frac{1}{(1+a)\left[1-(1-a)A_T^{-1}\right]} \left\{ \frac{1}{(1-a)^2 A_T^{-1-a}} \left[\frac{1}{(1-a)^2 A_T^{-1-a}} \right] \right\}$	$\frac{t_{CP}}{t_{CP}} = \frac{1}{h_{F}^{*}(1+a)(1-a^{2})[1-(1-a)A_{F}^{*}]} \left\{ \frac{(7a^{2}-2a^{4}+1)-2A_{F}^{*}(1-a^{2})^{2}[2a+(1+a^{2})A_{F}^{*}]}{n} + \frac{n}{h_{F}^{*}(1+a)(1-a^{2})A_{F}^{*}[1-a^{2})$
$P = \frac{1}{(1+a)} \left(1 + \frac{a}{\pi} \cos^{-1}a - \frac{\sqrt{1-a^2}}{\pi} \right) \qquad \text{tcp.}^{'} = \frac{1}{4P(1+a)(1-a^2)}$ $P = \frac{1}{2}$ $\left[\frac{1}{2} - (1+a)A_F^{'} \right] \left\{ \frac{2\sqrt{A_F'(1+a)} \left[\frac{1}{2} - A_F'(1+a) \right]}{\pi} - \frac{1}{4c} + \frac{1}$		= 1 - (1 - 8 Ag'\1 - 8	
$\frac{1}{[1-(1+a)Ar^{1}]} \left\{ \frac{2[M_{2}^{1}(1+a)[1-Ar^{1}(1+a)]}{\pi} - \frac{t_{CD}^{1}}{r} = \frac{1}{[6p^{4}(1+a)[1-(1+a)Ar^{1}]} \right\} $ $= \frac{1}{1-(1+a)Ar^{1}} \left\{ \frac{1}{\pi} \cos^{-1} [2Ar^{1}(1+a) - 1] \right\} $ $= \frac{1}{1-(1+a)Ar^{1}} \left\{ \frac{1}{\pi} \cos^{-1} [2Ar^{1}(1+a) - 1] - \frac{r_{CD}^{1}}{\pi} = \frac{1}{6p^{4}Ar^{1}[1-(1+a)Ar^{1}]} \right\} $ $= \frac{1}{[6p^{4}(1+a)[1-(1+a)Ar^{1}]} \left\{ \frac{1}{\pi} \cos^{-1} [2Ar^{1}(1+a) - 1] - \frac{r_{CD}^{1}}{\pi} = \frac{1}{6p^{4}Ar^{1}[1-(1+a)Ar^{1}]} \right\} $ $= \frac{2[1+2Ar^{1}(1+a)]}{r^{1}(1+a)Ar^{1}} \left\{ \frac{1}{\pi} \cos^{-1} [2Ar^{1}(1+a) - 1] - \frac{r_{CD}^{1}}{\pi} = \frac{1}{6p^{4}Ar^{1}[1-(1+a)Ar^{1}]} \right\} $		$P = \frac{1}{(1+a)} \left(1 + \frac{a}{\pi} \cos^{-1} a - \frac{\sqrt{1-a^2}}{\pi} \right)$	$t_{Cp} = \frac{1}{4P(1+a)(1-a^2)} \left[8a + (1+a^2) + \frac{7a^2 - 2a^4 + 1}{x} \cos^{-1} a - \frac{a(7-a^2)\sqrt{1-a^2}}{x} \right]$
$\frac{1}{[1-(1+a)A_f^{-1}]} \left\{ \frac{2\sqrt{A_f^{-1}(1+a)}\left[\frac{1}{2} - A_f^{-1}(1+a)\right]}{\pi} - \frac{t_{Cp}^{-1}}{1} \frac{1}{(Dp^{-1}(1+a)\left[1-(1+a)A_f^{-1}\right]} \right\} \right.$ $\frac{A_f^{-1}(1+a)}{\pi} = \frac{1}{1-(1+a)A_f^{-1}} \left\{ \frac{1}{2}\cos^{-1}\left[2A_f^{-1}(1+a) - 1\right] - \frac{1}{1} - \frac{1}{1} \right\} \right.$ $\frac{2\left[\frac{1}{2}a^{2} + 6a - 3 - 2A_f^{-1}(1+a)}{\pi}\right]}{2\sqrt{A_f^{-1}(1+a)A_f^{-1}}} \right\} = \frac{1}{\pi} \frac{1}{\pi} \left(\frac{1}{\pi} + \frac{1}{\pi$		~ Q 1 8	$t_{\rm Cp}$ ' = $\frac{5-8a-3a^2}{8(1+a)}$
$= \frac{1}{1 - (1 + a)A_{E'}} \left\{ \frac{1}{4} \cos^{-1} \left[2A_{E'} (1 + a) - 1 \right] - \frac{r_{cp}^{*}}{1 - (1 + a)A_{E'}} \right\} $ $= \frac{1}{1 - (1 + a)A_{E'}} \left\{ \frac{1}{4} \cos^{-1} \left[2A_{E'} (1 + a) - 1 \right] - \frac{r_{cp}^{*}}{1 - (1 + a)A_{E'}} \right\} $		4)ArJ	$ \mathbf{t_{cp}}^{**} = \underbrace{\frac{16P^{*}(1+a)[1-(1+a)Ar^{2}]}{\pi}} \left\{ \underbrace{\frac{[3-8a-5a^{2}-8A_{f},(1+a)^{2}[A_{f},(1+a^{2})-2a]}{\pi} \cos^{-1}[2A_{f},(1+a)-1] - \frac{1}{2} - \frac{1}{2} \cos^{-1}[2A_{f},(1+a)^{2}]}_{R} \right\} $
*) = * (*)		= 1 - (1 +	$z_{\text{CD}^*} = \frac{1}{6P^4 \pi^4 \left[1 - (1 + a)A_T^{-1}\right]} \left[\frac{3(1 - 2aA_T^{-1})}{\pi} \cos^{-1} \left[2A_T^{-1}(1 + a) - 1\right] - \frac{2\left[1 + 2A_T^{-1}(1 - 2a)\right]}{\pi} A_T^{-1} + \frac{1}{2}A_T^{-1} A_T^{-1} \right]$

TABLE III.- COMPONENT PARTS OF EQUATIONS USED IN CALCULATING CHARACTERISTICS OF DEFLECTED CONTROLS HAVING UNTAFERED PLAN FORMS - Concluded

(b) Geometric Parameters.

$$S_{\mathbf{f}} = \frac{\beta \mathbf{b}^2}{A_{\mathbf{f}}^*},$$

$$2M_{\mathbf{a}} = \frac{\beta^2 \mathbf{b}^3}{A_{\mathbf{f}}^{*2} \sqrt{1 + \beta^2 \mathbf{a}^2}}$$

Region (fig. 1)	s _L /s _f	s _L ý/b _f s _f	S _L x̄/2M _a
I	$\frac{1}{A_f'(1-a^2)}$	$\frac{S_{L}}{Sr} \frac{\left(1 + 4_{a}\right)}{6A_{r}'\left(1 - a^{2}\right)}$	2 S <u>L</u> 3 Sf
Ia	$\frac{1 - A_{f}'(1 - a)}{2A_{f}'(1 - a)}$	$\frac{s_{L}}{s_{f}} \frac{2(t_{cp'} - a)}{3A_{f'}(1 + a^{2})}$	$\frac{2}{3} \frac{s_L}{s_f}$
ı,	1 - Ap'(1 - a)	2 ^S L 3 ^S f	2 S _L A _f '(r _{cp} '- a)
· Ic			1 3A _f '(1 - a)
11	$\frac{1}{A_{\mathbf{f}}'(1-a^2)}$	$\frac{S_{L}}{S_{T}}\left[1-\frac{\left(1-\frac{L}{a}\right)}{6A_{T}'\left(1-a^{2}\right)}\right]$	2 SL 3 Sr
. II _a			$\frac{1 - A_{f}'(1 + a)}{3A_{f}'(1 + a)}$
IIb			$\frac{A_{\mathbf{f}'}(\mathbf{r}_{\mathbf{cp}} + \mathbf{a})\left[\widetilde{\mathbf{i}} - A_{\mathbf{f}'}(1 + \mathbf{a})\right]}{3}$
II _e			$\frac{1}{3A_{\mathbf{f}'}(1+\mathbf{a})}$
ın	2A _f '(1 + a)	$\frac{S_L}{S_f} \left[1 - \frac{5}{12A_f!(1+a)} \right]$	3 St
IIIa			$\frac{1 - A_{f}'(1 + a)}{3A_{f}'(1 + a)}$
IIIÞ	-		$\frac{A_{f}'(r_{cp} + a)[1 - A_{f}'(1 + a)]}{3}$
Two- dimensional	$\frac{A_{f}'(1-a^2)-1}{A_{f}'(1-a^2)}$	$\frac{3A_{f}'(1-a)(1-a^{2})\left[A_{f}'(1+a)-1\right]-a_{a}}{6A_{f}'^{2}(1-a^{2})^{2}}$	$\frac{3A_{f}'(1-a^{2})-4}{6A_{f}'(1-a^{2})}$

NACA

TABLE IV, - EXAMPLE OF NUMERICAL INTEGRATION OF PRESSURES ALONG AN INCLINED SECTION INTERSECTING WING-ROOT MACH CONE

												*.		(18)	(12) ~ (13)	/ / ·	0,0980	.1348	.1620	.1837	. 2018	.2171	.2305	.2417	.2513	.2595	3	¥
														(11)	-I		10.0000	5.0000	3.3333	2,5000	2.0000	1.6667	1.4286	1.2500	1.1111	1.0000	NACA	3
													do.	(16)	(14)	(12)	0.9482	.9021	.8522	.8012	.7493	.6965	.6430	.5887	.5337	.4783		
				•			1.50		•					(12)	(12) -	$K_1 \times (13)$	0.009672 0.9482 10.0000	.026307	,046869	.070012	.094969	.121139	.148054	.175321	.202594	.229540		
		Ç	2i	an 1 = 0.20	ا ما	125	$K_2 = 2(1 - g^2) = \frac{1.50}{1.50}$	•	•					(14)	(19) - (18)	(01) _ (01)	0,009171	.023732	.039940	,056091	.071158	.084378	.095194	.103203	.108120	.109789		
		9 03		K ₁ = tan η	• •	8 = 0.25	K ₂ = 2							(13)	∏.rou	(11)mom.	0,000628	003218	.008661	.017401	029764	.045951	066075	.090148	.118092	149689		
									•					(12)	Incr. ∑	(1) to (10) (11)area	0.009797 0.000628	.026951	.048601	.073492	.100922	.130329	.161269	.193351	.226212	.259478		
1 - P	(8)	$\frac{\cos^{-1}(7)}{\pi}$	0,1431	.1967	.2342	,2627	2850	.3024	.3158	.3253	.3313	.3333		(11)	×(' q - 1)Χ	(1) to (10)	767600.0	.017154	,021650	.024891	,027430	.029407	.030940	.032082	.032861	.033266		0,000626
į	(2)	(6) - 1	0,9007	.8151	.7414	.6784	6253	.5816	.5470	.5216	.5056	.5000		(10)		1.0	0	0	0	0	0	0	.004167	020833	.079167	.037500		0
ş	(9)	K ₂ (5)	1,9007	1,8151	1.7414	1.6784	1,6253	1.5816	1,5470	1,5216	1.5056	1.5000		(6)		6.0	0	0	0	0	0	0	004167	.054167	.054167	004167		0
į	(2)	1 - g2× (4)	0.7892	.8264	.8614	.8937	. 9229	9484	9696	.9858	.9963	1,0000		(8)		8.0	0	0	0	0	0	0	.037500	.079167	020833	.004167		0
	(4)	2 (3)(5)	0.8434	.6944	.5545	.4253	.3086	.2066	.1217	£990°	.0149	0		(7)		0.7	0	0	0	.004167	020833	.079167	.037500	0	0	0		0
[(3)	$K_1 \times (1)$	0.98	96*	.94	26*	8	88*	98*	*84	.82	08*		(9)	MULTIPLIERS	9.0	0	0	0	004167	.054167	.054167	004167	0	0	0		0
	(2)	(1) - (1)	6.0	8.	۲.	9.	5.	4.	<i>ي</i>	2.	7:	0		(2)	MULT	0.5	0	0	0	.037500	.079167	020833	.004167	0	0	0		٥
	(1)	u	0.1	.2	E.	₹.	rō.	9.	۲.	æ.	6.	1.0		(4)		0.4	-0.004167 0.004167	.054167020833 0	.079167	.037500	0		۰	0	0	0		0
														(3)		0.3	-0.004167		.054167	004167		0	0	0	0	0		۰
														. (2)		0.2	0.037500	.079167	020833	.004167	0	0	0	, 0	0	0		0.006667
														(1)		n = 0.1	0.130786		0	0		0	٥	0	٥	0		0.006667 0.006667

1	1.0 33330	9 6	0	0	5	n		9	101200.	004107	oneren.	002550. 005150. 101500 101500.	. C384 (8 .14800	4200
-														
ı -	0.10,143	0.1431 0.006667	0.006667	0	٥		0	0	0	0	0	0,000626		
	.196	.1967001667	.008333	.007500	-:000833 0.000833	0.000833	0	0	0	0	. 0	.002593		
	.3 .2342	20	0	.023750	.016250	016250006250	0	0	0	0	0	.005442		
J	.4 ,2627	7 0	0	008333	.021667	.031667	0	0	0	0	0	.008740		
ENJ	.5 ,2850	0 O	0	.002083	002083002083	.018750	.018750	.018750002083	.002083	0	0	.012363		
WO	.6 3024	4 0	0	0	0	0	.047500	.032500	012500	0	0	.016187		
M	.31580	08	0	0	0	0	014583	.037917	.055417	0	0	.020124		
	.8 ,3253	30	0	0	0	0	.003333	003333	.030000	.033333	.033333006667	.024073		
	.9 3313	30 ·	0	0	0	0	0	0	0	.060000	.060000	.027944		
	1.0 .33330	30	0	0	0	0	0	0	0	008333	.041667	.031597		
۱														

TABLE V. - EXAMPLE OF NUMERICAL INTEGRATION OF PRESSURES ALONG A STREAMMLES SECTION INTERSECTING WING-ROOT MACH CONE.

												乱	(12)	-	(12)×(16)	0.1074	.1414	.1649	.1825	.1964	.2077	.2172	.2252	.2322	.2383	A	\ \									
													(16)	T	ŗ,	0.9409 10.0000	5.0000	3.3333	2,5000	2.0000	1.6667		1.2500	1.1111	1.0000	NACA	3									
								= 0.50			•	ţ	(15)	(3)	(14)	0.9409	.8951	.8514	.8121	.7766	.7444	.7150	.6879	.6630	.6400											
						25	?. !	$\mathbf{K}_1 = \left(1 - 2\mathbf{g}^2\right) = 0$					(14)		(12) + (13)	0,011413	.031594	.058111	.089872	,126415	167405	.212625	.261914	.315160	.372283											
					g = 0.50	52 = 0.25	•	$\mathbf{K_1} = (1$					(13)	10.4	(11)mom.	0,000674	.003315	.008635	.016886	.028237	.042788	909090	.081733	,106200	.134031											
								*					(12)	Incr 7	111)area	0.010739	.028279	.049476	.072986	.098178	.124617	.152019	,180181	.208960	.238252											
													(11)	5/1- D/x	(1) to (10)	0.010739	.017540	.021197	.023510	.025192	.026439	.027402	.028162	.028779	.029292		0.000674	.002641	.005320	.008251	.011351	.014551	.017818	.021127	.024467	.027831
1 - P'	(9)	cos ⁻¹ (5)	0.1503	.1967	.2250	.2445	.2587	.2696	.2781	.2849	.2905	2952	(10)		1.0	0	0	0	. 0	0	0	.004167	020833	.079167	.037500		0	0	0	. 0	, 0	0	0	.033333006667	.060000	.041667
	(2)	<u>(4)</u>	0.8906	.8151	.7604	7193	.6875	.6623	.6420	.6254	.6116	0009*	(6)		6.9	0	0	0	0	0	0	004167	.054167	.054167	004167		0	0	0	0	0	0	0	.033333	.060000	008333
	(4)	(2) - g ²	96.0	1,19	1,44	1,71	2.00	2,31	2,64	2.99	3,36	3.75	(8)		9.0	0	0	۰	0	0	0	.037500	.079167	020833	.004167		0	. 0	0	0	.002083	012500	.055417	.030000	0	•
	(3)	$g^2 + K_1 \times (2)$	0,855	970	1,095	1,230	1,375	1.530	1,695	1,870	2,055	2,250	6		0.7	0	0	. 0	.004167	020833	.079167	.037500	0	0	0		0	0	0	0	002083	.032500	.037917	003333	0	0
	(2)	[1 + (1)] ²	1.21	1.44	1.69	1.96	2.25	2.56	2.89	3.24	3.61	4.00	. (9)	MULTIPLIERS	9.0	0	0	0	004167	.054167	.054167	004167	ŏ	0	0		0	0	, 0	0	.018750	.047500	014583	.003333	0	0
	(1)	r'	0.1	.2	.3	.4	.5	9.	7.	8.	6.	1.0	(2)	MULT	0.5	0	0	0	.037500	.079167	020833	.004167	0	0	0		0.	.000833	006250	.031667	.018750	0	0	0	0	0
													(4)		4.0	0.004167	020833	.079167	.037500.		0	0	0	0	0		0	-,000833	.016250	.021667	002083	0	0	0	0	0
													(6)		0.3	-0.004167	.054167	.054167	004167	0	0		0	0	0		0	.007500	.023750	008333	.002083	0	0	0	0	0
		•											(3)		0.2	0.037500	.079167	020833	.004167	0	0	0	0	0	0		0.006667	.008333	0	0	0	0	0	0	0	
			ı										3		r'= 0.1	0.130786	045340	0	0	0	0.		0	0	0		1503 0.006667	001667	0	0				0	0	
						•								L	1 - P'	0,1503	.1967	.2250	.2445 0	.2587 0	0. 9692*	.2781 0	.2849 0	.2905 0	.2952		0,1503	.1967	,2250	.2445 0	.2587 0	.2696 0	.2781 0	.2849 0	2905	.2952 0

TABLE V. - EXAMPLE OF NUMERICAL INTEGRATION OF PRESSURES ALONG A STREAMMISE SECTION INTERSECTING WING-ROOT MACH CONE - Concluded

				$\mathbf{g} = \frac{0.50}{0.25}$ $\mathbf{g}^2 = \frac{0.25}{0.25}$ $\mathbf{K}_1 = (1 - 2\mathbf{g}^2) = \frac{0.50}{0.50}$								•
									•			
1 - p'	(9)	cos-1(5)	0.3173	.3245	.3277	.3295	.3305	.3312	.3316	.3319	.3322	
	(2)	(4)	0.5429	.5238	.5152	5105	.5077	.5059	.5046	.5038	.5031	
	(4)	(2) - g ²	8.75	15.75	24.75	35,75	48.75	63.75	80.75	99.75	120.75	
	(3)	$\begin{array}{c} g^2 + \\ K_1 \times (2) \end{array}$	4.750	8,250	12,750	18,250	24.750	32,250	40.750	90,250	60.750	
	(2)	[[1 + (1)] z	9.00	16.00	25.00	36.00	49.00	64.00	81.00	100.00	121.00	
	(E)	т.	2.0	3.0	4.0	0.5	6.0	7.0	8.0	9.0	10.0	

ž,	(16)	(11) × (15)	(20) (10)		0.2731	.2893	.2985	.3045	.3088	3119	.3144	.3163	.3179	MACA
	(12)	i	r.		0.50000	.33333	.25000	.20000	.16667	.14286	.12500	.11111	.10000	
tcp	(14)	(11)			0.4770	.3822	.3193	.2745	.2408	2146	.1936	.1763	.1619	
	(13)	Σ(1-P')× Incr. Σ Incr. Σ (11). (12)	(44) 7 (48)		1,14513 0.4770 0.50000 0.2731	2,27096	3.73927	5.54726	7.69261	7,99066 10,17412	12,99117	16,14285	19,62937	-
	(12)	Incr. Z	(10)mom.	0.13403	.59893	1,40307	2.54540	4.02470	5.84000		2.51487 10.47630 12,99117	13,29623 16,14285	.33205 3.17867 16.45070 19.62937	
	(11)	Incr. Σ	(10)area (10)mom.	0.23825	.54620	.86789	1,19387	1.52256	1.85261	33085 2,18346	2.51487	.33175 2.84662	3,17867	
	(10)	$\Sigma(1-P')\times$	(1) to (9)	0,23825	30795	.32169	.32598	.32869	:33005	- 1	.33141			
	(6)		10.0	0	0	0	0	0	, 0	041667	208333	.791667	.375000	
	(8)		9.0	0	0	0	0	0	0	.375000041667	.541667	.541667	.041667041667	
		١.								8	.791667	333	1667	
	E		8.0	٥	0	0	0	0	0	.375	.791	208333	.041	
	(6)	PLIERS	7.0 8.0	0 0	0	0	.041667 0	208333 0	.791667 0	.375000 .375	0 .791	0208	0 041	
	\vdash	MULTIPLIERS	<u> </u>	0 0 0	0 0	0 0	_	ļ	.541667	.375000	167. 0 0	0208	0 0 041	
	(9)	MULTIPLIERS	7.0	0 0 0	0 0 0	0 0 0	.375000041667 .041667 0	ļ	Ш		0 0 0	0 0208	0 0 0	
	(9) (9)	MULTIPLIERS	6.0 7.0	0.041667 0 0 0 0	208333 0 0 0 0	0 0 0 0	.375000 .375000041667	0 .791667 .541667	.541667	.375000	167. 0 0 0 0	0 0 0 0 0	0 0 0 0	
	(4) (5) (6)		5.0 6.0 7.0	1667 0.	.541667208333 0 0 0 0	867	67 .375000 .375000041667	0 .791667 .541667	.541667	.375000	167. 0 0 0 0	0 0 0 0 0	0 0 0 0 0	
	(3) (4) (5) (6)		0 4.0 5.0 6.0 7.0	-0.04 40.04	.541	.541667	041667 .375000 .375000041667	0 .791667 .541667	0208333 .541667	0 .041667041667 .375000	167. 0 0 0 0 0	0 0 0 0 0 0	0 0 0 0 0	
	(2) (3) (4) (5) (6)		3.0 4.0 5.0 6.0 7.0	0 -0.04	3173 791667 .541667 208333 0 0 0 0	867	041667 .375000 .375000041667	0 0 .791667 .541667	0208333 .541667	0 .041667041667 .375000	33160 0 0 0 0 0 0 0	802 0 0 0 0 0 0 0 0 S15.	.3322 0 0 0 0 0 0 0 0 0 0 0 0 0 0 141	

0.13403	.46490	.80414	1,14233	1.47930	1,81530	.291667 2.15066	2,48564	2.81993	3.15447	
0	0	0	0	0	0	.291667	-1.666667	7.125000 2.81993	3.750000	
0	0	0	0	0	0	291667	6.33333 4.33333 -1.666667 2.48564	-1.875000 4.875000	416667416667 3.750000 3.15447	
. 0	0	0	0	0	0	2.625000	6.33333	-1.875000	.416667	
0	0	0	.166667	3.958333 2.708333 -1.041667	4.750000	291667291667 2.625000 2.625000291667	0	0	0	
0	0	0	-,166667	2,708333	-1.250000 3.250000	291667	0	0	0	
0	0	0	166667 1.500000 1.500000166667	3.958333	-1.250000	.291667	0	0	0	
0.041667	.083333416667	1.625000 2.375000	1.500000	0	0	0	0		0	
-0.041667	1.083333	1.625000	166667		0	0	٥	0	0	
1.0 0.2952 0.375000 -0.041667 0.041667	1.583333	.3245625000	.166667	0	0	0	0	0	0	
0.2952	.3173	.3245	.3277	.3295	.3305	.3312	.3316	.3319	.3322 0	
1.0	2.0	3.0	6.	5.0	0.9	7.0	8.0	9.0	10.0	
L_	MOMENT									

OF DEFLECTED CONTROLS HAVING TAPERED PLAN FORMS

(a) Average Pressure Ratio

[Values of P, for regions II, II_a, II_b, and II_c are obtained by substituting -a, -d, and $1/\lambda_f$ for a, d, and λ_f in equations for regions I, I_a, I_b, and I_c, respectively. In cases where plus and minus signs are together (±), the upper sign must be used when values of a and d substituted are such that a - d is negative and the lower sign must be used when values of a and d substituted are such that a - d is positive.]

Region (fig. 1)	Average pressure ratio
I	$P = \frac{\sqrt{(1-a^2)(1-d^2)} - (1-a)(1+d)}{2(a-d)}$
Ia	$P^* = \frac{1 - d}{\lambda_f(1 - d) - (1 - a)} \left\{ \frac{\lambda_f}{\pi} \cos^{-1} \left[\frac{(1 - a^2) - \lambda_f(1 - ad)}{\lambda_f(a - d)} \right] - \frac{1}{\pi} \sqrt{\frac{1 - a^2}{1 - d^2}} \cos^{-1} \left[\frac{(1 - ad) - \lambda_f(1 - d^2)}{(a - d)} \right] \right\}$
Ib	$P^* = \frac{1}{\lambda_f(1-d) - (1-a)} \left\{ \frac{\lambda_f}{\pi} (a-d)\cos^{-1} \left[\frac{(1-a^2) - \lambda_f(1-ad)}{\lambda_f(a-d)} \right] + \frac{(1-\lambda_f)\sqrt{1-a^2}}{\pi} \log_e \left[\frac{(a-\lambda_f d) \pm \sqrt{2\lambda_f(1-ad) - \lambda_f^2(1-d^2) - (1-a^2)}}{1-\lambda_f} \right] \right\}.$
Ic	$P = \frac{1 - d}{a - d} \sqrt{\frac{1 - a^2}{1 - d^2}} \left(1 - \frac{1}{\pi} \cos^{-1} d \right) + \frac{1}{\pi} \cos^{-1} a - \frac{1 - a}{1 - d}$
III	$P = \frac{(1 + a) - \sqrt{(1 + a)(1 + d)}}{a - d}$
III _a	$P^* = \frac{1}{(1+d) - \lambda_f(1+a)} \left\{ \frac{1+d}{\pi} \cos^{-1} \left[\frac{(2+a+d) - 2\lambda_f(1+a)}{(a-d)} \right] - \frac{\lambda_f \sqrt{(1+a)(1+d)}}{\pi} \cos^{-1} \left[\frac{2(1+d) - \lambda_f(2+a+d)}{\lambda_f(a-d)} \right] \right\}$
III _P	$P^* = \frac{1}{\lambda_f(1+a) - (1+d)} \begin{cases} a - d \\ \pi \end{cases} \cos^{-1} \left[\frac{(2+a+d) - 2\lambda_f(1+a)}{(a-d)} \right] \mp$ $\frac{2}{\pi} \sqrt{(1+a)(1-\lambda_f) \left[\lambda_f(1+a) - (1+d) \right]}$

~NACA_

OF DEFLECTED CONTROLS HAVING TAPERED PLAN FORMS - Continued

(b) Center-of-Pressure Ray Location.

[Values of t_{cp} ' (or r_{cp}) for regions II, II_a, II_b, and II_c are obtained by substituting -a, -d, and $1/\lambda_f$ for a, d, and λ_f in equations for regions I, Ia, Ib, and Ic, respectively. In cases where plus and minus signs are together (±), the upper sign must be used when values of a and d substituted are such that a - d is negative and the lower sign must be used when values of a and d substituted are such that a - d is positive.]

Region (fig. 1)	Center-of-pressure ray location (t _{cp} ' or r _{cp})
I	$t_{cp'} = \frac{1}{4P(a-d)^2} \left\{ \sqrt{\frac{1-a^2}{1-d^2}} \left(1 + 3ad - 3d^2 - ad^3\right) - \frac{1+d}{1-d} \left[(1-a^2)(1-d^2) - 2d(1-a)^2 \right] \right\}$
	$t_{cp}^{**} = \frac{1}{2P^{*}(a-d)(1+d)[\lambda_{f}(1-d)-(1-a)]} \left\{ \frac{1-d^{2}}{\pi} \left[2\lambda_{f}(1+ad) - \lambda_{f}^{2}(1+d^{2}) \cos^{-1} \left[\frac{(1-a^{2})-\lambda_{f}(1-ad)}{\lambda_{f}(a-d)} \right] - \frac{(1-a^{2})^{2}}{\pi} \right\} \right\}$
Ia	$\frac{1}{\pi} \sqrt{\frac{1-a^2}{1-d^2}} \left(1 + 3ad - 3d^2 - ad^2\right) \cos^{-1} \left[\frac{(1-ad) - \lambda_f(1-d^2)}{a-d} \right] \pm$
	$\frac{(1+d^2)}{\pi} \sqrt{(1-a^2) \left[2\lambda_f (1-ad) - \lambda_f^2 (1-d^2) - (1-a^2) \right]} $
	$r_{cp}^* = \frac{1}{2p^* \left[\lambda_f (1-d) - (1-a) \right]} \cdot \frac{\left[\lambda_f (a-d) \left[2a - \lambda_f (a+d) \right]}{\pi (1-\lambda_f)} \cdot \cos^{-1} \left[\frac{(1-a^2) - \lambda_f (1-ad)}{\lambda_f (a-d)} \right] \pm \frac{1}{(1-a^2)^2 + (1-a^2)^2 + (1-a^2)$
Ib	$\frac{\sqrt{(1-a^2)[2\lambda_f(1-ad)-\lambda_f^2(1-d^2)-(1-a^2)]}}{\pi} +$
	$\frac{a(1-\lambda_{f})\sqrt{1-a^{2}}}{\pi}\log_{e}\left[\frac{(a-\lambda_{f}d)\pm\sqrt{2\lambda_{f}(1-ad)-\lambda_{f}^{2}(1-d^{2})-(1-a^{2})}}{1-\lambda_{f}}\right]$
	$t_{cp}' = \frac{1}{2P(1+d)(a-d)^2} \left\{ \sqrt{\frac{1-a^2}{1-d^2}} (1+3ad-3d^2-ad^3) \left(1-\frac{1}{\pi}\cos^{-1}d\right) + \frac{(a-d)(1+d^2)\sqrt{1-a^2}}{\pi} - \frac{1}{2P(1+d)(a-d)^2} \left(1+\frac{1}{2}ad^2-ad^3\right) \left(1-\frac{1}{2}ad^2-ad^3\right) + \frac{(a-d)(1+d^2)\sqrt{1-a^2}}{\pi} - \frac{1}{2P(1+d)(a-d)^2} \left(1+\frac{1}{2}ad^2-ad^3\right) \left(1-\frac{1}{2}ad^2-ad^3\right) + \frac{(a-d)(1+d^2)\sqrt{1-a^2}}{\pi} - \frac{1}{2P(1+d)(a-d)^2} + $
Ic	$\frac{1+d}{1-d}\left[(1-a^2)(1-d^2)-2d(1-a)^2\right]+\frac{(1-d^2)(1+2ad-d^2)}{\pi}\cos^{-1}a$
	$t_{cp}' = \frac{1}{4P(1+d)(a-d)^2} \left\{ \sqrt{(1+a)(1+d)} \left[(2-a+d)(1-d^2) + 2ad(1+d) + 2d(1+a) \right] - \frac{1}{4P(1+d)(a-d)^2} \right\}$
III	$2\left[\left(1-a^{2}\right)\left(1-d^{2}\right)+2d(1+a)^{2}\right]$
	$t_{cp}^{**} = \frac{1}{4p^{*}(a-d)\left[\lambda_{f}(1+a)-(1+d)\right]} \left\{ \frac{2(1+d)\left[2\lambda_{f}(1+ad)-(1+d^{2})\right]\cos^{-1}\left[\frac{(2+a+d)-2\lambda_{f}(1+a)}{a-d}\right] \pm \frac{1}{2(1+d)\left[2\lambda_{f}(1+ad)-(1+d^{2})\right]\cos^{-1}\left[\frac{(2+a+d)-2\lambda_{f}(1+a)}{a-d}\right] \pm \frac{1}{2(1+d)\left[2\lambda_{f}(1+ad)-(1+d^{2})\right]\cos^{-1}\left[\frac{(2+a+d)-2\lambda_{f}(1+a)}{a-d}\right] \pm \frac{1}{2(1+d)\left[2\lambda_{f}(1+ad)-(1+d^{2})\right]\cos^{-1}\left[\frac{(2+a+d)-2\lambda_{f}(1+a)}{a-d}\right] \pm \frac{1}{2(1+d)\left[2\lambda_{f}(1+ad)-(1+d^{2})\right]\cos^{-1}\left[\frac{(2+a+d)-2\lambda_{f}(1+a)}{a-d}\right] \pm \frac{1}{2(1+d)\left[2\lambda_{f}(1+ad)-(1+d^{2})\right]\cos^{-1}\left[\frac{(2+a+d)-2\lambda_{f}(1+a)}{a-d}\right] \pm \frac{1}{2(1+d)\left[2\lambda_{f}(1+a)-(1+d^{2})\right]\cos^{-1}\left[\frac{(2+a+d)-2\lambda_{f}(1+a)}{a-d}\right] \pm \frac{1}{2(1+d)\left[2\lambda_{f}(1+a)-(1+d^{2})\right]\cos^{-1}\left[\frac{(2+a+d)-2\lambda_{f}(1+a)}{a-d}\right] \pm \frac{1}{2(1+d)\left[2\lambda_{f}(1+a)-(1+d^{2})\right]}\cos^{-1}\left[\frac{(2+a+d)-2\lambda_{f}(1+a)}{a-d}\right] \pm \frac{1}{2(1+d)\left[2\lambda_{f}(1+a)-(1+d^{2})\right]}\cos^{-1}\left[\frac{(2+a+d)-2\lambda_{f}(1+a)}{a-d}\right] \pm \frac{1}{2(1+d)\left[2\lambda_{f}(1+a)-(1+d^{2})\right]}\cos^{-1}\left[\frac{(2+a+d)-2\lambda_{f}(1+a)}{a-d}\right] \pm \frac{1}{2(1+d)\left[2\lambda_{f}(1+a)-(1+d^{2})\right]}\cos^{-1}\left[\frac{(2+a+d)-2\lambda_{f}(1+a)}{a-d}\right]$
IIIa	$\frac{2(1+d^2)}{\pi}\sqrt{(1+a)\left[\lambda_f(2+a+d)-\lambda_f^2(1+a)-(1+d)\right]}$
	$\frac{\lambda_{\mathbf{f}}}{\pi} \sqrt{\frac{1+a}{1+a}} \left[(2-a+d)(1-d^2) + 2ad(1+d) + 2d(1+a) \right] \cos^{-1} \left[\frac{2(1+d) - \lambda_{\mathbf{f}}(2+a+d)}{\lambda_{\mathbf{f}}(a-d)} \right] $
	$r_{cp}^* = \frac{1}{6p^*(1 - \lambda_f)\left[\lambda_f(1 + a) - (1 + d)\right]} \begin{cases} \frac{3(a - d)\left[2a\lambda_f - (a + d)\right]}{\pi} \cos^{-1}\left[\frac{(2 + a + d) - 2\lambda_f(1 + a)}{a - d}\right] \pm \frac{(2a\lambda_f - (a + d))\left[2a\lambda_f - (a + d)\right]}{\pi} \cos^{-1}\left[\frac{(2 + a + d) - 2\lambda_f(1 + a)}{a - d}\right] \pm \frac{(2a\lambda_f - (a + d))\left[2a\lambda_f - (a + d)\right]}{\pi} \cos^{-1}\left[\frac{(2 + a + d) - 2\lambda_f(1 + a)}{a - d}\right] \pm \frac{(2a\lambda_f - (a + d))\left[2a\lambda_f - (a + d)\right]}{\pi} \cos^{-1}\left[\frac{(2 + a + d) - 2\lambda_f(1 + a)}{a - d}\right] \pm \frac{(2a\lambda_f - (a + d))\left[2a\lambda_f - (a + d)\right]}{\pi} \cos^{-1}\left[\frac{(2 + a + d) - 2\lambda_f(1 + a)}{a - d}\right] \pm \frac{(2a\lambda_f - (a + d))\left[2a\lambda_f - (a + d)\right]}{\pi} \cos^{-1}\left[\frac{(2 + a + d) - 2\lambda_f(1 + a)}{a - d}\right] + \frac{(2a\lambda_f - (a + d))\left[2a\lambda_f - (a + d)\right]}{\pi} \cos^{-1}\left[\frac{(2 + a + d) - 2\lambda_f(1 + a)}{a - d}\right] + \frac{(2a\lambda_f - (a + d))\left[2a\lambda_f - (a + d)\right]}{\pi} \cos^{-1}\left[\frac{(2 + a + d) - 2\lambda_f(1 + a)}{a - d}\right] + \frac{(2a\lambda_f - (a + d))\left[2a\lambda_f - (a + d)\right]}{\pi} \cos^{-1}\left[\frac{(2 + a + d) - 2\lambda_f(1 + a)}{a - d}\right] + \frac{(2a\lambda_f - (a + d))\left[2a\lambda_f - (a + d)\right]}{\pi} \cos^{-1}\left[\frac{(2 + a + d) - 2\lambda_f(1 + a)}{a - d}\right] + \frac{(2a\lambda_f - (a + d))\left[2a\lambda_f - (a + d)\right]}{\pi} \cos^{-1}\left[\frac{(2 + a + d) - 2\lambda_f(1 + a)}{a - d}\right] + \frac{(2a\lambda_f - (a + d))\left[2a\lambda_f - (a + d)\right]}{\pi} \cos^{-1}\left[\frac{(2 + a + d) - 2\lambda_f(1 + a)}{a - d}\right] + \frac{(2a\lambda_f - (a + d))\left[2a\lambda_f - (a + d)\right]}{\pi} \cos^{-1}\left[\frac{(2a\lambda_f - (a + d))\left[2a\lambda_f - (a + d)\right]}{a - d}\right] + \frac{(2a\lambda_f - (a + d))\left[2a\lambda_f - (a + d)\right]}{\pi} \cos^{-1}\left[\frac{(2a\lambda_f - (a + d))\left[2a\lambda_f - (a + d)\right]}{\pi} \cos^{-1}\left[\frac{(2a\lambda_f - (a + d))\left[2a\lambda_f - (a + d)\right]}{\pi}\right] + \frac{(2a\lambda_f - (a + d))\left[2a\lambda_f - (a + d)\right]}{\pi} \cos^{-1}\left[\frac{(2a\lambda_f - (a + d))\left[2a\lambda_f - (a + d)\right]}{\pi} \cos^{-1}\left[\frac{(2a\lambda_f - (a + d))\left[2a\lambda_f - (a + d)\right]}{\pi}\right]} \cos^{-1}\left[\frac{(2a\lambda_f - (a + d))\left[2a\lambda_f - (a + d)\right]}{\pi} \cos^{-1}\left[\frac{(2a\lambda_f - (a + d))\left[2a\lambda_f - (a + d)\right]}{\pi} \cos^{-1}\left[\frac{(2a\lambda_f - (a + d))\left[2a\lambda_f - (a + d)\right]}{\pi}\right]} \cos^{-1}\left[\frac{(2a\lambda_f - (a + d))\left[2a\lambda_f - (a + d)\right]}{\pi} \cos^{-1}\left[\frac{(2a\lambda_f - (a + d))}{\pi}\right]} \cos^{-1}\left[\frac{(2a\lambda_f - (a + d))}{\pi} \cos^{-1}\left[\frac{(2a\lambda_f - (a + d))}{\pi}\right]} \cos^{-1}\left[\frac{(2a\lambda_f - (a + d))}{\pi}\right]} \cos^{-1}\left[\frac{(2a\lambda_f - (a + d))}{\pi}\right] \cos^{-1}\left[\frac{(2a\lambda_f - (a + d))}{\pi}\right] \cos^{-1}\left[\frac{(2a\lambda_f - (a + d))}{\pi}\right]$
III	$\frac{2\left[2\lambda_{f}(1-2a)-(2-3a-d)\right]}{\pi}\sqrt{(1+a)\left[\lambda_{f}(2+a+d)-\lambda_{f}^{2}(1+a)-(1+d)\right]}$
	,

NACA

TABLE II.- COMPONENT PARTS OF EQUATIONS USED IN CALCULATING CHARACTERISTICS OF DEFLECTED CONTROLS HAVING TAPERED PLAN FORMS - Concluded

(c) Geometric Parameters,

$$S_f = \frac{\beta b_f^2(a-d)(1+\lambda_f)}{2(1-\lambda_f)}$$

$$2M_{a} = \frac{\beta^{2}b_{f}^{3}(a - d)^{2}(1 - \lambda_{f}^{3})}{3(1 - \lambda_{f}^{3})\sqrt{1 + \beta^{2}a^{2}}}$$

Region (fig. 1)	s _L /s _f	$s_L \overline{y}/b_f s_f$	S _L ₹/2M _a
ī	$\frac{2(a-d)}{(1-\lambda_f^2)(1-d^2)}$	$\frac{s_{L}}{s_{f}} \frac{2(a-d)(t_{cp}'-d)}{3(1-\lambda_{f})(1+d^{2})}$	$\frac{g_{L}}{g_{f}} \frac{1 - \lambda_{f}^{2}}{1 - \lambda_{f}^{3}} \frac{\left[(1 + ad) - (a - d)t_{cp}^{1} \right]}{1 + d^{2}}$
Ia	$\frac{\lambda_{\mathbf{f}}(1-d)-(1-a)}{(1'-\lambda_{\mathbf{f}}^2)(1-d)}$	$\frac{s_L}{s_f} \frac{2(a-d)(t_{cp}'-d)}{3(1-\lambda_f)(1+d^2)}$	$\frac{g_L}{g_f} \frac{1 - \lambda_f^2}{1 - \lambda_f^3} \left[(1 + ad) - (a - d)t_{cp}' \right]$
I _b	$\frac{\lambda_{\mathbf{f}}(1-d)-(1-a)}{(1+\lambda_{\mathbf{f}})(a-d)}$	2 ^S L 3 ^S f	$\frac{g_L}{g_T} \frac{1 - \lambda_T^2}{1 - \lambda_T^3} \left[\frac{(1 - \lambda_T)(r_{cp} - a)}{a - d} \right]$
I _c			$\frac{(a-d)[(1+ad)-(a-d)t_{cp}]}{(1-\lambda_{r}^{3})(1-d)(1+d^{2})}$
11	$\frac{2\lambda_{f}^{2}(a-d)}{(1-\lambda_{f}^{2})(1-d^{2})}$	$\frac{s_{L}}{s_{f}} \left[1 - \frac{2\lambda_{f}(a-d)(t_{cp}'+d)}{3(1-\lambda_{f})(1+d^{2})} \right]$	$\frac{s_{L}}{s_{r}} \frac{1 - \lambda_{r}^{2}}{1 - \lambda_{r}^{3}} \frac{\left(1 + ad\right) + (a - d)t_{cp}}{1 + d^{2}}$
· IIa			$\frac{\lambda_{f}^{2} \left[\lambda_{f} (1+a) - (1+d) \right] \left[(1+ad) + (a-d) t_{cp}^{\dagger} \right]}{(1-\lambda_{f}^{3})(1+d)(1+d^{2})}$
· II _b			$\frac{(1-\lambda_{\rm f})^2 \left[\lambda_{\rm f} (1+a) - (1+d)\right] (r_{\rm cp}+a)}{(1-\lambda_{\rm f}^3)(a-d)^2}$
II _c			$\frac{\lambda_{f}^{3}(a-d)[(1+ad)+(a-d)t_{cp}]}{(1-\lambda_{f}^{3})(1+d)(1+d^{2})}$
III	$\frac{\lambda_f^2(a-d)}{(1-\lambda_f^2)(1+d)}$	$\frac{g_{L}}{g_{f}} \left[1 - \frac{2\lambda_{f}(a-d)(t_{cp}^{\prime}+d)}{3(1-\lambda_{f})(1+d^{2})} \right]$	$\frac{\lambda_{f}^{3}(a-d)\left[(1+ad)+(a-d)t_{cp}\right]}{(1-\lambda_{f}^{3})(1+d)(1+d^{2})}$
III _a			$\frac{\lambda_{f}^{2} \left[\lambda_{f} (1+a) - (1+d) \right] \left[(1+ad) + (a-d) t_{cp} \right]}{(1-\lambda_{f}^{3})(1+d)(1+d^{2})}$
III ^p			$\frac{(1-\lambda_f)^2 \left[\lambda_f (1+a) - (1+d) \right] (r_{cp}+a)}{(1-\lambda_f^3)(a-d)^2}$
Two- dimensional	$\frac{\left(\frac{1-a}{1-d}\right)-\lambda_{f}^{2}\left(\frac{1+a}{1+d}\right)}{(1-\lambda_{f}^{2})}$	$ \frac{\left\{ (1+a)(1-\lambda_f) - \frac{(a-d)^3}{(1-\lambda_f)^2(1-d)^2} - \frac{\left[(1+d) - \lambda_f(1+a) \right]^3}{(1-\lambda_f)^2(1+d)^2} \right\}}{3(a-d)(1+\lambda_f)} $	$\frac{\left(\frac{1-a}{1-d}\right)^2 - \lambda_f^3 \left(\frac{1+a}{1+d}\right)^2}{2(1-\lambda_f^3)}$
		3(a - d)(1 + \(\lambda_f\)	

TABLE III.- COMPONENT PARTS OF EQUATIONS USED IN CALCULATING CHARACTERISTICS OF DEFLECTED CONTROLS HAVING UNIAPERED FLAN FORMS

(a) Average Pressure Ratio and Center-Of-Pressure Ray Location.

[Values of P and tcp' (or rcp) for regions II, IIa, IIb, and IIc are obtained by substituting .a for a in equations for regions I, Ia, Ib, and Ic, respectively.]

_		,		,		, .	,			
	Center-of-pressure ray location (tcp' or rcp)	$t_{Cp} = \frac{8a + \frac{(1 + a^2)}{h(1 - a^2)}$	$\frac{t_{\text{cp}}^{+*}}{t_{\text{tp}}^{*}(1+a)\left(1-a^{2}\right)\left[1-(1-a)A_{T}^{-1}\right]} \left\{ \frac{\left(7a^{2}-2a^{4}+1\right)-2A_{T}^{-}\left(1-a^{2}\right)^{2}\left[2a+\left(1+a^{2}\right)A_{T}^{-1}\right]}{\pi} \cos^{-1}\left[\left(1-a^{2}\right)A_{T}^{-}\right] + \left(1-a^{2}\right)A_{T}^{-}\right]} \right\}$		$t_{CP} = \frac{1}{4P(1+a)(1-a^2)} \left[8a + (1+a^2) + \frac{7a^2 - 2a^4 + 1}{\pi} \cos^{-1}a - \frac{a(7-a^2)\sqrt{1-a^2}}{\pi} \right]$	$t_{\rm Cp}' = \frac{5 - 8a - 3a^2}{8(1 + a)}$	$ t_{\mathrm{CP}}^{1*} = \frac{1}{16F^{*}(1+a)[1-(1+a)Ag^{*}]} \left\{ \frac{3-8a-5a^{2}-8Ag^{*}(1+a)^{2}[Ag^{*}(1+a^{2})-2a]}{\pi} \cos^{-1}[2Ag^{*}(1+a)-1] - \frac{1}{1} - \frac{1}{1} \right\} $	$2\left[\frac{5a^{2}+8a-3-2A_{\mathbf{f}}'(1+a)(1+a^{2})}{x}\right]\sqrt{A_{\mathbf{f}}'(1+a)\left[1-A_{\mathbf{f}}'(1+a)\right]}\right\}$	$r_{Cp} = \frac{1}{6p^2 A_f^* \left[\frac{1}{L} - (1 + a) A_f \right]} \left\{ \frac{3(1 - 2aA_f^*)}{\pi} \cos^{-1} \left[\frac{2}{L} A_f^* (1 + a) - 1 \right] - \frac{1}{L} \right\}$	$ \frac{2\left[1 + 2A_{2}'(1 - 2a)\right]}{\pi} \sqrt{A_{2}'(1 + a)\left[\frac{1}{2} - (1 + a)A_{2}'\right]} $
	Average pressure ratio	-40 11 2.	$P^{*} = \frac{1}{(1+a)\left[1-(1-a)Ar^{\frac{3}{2}}\right]} \left\{ \frac{\sqrt{(1-a^2)\left[1+2aAr^{\frac{3}{2}}-(1-a^2)Ar^{\frac{3}{2}}\right]}}{x} \frac{x}{(1-a^2)Ar^{\frac{3}{2}}-a} \frac{(1-a^2)Ar^{\frac{3}{2}}-a^2}{x} \right\}$	$P^* = \frac{1}{1 - (1 - a)A_F}, \left\{ \frac{1}{\pi} \cos^{-1} \left[(1 - a^2)A_F - a \right] + A_F \cdot \left[\frac{1}{1 - a^2} \right] + A_F \cdot \left[\frac{1}{1 - a^2} \right] \right\}$	$P = \frac{1}{(1+a)} \left(1 + \frac{a}{\pi} \cos^{-1} a - \sqrt{\frac{1-a^2}{\pi}} \right)$	대입 명 요	$P^* = \frac{1}{2[1 - (1 + a)A_F]} \left\{ \frac{2\sqrt{A_F'(1 + a)[1 - A_F'(1 + a)]}}{\pi} - \frac{1}{4} \right\}$	$\frac{2h_{\xi^*}(1+a)-1}{\pi}\cos^{-1}\left[2h_{\xi^*}(1+a)-1\right]$	$P^* = \frac{1}{1 - (1 + a)At'} \left\{ \frac{1}{4} \cos^{-1} \left[2A_{1}'(1 + a) - 1 \right] - \right.$	$2 A_T'(1+a)[\underline{1}-(1+a)A_T]$
Region	(fig. 1)	н	I.a.	¹	Ic	H	III.		III	

TABLE III.- COMPONENT PARTS OF EQUATIONS USED IN CALCULATING CHARACTERISTICS OF DEFLECTED CONTROLS HAVING UNTAPERED PLAN FORMS.- Concluded

(b) Geometric Parameters.

$$S_{\mathbf{f}} = \frac{\beta b^2}{A_{\mathbf{f}}!}$$

$$2M_{\mathbf{a}} = \frac{\beta^2 b^3}{A_{\mathbf{f}}!^2 \sqrt{1 + \beta^2 a^2}}$$

Region (fig. 1)	s _L /s _f	S _L ȳ/b _f S _f	S _L x/≥M _a
1	$\frac{1}{A_{\mathbf{f}}'(1-a^2)}$	$\frac{S_L}{S_f} \frac{(1+h_a)}{6A_f'(1-a^2)}$	<u>2</u>
Ia	$\frac{1 - A_{f}'(1 - a)}{2A_{f}'(1 - a)}$	$\frac{s_{L}}{s_{f}} \frac{2(t_{cp'} - a)}{3A_{f'}(1 + a^{2})}.$	<u>e</u> s <u>t</u> 3 s _r
Ib	$\frac{1-A_{\mathbf{f}'}(1-a)}{2}$	2 SL 3 Sr	$\frac{2}{3} \frac{s_L}{s_f} A_f'(r_{cp} - a)$
I _c			3A _f '(1 - a)
11	. Ar'(1 - a ²)	$\frac{s_L}{s_f} \left[1 - \frac{\left(1 - \frac{k_a}{a}\right)}{6A_f'\left(1 - a^2\right)} \right]$	<u>은</u> S <u>L</u> 3 S _f
IIa			$\frac{1 - A_{f}'(1 + a)}{3A_{f}'(1 + a)}$
II _b			$\frac{A_{\mathbf{f}}'(\mathbf{r}_{\mathbf{cp}} + \mathbf{a})\left[\tilde{1} - A_{\mathbf{f}}'(1 + \mathbf{a})\right]}{3}$
. II _e			3A _f '(1 + a)
in	2A _f '(1 + a)	$\frac{S_{L}}{S_{f}} \left[1 - \frac{5}{12A_{f}'(1+a)} \right]$	2 SL 3 Sf
III _a			$\frac{1 - A_{f}'(1 + a)}{3A_{f}'(1 + a)}$
IIIP			$\frac{A_{f}'(r_{cp} + a)[1 - A_{f}'(1 + a)]}{3}$
Two- dimensional	$\frac{A_{f}'(1-a^{2})-1}{A_{f}'(1-a^{2})}$	$\frac{3A_{f}'(1-a)(1-a^{2})\left[A_{f}'(1+a)-1\right]-4_{a}}{6A_{f}'^{2}(1-a^{2})^{2}}$	$\frac{3A_{f}'(1-a^2)-4}{6A_{f}'(1-a^2)}$

NACA

TABLE IV. - EXAMPLE OF NUMERICAL INTEGRATION OF PRESSURES ALONG AN INCLINED SECTION INTERSECTING WING-ROOF MACH CONE

						•							
	٠												(44)
											,	d.	(40)
			0			= 1.50							(4.6)
			1 = 0.20	 	0, 25 0	1 - 82) =							1
	0.50	•	K ₁ = tan η	ָ	, 100	$K_2 = 2$			•				(6.5)
													(0.)
(8)	$\frac{\cos^{-1}(7)}{\pi}$	0,1431	.1967	.2342	.2627	2850	.3024	.3158	.3253	.3313	,3333		(5.5)
(1)	(6) - 1	0,9007	.8151	.7414	£878 .	.6253	.5816	.5470	.5216	.5056	.5000		(0,0
(6)	K ₂ ' (5)	1,9007	1,8151	1,7414	1,6784	1,6253	1,5816	1.5470	1,5216	1.5056	1.5000		3
(2)	1 - g ² × (4)	7882	.8264	.8614	.8937	. 9229	.9484	9696*	.9858	6966	1,0000		3
(4)	[(3)] Z	0.8434	.6944	.5545	.4253	.3086	.2066	,1217	.0567	.0149	0		١
(3)	1 - K ₁ × (1)	96.0	96*	.94	26*	06	88	98.	.84	.82	.80		
(2)	1 - (1)	6.0	æ	.7	9.	5.	4.	w.	2.	ι.	0		
(1)	c	0.1	5.	₆ .	4.	5.	9.	7.	æ	6.	1.0		
	,		,										
													ŀ

ř.

MULTIPLIERS Decided of the control of t	(3) (4)	(2)	(9)	(7)	(8)	(6)	(10)	(11)	(12)	(13)	(14)	(15)	(16)	(11)	(18)
0,5 0,6 0,7 0,8 0,9 1,0 (1) to (10) (11) area 1 0 0 0 0 0,009797 0,		MULTI	PLIERS					Σ(1 - P')×	Incr. Z	Incr. Z	(12) - (13)	(12) -	<u>4</u>	1 (12	12) × (1.2)
0 0	0.3 0.4	0.5	9.0	0.7	0.8	0.9	\neg	(1) to (10) (11)area	(11)mom.	(==)	$K_1 \times (13)$	(12)	u	
0 0	0.037500 -0.004167 0.004167	0	0	0.	0	0	•		767600.0	0,000626	0,009171	0.009672 0.9482 10.0000	0.9482 10.		0,0980
.079167 0 0 0 0 0 0.021650 .046601 .037500 .004167 .004167 0 0 0 .024891 .073482 0 .079167 .054167 .020833 0 0 0 .027430 .100922 0 020633 .079167 .079167 .079167 .029407 .130329 0 .004167 .037500 .004167 .037500 .004167 .037500 .161269 0 0 0 .079167 .079167 .020833 .032083 .183351 0 0 0 .020833 .054167 .079167 .032861	.054167020833	o	0	0	0	0	0	.017154	.026951	.003219	.023732	.026307	.9021 5.	5.0000	1348
.037500 .004167 .004167 0 0 0 .024891 .073492 0 .079167 .054167 .020833 0 0 .027430 .100922 0 .020433 .078167 0 0 0 .029407 .130329 0 .004167 .037500 .004167 .037500 .004167 .030940 .161269 0 0 0 .079167 .079167 .004167 .030940 .161269 0 0 0 .079167 .064167 .030940 .161269 0 0 0 .079167 .020833 .054167 .032861 .236212	.054167 .079167	o	0	0	0	٥	0	,021850	.048601	.008661	.039940	.046869	.8522 3.	3.3333	.1620
.054167 020833 0 0 .027430 .100922 .054167 .079167 0 0 0 .130329 004167 .037500 .004167 .004167 .039407 .130329 0 .075167 .004167 .030940 .161269 0 .079167 .054167 .020833 .132861 0 .0220833 .03467 .032861 .236212	004167 .037500	.037500	004167	.004167	0	0	0	.024891	.073492	.017401	.056091	.070012	.8012 2 .	2,5000	.1837
.054167 .079167 0 0 .029407 .130329 004167 .037500 .037500 004167 .030940 .161269 0 0 .079167 .054167 020833 .032082 .193361 0 0 020833 .054167 .079167 .232821	0 0	.079167	.054167	020833	0	. 0	0	.027430	100922	.029764	,071158	.094969	.7493 2.	2.0000	.2018
004167 .037500 .037500 004167 .004167 .020940 .161269 0 0 .079167 .054167 020633 .032082 .193351 0 0 020833 .054167 .079167 .032861	0 0	020833	.054167	.079167	0	0	0	.029407	.130329	.045951	.084378	.121139	.6965 1.	. 5867	2171
.054167020833 .032082 .193351 .054167 .079167 .032861 .226212	0	_	004167	i .	.037500	004167	.004167	.030940	.161269	.066075	,095194	.148054	.6430 1.	1.4286	2305
.054167 .079167 .032861 .226212	0 . 0	0	0	0	.079167	.054167	020833	.032082	.193351	.090148	.103203	175321	.5887 1.	. 2500	2417
	0 0	0	0	0	020833	.054167	.079167	.032861	.226212	118092	.108120	.202594	.5337 1.	1.1111	2513
0 0 0 0 0 0 0.004167004167 0.037500 0.33266 259478 .14968	0	0	0	0		004167	.037500	.033266	.259478	.149689	.109789	.229540	.4783 1.	1.0000	.2595

0.1 0.1 0.1 0 </th <th></th>											
0.10_11431 0.006667 0		0,000626	.002593	.005442	.008740	.012363	.016187	.020124	.024073	.027944	
0.1 0.1431 0.006687 0		0	0	0	. 0	0	0	0	006667	.060000	.041667
0.1 0.1431 0.006667 0		0	0	0	0	0	0	0	.033333	.060000	008333
0.10.1431 0.006667 0		0	0	0	0	.002083	012500	.055417	.030000	0	0
0.10.1431 0.006667 0		0	. 0	0	0	002083	ı,	.037917	003333	0	0
0.10.1431 0.006667 0 0 0 0 0 0 0 0 0 0 0 0 0 0 0 0 0.00833 0.00683 0		0	0	0	0	.018750	.047500	014583	.003333	. 0	0
0.10.1431 0.006867 0.006867 0 .2 .1967001667 0.006333 .3 .2342 0 0			0.000833	006250	.031667	.018750	0	0	0	0	0
0.10.1431 0.006867 0.006867 0 .2 .1967001667 0.006333 .3 .2342 0 0		0	-:000833	.016250	.021667	002083	0	0	0	0	0
0.10.1431 0.006667 0. 2. 1967001667 . 3. 2242 0 0 0 0. 4. 2827 0 0 0 0. 5. 3024 0 0 0 0 0. 7. 3158 0 0 0 0 0. 8. 3253 0 0 0 0 0. 9. 3333 0 0 0 0.		0	.007500	.023750	008333	.002083	0	0	0	0	0
0.10.1431 0.006667 .2 .1967001667 .3 .2042 0 .4 .2867 0 .5 .2850 0 .6 .3024 0 .7 .3158 0 .8 .3253 0 .8 .3253 0 .9 .3333 0		0.006667	.008333	0	0		0	0	0	0	0
010 8 4 5 8 6 0 0			001667	0	0	0	0	0	0		0
MOMENT S		10.1431	2 .1967	3 .2342	4 .2627	5 ,2850	6 ,3024	7 .3158	8 .3253	9 ,3313	.3333
	}	6	Ľ	<u> </u>	<u> </u>	EN3	MC	M.		<u>. </u>	H

TABLE V. - EXAMPLE OF NUMERICAL INTEGRATION OF PRESSURES ALONG A STREAMMISE SECTION INTERSECTING WING-ROOT MACH CONE

					6 = 0.50	22 = 0.25		$\mathbf{K}_1 = (1 - 2\mathbf{g}^2) = 0.50$		•			do ₁
1 - P	(9)	cos ⁻¹ (5). π	0.1503	.1967	.2250	.2445	.2587	,2696	.2781	2849	2905	.2952	
	(5)	(3) (4)	0.8906	.8151	.7604	7193	.6875	.6623	.6420	.6254	.6116	.6000	
	(4)	(2) - g ²	96.0	1,19	1,44	1,71	2,00	2,31	2,64	66.2	3,36	3.75	
	(3)	${g^2\atop K_1\times (2)}$	0.855	.970	1,095	1,230	1,375	1,530	1,695	0.81	250.2	2,250	
	(2)	$\left[\overline{1} + (1)\right]^2$	1.21	1.44	1.69	1.96	2.25	2.56	2.89	3.24	3.61	4.00	
	(1)	. I	0.1	.2	.3	4.	.5	9.	7.	8.	6.	1.0	

	_	_			_									
	(11)	(01)	(12)×(10)	0.1074	.1414	.1649	.1825	1964	.2077	.2172	.2252	.2322	.2383	CAN
	(16)	1	Īh	10,0000	5.0000	3.3333	2.5000	2.0000	1.6667	1.4286	1.2500	1,1111	1.0000	NACA
,	(12)	(12)	(F)	0.9409	.8951	.8514	.8121	.7766	.7444	.7150	.6879	.6630	.6400	
	(14)	(0+)	(12) + (13)	0.011413	.031594	.058111	278980.	,126415	,167405	.212625	.261914	.315160	.372283	
	(13)	Incr.Σ	(11)mom.	0,000674	003315	.008635	.016886	.028237	.042788	909090	.081733	.106200	134031	
	(13)	Σ(1 - P')× Incr. Σ	(11)area	0,010739	.028279	.049476	.072988	921860	124617	.152019	,180181	096802	.238252	
	(11)	Σ(1 - P')×	(1) to (10)	0.010739	.017540	,021197	.023510	.025192	.026439	.027402	.028162	,028779	.029292	
	(10)		1.0	0	0	0	0	0	0	.004167	020833	.079167	.037500	
	(6)		6.0	0	0	0	0	0	0	004167	.054167	.054167	004167	
	(8)		8.0	0	0	0	0	0	0	.037500	.079167	020833	.004167	
	(2)		0.7	0,	0	0	.004167	020833	.079167	.037500	0	0	0	
	(9)	MULTIPLIERS	9.0	0	0	0	.037500004167	.054167	.054167	004167	0	0	0	
	(2)	MULT	0.5	0	0	0	.037500	.079167	020833	.004167	0	0	0	•
	(4)		9.0	7 0.004167	020833	.079167	.037500	ó	0	0	0	0	0	
	(8)		0.3	9	.054167	.054167	004167	0	0	0	0	0	0	
	(2)		0.2	0.037500 -0.0041	.079167	020833	.004167	0	0	0	0	0	0	
	(1)		r' = 0.1	0.130786	.1967045340	0	0	0	0.	0	0	0	0	
		,	7 - 1	0,1503	.1967	.2250	.2445	.2587	,2696	.2781	.2849	.2905	2362	
	,		H	3	?	e.	*	3	9.	۲.	.8	.9	1.0	
		L					A 3	IAA						

						,				
	0,000674	,002641	0028300*	,008251	.011351	.014551	.017818	.021127	.024467	.027831
	0	0	0	0	0	0	0	.033333006667	.060000	008333 .041667
	0	0	0	0	0	. 0	0	.033333	.060000	008333
	0	0	0	0	.002083	012500	.055417	.030000	0	0
,	0	0		0	002083	.032500	.037917	003333		0
	. 0	0	0	0	.018750002083002083	.047500	014583	.003333	0	
	0	.000833	006250	.031667	.018750		0		0	0
	0	000833	.016250006250	.021667	002083002083	0	0		0	0
	0	.007500000833	.023750	-,008333	.002083	0	0	0	0	0
	0.006667	.1967001667 .008333	0	0	0	0	0	0	0	0
	.10,1503 0.006667	001667	0	0	0	0	0	0	0	0
	2,1503	.1987	,2250	.2445	,2587	,2696	.2781	,2849	.2905	.2952
	=	~	8	4.	S.	8.	2.	8	6.	ó

TABLE V. - EXAMPLE OF NUMERICAL INTEGRATION OF PRESSURES ALONG A STREAMMISE SECTION INTERSECTING WING-ROOF MACH CONE - Concluded

					(Y () 8	, , , , , , , , , , , , , , , , , , ,	$g^4 = 0.25$	$K_{-} = (1 - 3\sigma^2) = 0.50$					(19) (18)
1 - P'.	(9)	cos-1(5)	0.3173	.3245	-3277	.3295	.3305	.3312	.3316	.3319	.3322		(01)
	(2)	(3) (4)	0.5429 (.5238	.5152	.5105	.5077	.5059	.5046	.5038	.5031		(0)
	(\$)	(2) - g ²	8.75	15.75	24.75	35.75	48.75	63.75	80.75	99.75	120.75		ξ,
	(3)	$\begin{matrix} g^2 + \\ K_1 \times (2) \end{matrix}$	4.750	8.250	12.750	18,250	24.750	32,250	40.750	50.250	60,750		(9)
	(2)	[i + (1)] ²	9.00	16.00	25.00	36.00	49.00	64.00	81,00	100.00	121.00		ú
	Ξ	ı,	2.0	3:0	4.0	5.0	6.0	7.0	8.0	9.0	10.0		5
													[

i	* Д	(16)	$(11) \times (15)$	()		0.2731	,2893	.2985	.3045	.3088	.3119	.3144	.3163	.3179	Z V
		(12)	₩İ	т.		0.50000	.33333	.25000	.20000	.16667	14286	.12500	.11111	.10000	NACA
	tcp	(14)	Ξ	(13)		0.4770	.3822	.3193	.2745	.2408	2146	.1936	.1763	.1619	
		(13)	(11) (13)	(44) 7 (44)		1.14513 0.4770 0.50000	2,27096	3,73927	5,54726	7.69261	10,17412	12,99117	16.14285	19,62937	
		(12)	$\Sigma(1-P') \times \text{Incr.} \Sigma \text{Incr.} \Sigma$	(10) mom.	0.13403	.59893	1.40307	2,54540	4,02470	5.84000	7,99066	10,47630	13,29623	16.45070 19.62937	
		(11)	Incr. Z	(10)area	0,23825	.54620	.86789	1,19387	1,52256	1.85261	33085 2,18346	33141 2.51487	2,84662	.33205 3,17867	
		(10)	Σ(1 - P')×	(1) to (9)	0.23825 0.23825	.30795	.32169	,32598	.32869	.33005			.33175		
		(6)		10.0	0	0	0	ó	0	0	.041667	208333	.791667	.375000	
		(8)		9.0	0				٥	0	.375000041667	.541667	.541667	.041667041667	
		(1)		8.0	0	0	0	0			.375000	.791667	208333	.041667	
		(9)	MULTIPLIERS	7.0	0	0	0	.041667	208333	.791667	.375000	•	0	0	
		(2)	MULTI	8.0	0	0	0	375000041667	.541667	.541667	.041667041687	0	. 0	0	
		€		5.0	0	0	0	375000	.791667	-,208333	.041667	0	0	0	
		(8)		4.0	1667 0.041667	667208333	.791667	1	1		0	0	0	0	
		(2)		3.0		.541667	.541667	- 041887				-	0	0	
		Ξ		r'= 2.0	١.	791667	208333	041667	10		_				
				1 - P	0.2952	.3173	3245	2577	+-	3305	3312	3316	3319	.3322	
			•	.	12	2.0	ြင္တ	5	9 0	0.0	5	2		0	

0.13403	.46490	.80414	1,14233	1,47930	1,81530	.291667 2.15066	2,48564	2,81993	3,15447
0	0	0	0	0 .	0	.291667	-1.666667 2.48564	7.125000 2.81993	3.750000
0	0	0	0	0	0	291667	6.333333 4.333333	-1.875000 4.875000	416667416667 3.750000 3.15447
0	0	0	0	0	. 0	2.625000	6.333333	-1.875000	.416667
0	0	0.	.166667	-1.041667	4.750000	2.625000 2.625000291667	. 0	0	0
0	0	0	1,500000166667	3.958333 2.708333 -1.041667	3.250000	291667291667	0	۰	0
0	0	. 0	Ι' `	3.958333	-1.250000 3.250000	.291667	0	0	0
0.041667	1.083333416667	1.825000 2.375000	166667 1.500000	0	٥	٥	0	0	0
-0.041667	1.083333	1.625000	166667		0	0	0	0	0
3.2952 0.375000 -0.041667 0.041667	1.583333	.3245625000	.166667	0	٥	0	٥	0	
0.2952	.3173	.3245	.3277	.3295	.3305	.3312	.3316	.3319	.3322
1.0	5.0	3.0	4. 0.	50 50 50	WOI	M 0.	8.0 0.0	9.0	0.0

TABLE VI.- EXAMPLE OF NUMERICAL INTEGRATION OF PRESSURES ALONG AN INCLINED SECTION INTERSECTING WING-TIP MACH CONE

											*0.	ı
	g = 0.50	v tan n = 0.20	9 - 14	$K_2 = (2 + g + K_1) = 2.70$	$K_0 = (g - K_1) = 0.30$		$K_4 = (1 + g) = \frac{1.50}{1.50}$		•		***	d'
(1)	$\frac{\cos^{-1}(\theta)}{\pi}$	0.1844	.2677	.3372	.4016	.4646	.5290	.5978	.6755	.7729	1.0000	
(9)	(3)	0.8367	.6667	.4894	.3044	.1111	0909	-,3023	-,5238	7561	-1.0000	
(5)	K4 - (4)	1.47	1,44	1.41	1.38	1.35	1.32	1.29	1.26	1.23	1.20	
(4)	K3 × (1)	0.08	8.	80.	.12	.15	:18	.21	.24	.27	08'	
ව	$K_2 \times (1) K_4 - (2) K_3 \times (1)$	1.23	96"	69.	.42	. 15 ,	12	39	99'-	93	-1.20	
(3)	$K_2 \times (1)$	0.27	72.	.81	1.08	1,35	1.62	1,89	2.16	2,43	2.70	
Ξ	g	0.1	2.	8:	4.	č.	9.	7.	8.	6.	1.0	
			,									

		3	<u>(S</u>	8	4	(2)	(9)	3	(8)	(8)	(10)	(11)	(12)	(13)	(14)	(15)	(10)	. (11)	(18)
<u> </u>		-				MULTIPLIERS	LIERS					$\sum (1 - P) \times$	Incr.		12) - (13)	(12) +	(14)	-1	(12)~(17)
=	7 - 1	n = 0.1	0.2	0.3	9.0	0.5	9.0	0.7	8.0	6.0	1.0	(1) to (10)	(11)area		(1)	$K_1 \times (13)$	(12)	٥	//a
0	10.1844	0.113301	0.037500	0.037500 -0.004167	0.004167	0	0	0	0	0	0	0.012065	0.012065	0.000766	0.011299 0.012218	0.012218	0.92481	0.000.0	0.1207
Ľ	2 . 2677	7032975	791670.	.054167	020833	0	0	0	0	0	0	.022757	.034822	.004243	.030579	.035671	.8573	5,0000	.1741
نــا	3372	3 0	020833	.054167	.079167	0	0	. 0	0	0	0	,030324	,065146	.011891	.053255	.067524	. 7887.	3.3333	.2172
	4 .4016	3 0	.004167	04167004167	.037500	.041667	008333	0	0	0	0	.036946	.102092	.024885	,077207	.107069	.7211	2.5000	.2552
<u></u>	5 .4646	3 0	0	•	0-	.066667	799990.	0	0	0	. 0	.043299	.145391	.044426	.100965	.154276	.6544	2,0000	.2908
Ľ	6 .5290	0	0	0	·	008333	.041667	.037500	004167	.004167	0	.049669	.195060	.071793	.123267	.209419	.5886	1.6667	.3251
Ľ	7 .5978	3 0	•	0	·	0	0	.079167	.054167	020833 0	0	.056311	.251371	.108464	.142907	.273064	.5233	1.4286	.3591
ت	6755	2 0	0	0	0	0	0	020833	.054167	.079167	.079167038494	.063546	.314917	.156182	.158735	.346153	.4586	1.2500	.3936
	.9 .7729	0 €	0	0	0		0	.004167	004167	.037500	.121105	.072212	.387129	.217654	.189475	.430660	.3935	1.1111	.4301
Ŀ	0 1.0000	0 0	0	•	•	•	٥	0	0	0	.017389	.084988	.472117	.298483	.173634	.531814	.3265	1.0000	.4721
ĺ																			

							. •		
0.000766	.003477	007648	012994	019541	.027367	086671	.047718	.061472	080829
0.0	9.	0.	0.	0.	0.	0' (-	. 108995	0.17389
0	0	0	0	0	.002200	014583	.063334030795	.033750	0
0	0	0	0	0	002500	.037917	.043334	003750	۰
0	0	0	0	0	.022500	.055417	016667	.003750	0
0	0	.001250	008333	.039583	.022500	0	0	0	0
0	0	001250	.021667	.027083	002500	0	0	0	0
0	- 0	.011250	.031667	010416	.002200	0	0	0	0
0.005417 -0.002083	.015833	.011250	0	0	0	0	0	0	0
0.005417	.010833	001250	0	0	0	0	0	0	0
0.007917	004167	.001250	0	0	0	0	0.	0	0
0.1 0.1844	2677	.3372	4016	5 .4646	5290	8763.	3 .6755	6247. €	01.0000
	.2	ω.	_ <u>.</u>	Ę.	١.	7. N	۳	3:	ᆵ

-.008333 .041667 .040661

.6 .3590 **0** .4016 **0**

MOMENT

1.0 .4359 0

TABLE VII, - EXAMPLE OF NUMERICAL INTEGRATION OF PRESSURES ALONG A STREAMMISE

	-
CONE	
MACH	
WING-TIP	
INTERSECTING	
SECTION	

1 - P'

											₺,	(11)	(12) × (16)		0.1088	.1512	.1830	.2087	.2307	.2500	2672	.2828	.2970	.3101	\\\\\\\\\\\\\\\\\\\\\\\\\\\\\\\\\\\\\\	Į.						•			
												(18)	-1	-#	0.000	5.0000	3.3333	2.5000	2.0000	1.6667	1.4286	1.2500	1.1111	1.0000	NACA)									
											t _{cp}	(12)	(12)	(14)	-1	.8928	.8482	.8077	- 1	.7378	.7073	.6793	.6535	.6298	ν										
		•					$K_1 = (1 + g) = \frac{1.50}{1.50}$					(14)	(12) + (13)		\neg	.033879		.103360	$\overline{}$.203333	.264481	.333052	.409058	492507											
					g = 0.50		$K_1 = (1$					(13)		-,1	╗	.003631	.009828	.019872	.034245	.053322	.077422	.106818	.141748	,182409			•								
												(12)		- 0	0.010880 0.010880 0.000701	.030248	.054887	.083488	,115366	.150011	.187059	.226234	.267310	.310098											
				_		-						(11)	∑(1 - p') ×	(1) to (10) (11)area	0.010880	.019368	.024639	.028601	.031878	.034645	.037048	.039175	.041076	.042788		0.000701	.002930	.006195	.010046	.014373	.019077	.024100	.029396	.034930	.040861
(2)	$\frac{\cos^{-1}(4)}{\pi}$	0,1609	.2229	.2677	.3035	.3333	.3590	.3815	.4016	.4196	.4359	(10)		1.0	0	0	0	0	0	0	.004167	020833	.079167	.037500		0	0	0	0	0				.060000	041667
(4)	ଞ୍ଚାତ	0.8750	.7647	,6667	.5789	2000	.4286	.3636	.3043	.2500	2000	(8)		6.0	. 0	0	0	0	0	0	004167	.054167	.054167	004167		0	0	0	0	0	٥	0	.033333	.080000	- 008333
(3)	K ₁ + (1)	1.60	1.70	1,80	1.90	2,00	2,10	2.20	2,30	2,40	2.50	(8)		8.0	0	0	0	0	0	0	.037500	.079167	-,020833	.004167	,	0	0	0	0	.002083		.055417	.030000	0	_
(2)	K ₁ - (1)	1.40	1.30	1.20	1.10	1.00	6.	.80	0.4	9.	.20	3		0.7	0	0	0	.004167	020833	.079167	.037500	0	0	0.		0	0	0	0	002083	.032500	.037917	003333	0	_
(3)		0.1	2.	٤.	4.	ē.	9.	7.	8.	6.	1.0	(9)	MULTIPLIERS	9.0	0	0	0	004167	.054167	.054167	004167	0	0	. 0		0	0	0	0	.018750	.047500	014583	.003333	0	
									-			(5)	MULTI	0.5	0	0	0	.037500	.079167	020833	.004167	0	0	0		0	.000833	006250	.031667	.018750	. 0	0	0	0	•
												(4)		9.4	0.004167	-,020833	.079167	.037500	0	0	0	0	0	٥		0	000833	.016250	.021667	002083	0	0	0	٥	v
													ľ	0.3	04167	.054167	.054167	004167									.007500	.023750	008333	.002083					
												(6)		L	0.0	٩	Ľ.	ŀ	0	0	0	0	0	0		9			٠.	_	0	٥	٥	_	_
												(2)		0.2	0.037500 -0.004167	.079167	020833	├	├	0		0	0	0		0.006667	.008333	. 0	0 (0	0 0	0 0	0	0	,
														-	0.113301 0.037500 -0.0	032975 .079167	┖	├	0 0		0	0 0	0 0	0 0		\dashv	001667 .008333		0 0		0 0	0 0	0 0	0 . 0	
				•								(2)		0.2		.079167	020833	.3035 0 .004167	.3333 0 0	0	0	0	0	0		0.006667	.008333	0	0	0	0	0	0 0	0	

TABLE VII.- EXAMPLE OF NUMERICAL INTEGRACION OF PRESSURES ALONG A STREAMMISE SECTION INTERSECTING WING-TIP MACH CONE - Concluded

.:				1		9	•	$\mathbf{K_1} = (1 + \mathbf{g}) = 1.50$			· 1
1 - P	(2)	cos-1(4)	0.5456	.6082	.6502	.6810	.7048	.7240	.7398	.7533	.7647
	(4)	(<u>3)</u> (3)	-0.1429	-,3333	4545	-,5385	6000	-,6471	6842	7143	7391
	(3)	K ₁ + (1)	3.50	4.50	2.50	6,50	7.50	8.50	9.50	10,50	11.50
	(2)	K ₁ - (1)	-0.50	-1.50	-2,50	-3*20	-4.50	-5.50	-6.50	-7.50	-8.50
	(1)	,,	2.0	3.0	4.0	5.0	6.0	7.0	8.0	9.0	10.0

		(1)	(2)	(3)	(4)	(2)	(9)	(2)	8	(6)	(10)	(11)	(12)	(13)	(14)	(12)	(16)
-,	, ,					MULTI	MULTIPLIERS				Σ(1 - P)x Incr. Σ Incr. Σ	Incr. Σ	Incr. Z	(11) . (19)	(11)	1	(11) (15)
-	4 - 1	r'= 2.0	3.0	4.0	5.0	.0.9	7.0	8.0	9.0	10.0	(1) to (9)	(10)area	(10)area (10)mom.	(71) + (17)	(13)	Ī	(e1) × (11)
1.0	0.4359	0.375000	-0.041667	0.041667	0	0	0	0	. 0	0		0.31010	0.18241				
2.0	.5456	.791667	.541667	208333	0	0	0	0	0	0	0,49578	.80588	.93798	1.74386 0.4621 0.50000	0.4621	0.0003	0,4029
3.0		6082208333	.541667	.791667	0	0	0	0	0	0	.57972	1.38560	2,39084	3,77644	.3669	.33333	.4619
4.0	.6502	.041667	041667	.375000	.375000	041667	.041667	0	0	0	.62981	2,01541	4,60144	6,61685	.3046	.25000	.5039
5.0	.6810	0	0	0	.791667	.541667	208333	0		0	.66628	66628 2,68169	7,60253	10,28422	.2608	.20000	.5363
6.0	.7048	0	0	0	208333	.541667	.791667	0	0	0	.69338	3,37507	11,41797	14.79304	.2282	.16667	.5625
7.0	.7240	0	0	0	.041667	041667	.375000	.375000	.375000041667	.041667	Ι.	71468 4,08975	16,06526	20,15501	.2029	.14286	.5843
8.0	.7398 0	0	0	0	0	0	0	791667	.541667	208333	.73210	4,82185	21,55735	26,37920	.1828	.12500	.6027
9.0	.7533	0	0	0	0	٥	0	208333	.541667	.791667	ľ	74673 5.56858	27,90570	33,47428	.1664	11111.	.6187
10.0	.7647	0	0	0	0	.0	0	.041667	.041667041667	.375000	1	.75917 6.32775	35.11875 41.44650	41,44650	.1527	.10000	.6328

AREA

0.18241	.75557	1,45286	2,21060	3,00109	3.81544	.291667 4.64729	5,49209	6.34835	7.21305
0	0	0	0	0	0	.291667	-1.666667 5,49209	7.125000 6.34835	3.750000
0	0	0	0	0	0	291667	6.333333 4.333333	4.875000	416667416667 3.750000 7.21305
0	0	0	0	0	0	2.625000291667	6.333333	-1.875000 4.875000	.416667
0	0	0	.166667	-1.041667	-1.250000 3.250000 4.750000	291667291667 2.625000	0	•	0
0	. 0	0	166667	3.958333 2.708333 -1.041667	3.250000	-,291667	0	0	0
0	0	0	166667 1.500000 1.500000166667	3.958333	-1.250000	.291667	0	0	0
0.041667	1.083333416667	1.625000 2.375000 0	1.500000	0	0	0	0	0	0
-0.041667	1.083333		166667	0	, 0	0	0	0	0
1.0 0.4359 0.375000 -0.041667 0.041667 0	1.583333	.6082625000	.166667	0	0	0	0	0	0
0.4359	.5456		.6502	.6810	.7048	.7240	.7398	.7533	.7647
1.0	2.0	3.0	4.0	5.0	6.0	7.0	8.0	9.0	10.0
			T	VE!	NO.	V			

TABLE VIII.- CONTROL-SURFACE CHARACTERISTICS NOT INCLUDED IN FIGURES

(a) Tapered Controls.

8.	đ	λρ	$1/\lambda_{ m f}$		ling-tip		Inboard controls	a	đ	$\lambda_{\mathbf{f}}$		ling-tip		Inboard controls
				βC _{1δ} '	βCL _δ '	βC _{mδ} '	βC _{lδ} '				βC _{Zδ} '	βCL _δ '	βС т _б '	βC ₁₈ '
-0.95	{-0.80 90		0.95 .95	-0.2678 2778					-0.80 80 80	o .20 .49	0680	0.1164 .1139 .1053		0661
80	60 85 95 95	0.95 0 .20			0.2236	 -0.2751 2751	,	0.20	80 95 95 95	.60	2086 7606 9921	.0846 .2236 .2184		2106 7606 9917
	95 95 95 95	.60 .80		1076 2325 6156 -2.3878	.2218 .2184 .2074 .1399	2587	-0.2311 6306 -3.0759	.40	80 80 80 95	.20 .40	1369 9058	.1164 .1128 .1002	2133 2118 2004 -1.5823	1422
- 60	80 95 95	.20 .40		3349 1796 2420 3773	.2236 .2226 .2192	4925 4888	1796 2413 3762		95 95	.20 .40	-1.1787 -1.6605	.2161 .1896	-1.5715 -1.4907 0927	-1.1793 -1.7248
	95 95			6670 -1.4710	.2105	10 99	-1.6150	.60		.40 0 .20	0819 1148	.1164 .1109	0845 2392 2366	0819 1106
40	80 80 80 95	\$88€ 888€		 1747 3249	.2236	1038 0868 7109	1776 3249		80 95 95 95	.20 .40	-1.0510 -1.3642 -1.8747	.2123 .1737	2180 -1.8001 -1.7818 -1.6453	-1.0510 -1.3669 -1.9945
	95 95 95 95	.60		4299 6446 -1.0835 -2.1657	.2219 .2159 .2009 .1526	7097 7008 6705 5574	4289 6459 -1.1206 -2.5993		.75 .60 60 60	. 20			0990 0861	.1405 .2229
20	888888 	20 29 60 80 80		1106 2618 4701		1328 1241 0926 9287	 1050 2945 4701	.80	80 80 80	0 20 49 0 20	0991 1397 2121 -1.1963 -1.5463	.2236	2650 2602	
	95 95 95	.60		6175 9086 -1.4756	.2210 .2119 .1890		6165 9156 -1.5654		.90	•95 •95				.4493 .4359 0132
0	80 80 80 95 95 95	5 8 8 5 8 5 8 5 8 5 8 5 8 5 8 5 8 5 8 5		1617 6153 8050 -1.1680	.2236 .2199 .2067	1610 1566 1416 -1.1466 -1.1426 -1.1129	1578 6153 8041 -1.1853	.95	60 80 80 80 95 95	.49 0.29 0.20	-1.6659	.2236	0703 2844 2721 1812 -2.1813 -2.0869	0411 1121 1496 2302 -1.3052 -1.6952
	95			-1.8326		-1.0110			95		-1.7604		-1.3815	

NACA

TABLE VIII. - CONTROL-SURFACE CHARACTERISTICS NOT

INCLUDED IN FIGURES - Concluded

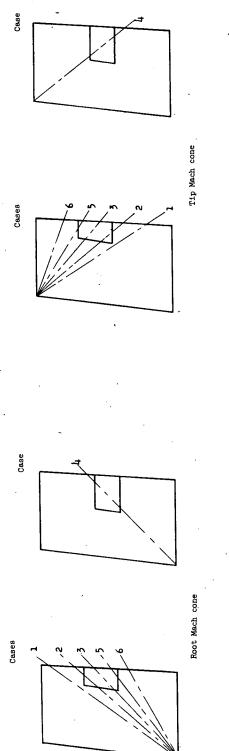
(b) Untapered Controls.

a	A _f '		Wing-tip controls	•	Inboard controls	a	A _f '		Wing-tip controls		Inboard controls
		βC l _δ '	βC _L δ'	βC _m δ'	βC 1 _{δ.} '		*	βC ₁₈ '	βC _L δ'	βC _{mδ} ,	βC ₁₈ '
-0.95	0.8 2.0 4.0 6.0 8.0 10.0	-1.1421 4242 1619 0720 0265 ,0009	0.1878 .2093 .2164 .2188 .2200 .2207	-0.0879 1022 1070 1086 1094 1099	-1.2498 4328 1605 0698 0244 .0029	0	6.0 8.0 10.0	0.0320 .0327 .0331 .0125 .0272	0.0669 .0676 .0681 .0446	-0.0330 0335 0337 0182 0282	0.0349 .0349 .0349 .0449
80	8 2.0 4.0 6.0 8.0 10.0	1061 0117 .0225 .0342 .0402	.0962 .1083 .1123 .1137 .1143 .1147	0447 0528 0555 0564 0568 0571	1034 .0065 .0259 .0366 .0420 .0452	.20	4.0 6.0 8.0 10.0	.0317 .0330 .0337 .0341 .0128 .0289	.0657 .0675 .0685 .0690	0319 0332 0338 0341 0158 0275	.0375 .0369 .0366 .0364 .0608
60	8 2.0 4.0 6.0 8.0 10.0	0190 .0173 .0302 .0346 .0369 .0382	.0702 .0804 .0839 .0850 .0856	0323 0391 0414 0421 0425 0427	0075 .0232 .0334 .0368 .0385 .0395	.40	4.0 6.0 8.0 10.0	.0341 .0356 .0362 .0366	.0682 .0709 .0722 .0730	0328 0346 0354 0360	.0426 .0411 .0404 .0399 .0948
40	8 2.0 4.0 6.0 8.0	.0005 .0226 .0302 .0328 .0341	.0592 .0694 .0728 .0739	0268 0336 0358 0366 0370	.0154 .0290 .0336 .0351 .0358	.60	4.0 6.0 8.0 10.0	.0384 .0406 .0415 .0420	.0736 .0782 .0804 .0818	0345 0376 0391 0400	.0539 .0505 .0487 .0477
20	10.0 8 2.0 4.0 6.0 8.0 10.0	.0349 .0078 .0245 .0301 .0319 .0328 .0334	.0748 .0527 .0638 .0675 .0688 .0694 .0698	0372 0233 0307 0332 0340 0344 0346	.0363 .0263 .0319 .0338 .0344 .0347	.80	2.0 4.0 6.0 8.0 10.0	.0296 .0441 .0508 .0535 .0549 0048	.0589 .0804 .0921 .0982 .1018	0222 0343 0420 0461 0485 .0032 0157	.1228 .0905 .0797 .0743 .0711 1.4733 .6564
٥	8 2.0 4.0	.0110 .0258 .0305	.0482 .0611 .0655	0205 0291 0320	.0349 .0349 .0349	.95	4.0 6.0 8.0 10.0	.0440 .0564 .0657 .0732	.0809 .0998 .1145 .1269	0282 0368 0438 0501	.3841 .2933 .2479 .2207

NACA

TABLE IX. - COMPUTING FORM FOR Cha.

(a) Dimensions and Preliminary Computing Form.



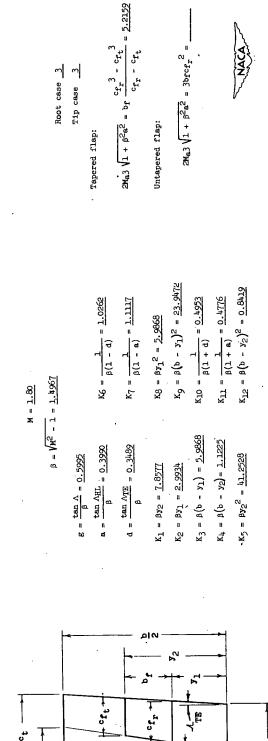


TABLE IX. COMPUTING FORM FOR Che - Concluded

	(9)	(5) × (4) × (5)	o	,o	-10.0832	0	9.5908	0	9.3941	-7.2778	0	0	4487	0	.3260	0	.5820	3025	∑ (6) = 1.7358
	(5)	T _{SS}	(1) × K ₅ =	(1) × K ₅ =	$(1) \times c_{\mathbf{r}}^{2} K_{6} = 15.65 \mu T$	$(1) \times c_{\mathbf{r}}^{2} K_{6} =$	$(1) \times x_{\rm r}^2 K_7 = 9.7865$	$(1) \times x_{\tau}^{-2}K_{\tau} = $	$(1) \times K_8 = 6.1017$	(1) × Kg = 4.4021	(1) × K ₉ =	(1) × K ₉ =	$(1) \times c_t^2 K_{10} = \frac{1.6833}{1.6833}$	(1) × c _t ² K ₁₀ =	$(1) \times x_t^2 K_{11} = 0.6616$	(1) × x _t ² K ₁₁ =	$(1) \times K_{12} = 0.9185$	$(1) \times K_{12} = 0.4722$	
of triangular segments of conical-flow region.	(†)	3x1/1 + B2a2	$\frac{\mathcal{K}_1(1-at_{op})}{t_{op}}-3x_r=$	3x _T - 2K1(1 - atop) =	$\frac{2c_{x}(1-at_{CD})}{(1-at_{CD})}-3x_{x}=\frac{-2.4965}{}$	$3x_T - \frac{2c_T(1 - at_{CP})}{(1 - at_{CP})} = \frac{1}{(1 - at_{CP})}$	<u>0000'†</u> = [₹] x		$3x_r - \frac{2K_2(1 - at_{cp})}{t_{cp}} = \frac{5.107h}{1}$	$\frac{2K_2(1-at_{cp})}{t_{cp}}$ - $3x_r = -5.9688$	$\frac{2K_3(1 + at_{cp})}{t_{cp}} - 3x_t = \frac{2K_3(1 + at_{cp})}{t_{cp}}$	3xt - 2K3(1 + atcp) =	$\frac{2c_{t}(1 + at_{cp})}{(1 + at_{cp})} - 3x_{t} = -0.9520$	$3x_{t} - \frac{2c_{t}(1 + at_{cp})}{(1 + at_{cp})} = \frac{1}{2c_{t}(1 + at_{cp})}$	xt = 2,2000	-x ² =	$3x_{\rm t} - \frac{2K_{\rm h}(1 + at_{\rm cp})}{t_{\rm cp}} = \frac{2.0179}{}$	$\frac{2K_{\rm h}(1+at_{\rm cp})}{t_{\rm cp}}$ - $3x_{\rm t}$ = -2.7150	<u> -0.0194</u>
lar ве <i>д</i> же	(3)	¢c⊅		-	0.736				3.645	1727			799				609.	.751	
f triangu	(2)	*4			0.258		.245		300	772:			.280		-22t	-	416.	.236	$\sum_{2M_{8}3 1/1+ p^{2}_{8}2}$
(b) Form for summing (PS _L x̄) o	(1)	Enter curve at following value of n or r'	$\frac{c_{L}}{K_{1}}$ - (1 - d) =	$\frac{x_T}{K_1} - (1 - a) = $	$1 - \frac{K_2}{c_r}(1 - d) = 0.6102$	$1 - \frac{K_1}{c_T}(1 - d) =$	$1 - \frac{K_2}{x_r}(1 - a) = \frac{0.5502}{1}$	$1 - \frac{K_1}{x_r}(1 - a) =$	$\frac{c_{\rm r}}{K_2}$ - (1 - d) = $\frac{1.0192}{1.0192}$	$\frac{\kappa_{\rm T}}{K_2}$ - (1 - a) = $\frac{0.7353}{0.7353}$	$\frac{c_t}{K_3} - (1 + d) =$	$\frac{x_{t}}{K_{3}} - (1 + a) = \dots$	$1 - \frac{K_{l_t}(1+\alpha)}{c_t} = \frac{0.4494}{}$	$1 - \frac{K_3(1+d)}{c_t} = \frac{1}{1 - \frac{1}{2}}$	$1 - \frac{K_{l_1}(1+a)}{x_t} = 0.2862$	$1 - \frac{K_3(1+a)}{x_t} = \frac{1}{x_t}$	$\frac{c_{t}}{K_{t_{t}}}$ - (1 + d) = $\frac{1.1010}{1.1010}$	$\frac{x_{t}}{K_{tt}} = (1 + a) = \frac{0.5609}{}$	$C_{h_{\alpha}} = \frac{-2}{57.38 \sqrt{1 - g_{\gamma}^2}} \left(1 - \frac{1}{3}\right)$
(a)	Column (6) = 0	for cases in table IX(a)	3, 5, 6	2, 3, 4, 5, 6	9	3, 5, 6	4, 5, 6	2, 3, 4, 5, 6	9	h, 5, 6	3, 5, 6	2, 3, 4, 5, 6	9	3, 5, 6	4, 5, 6	2, 3, 4, 5, 6	9	4, 5, 6	
		Region	٦	, a	۳,	#	5	9	7	8		2	т	न	• 5	9	7	80	
	Figures for	determining columns (2) and (3)	QQ S S S S S	D 10 10 10 10 10 10 10 10 10 10 10 10 10	Pigure 7	8 d	Figure 7	tan n = a	· · · · · · · · · · · · · · · · · · ·	o pingra	,	07 07 07 07 07 07 07 07 07 07 07 07 07 0	Figure 9	tan 1 = d	Figure 9	tan n = a		OT STORT	
						мась сов	Root							Nach con	q1T				

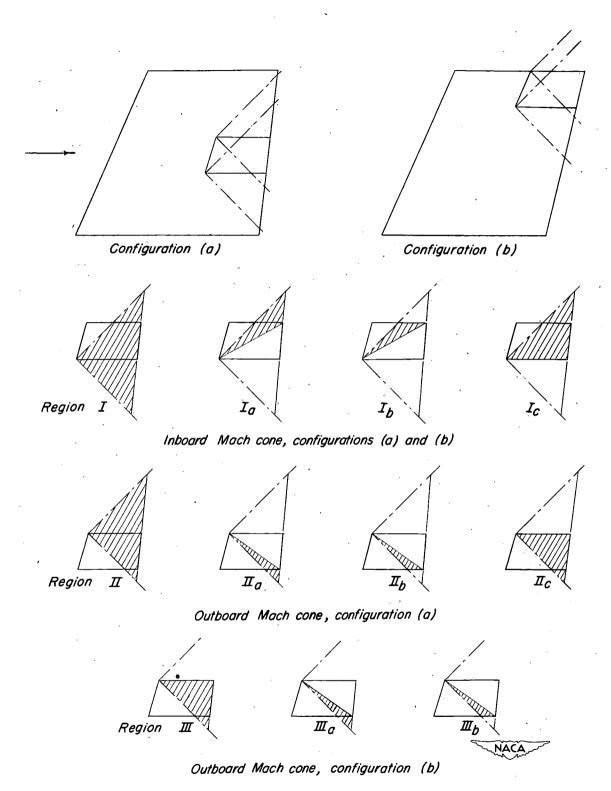
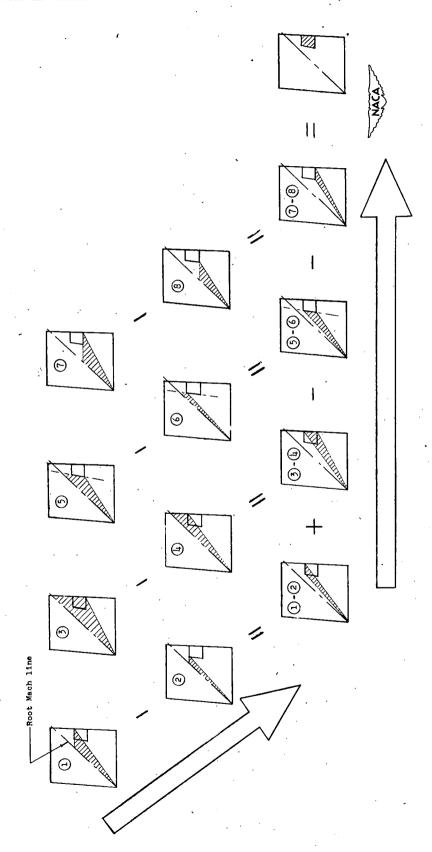
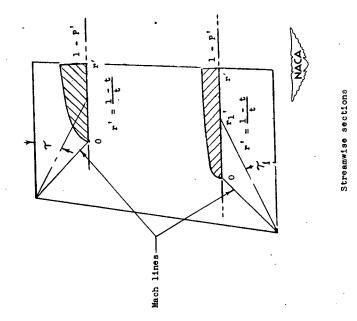
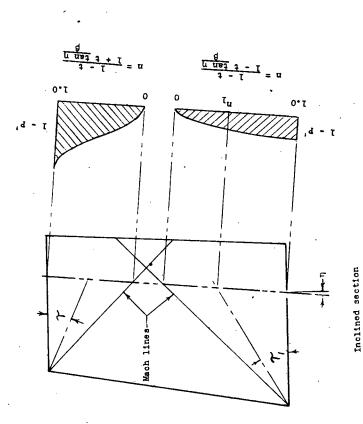


Figure 1.- Conical-flow regions for which solutions were obtained in the calculation of deflected control characteristics.



 $\left({{
m PS}_{
m L}}{
m z}
ight)^*$ of conical-flow regions for calculation of $\mathbb{C}_{h_{\mathbf{G}}}$. (Encircled numbers correspond to regions as Figure 2.- Procedure followed in summing designated in computing form for Ch_{α} .





segments of the wing-root and wing-tip Mach cones are obtained for use in determining $\text{Ch}_{\alpha}.$ Figure 3.- Illustration of method by which P* and

NACA TN 2221

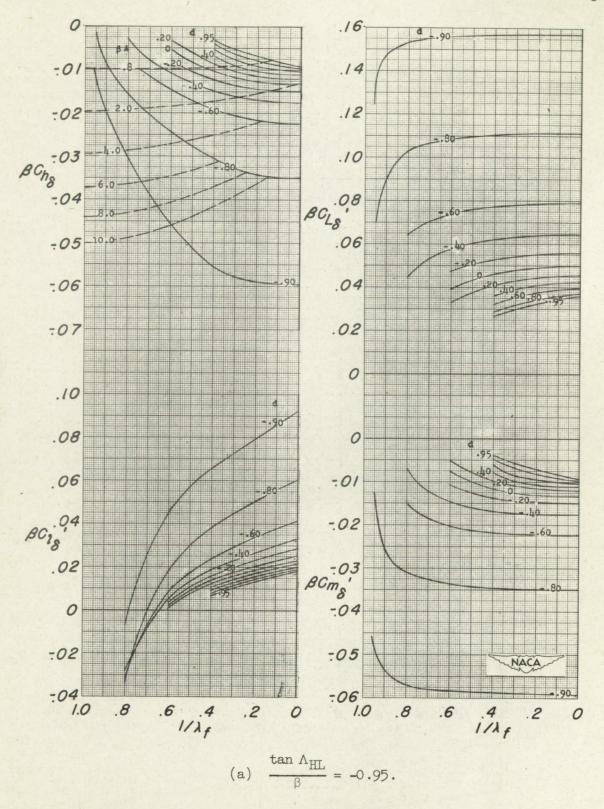


Figure 4.- Characteristics of deflected trailing-edge controls located at the wing tip. Results for values of $\lambda_f = \frac{1-a}{1-d}$ have been obtained by use of an approximation and should be used with caution.

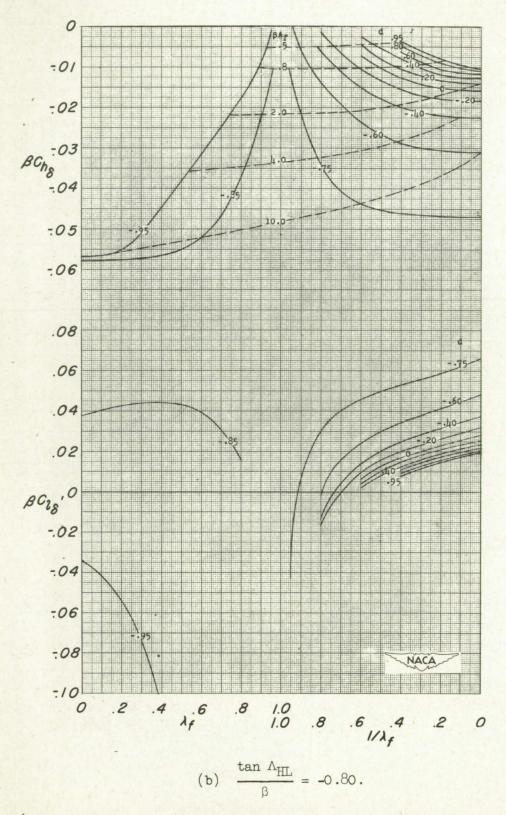
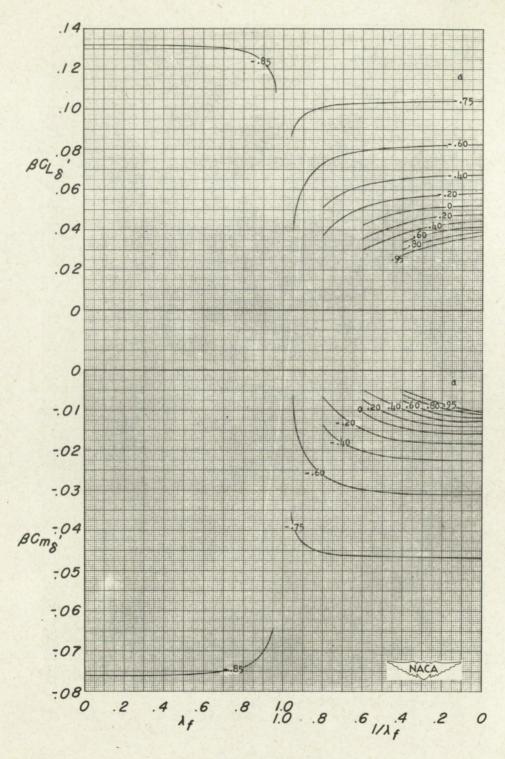


Figure 4.- Continued.



(b) Concluded.

Figure 4.- Continued.

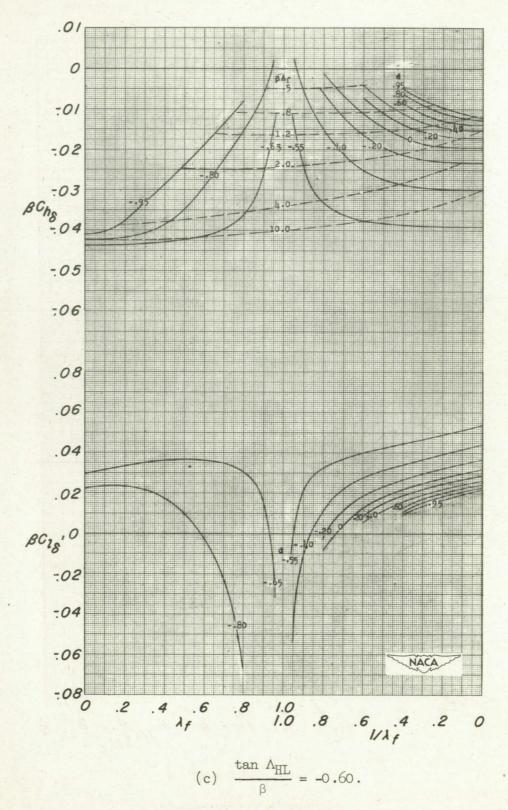
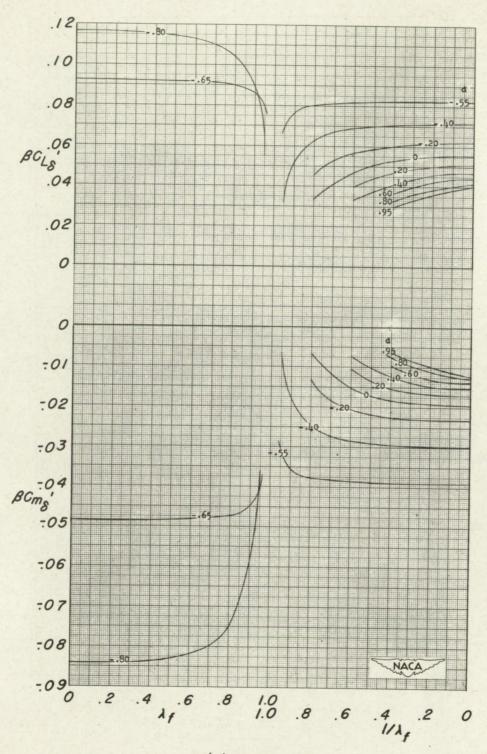
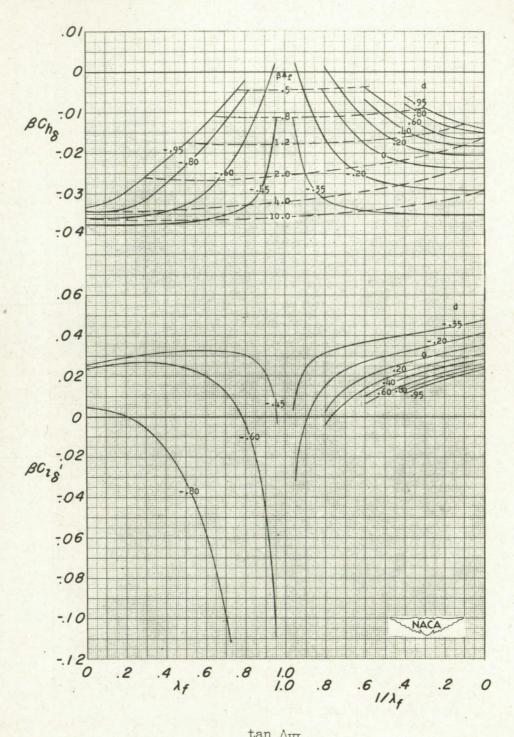


Figure 4. - Continued.



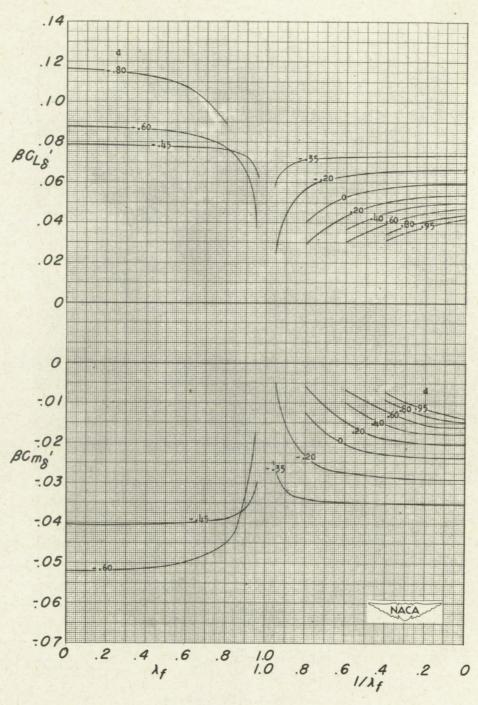
(c) Concluded.

Figure 4.- Continued.



(d) $\frac{\tan \Lambda_{\text{HL}}}{\beta} = -0.40$.

Figure 4.- Continued.



(d) Concluded.

Figure 4. - Continued.

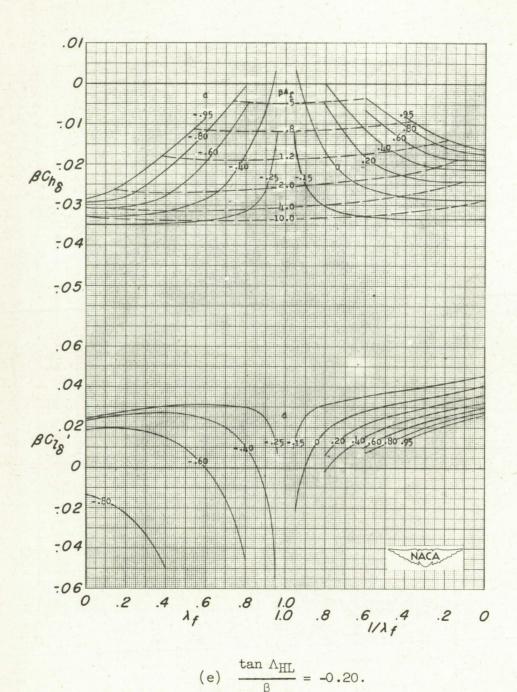
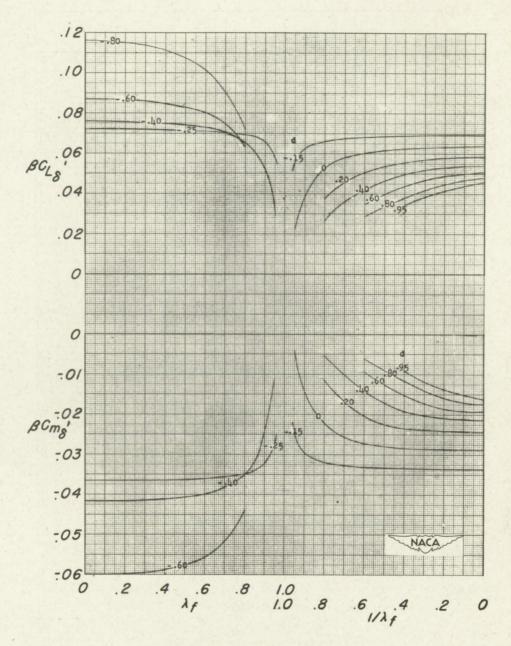


Figure 4. - Continued.



(e) Concluded.

Figure 4.- Continued.

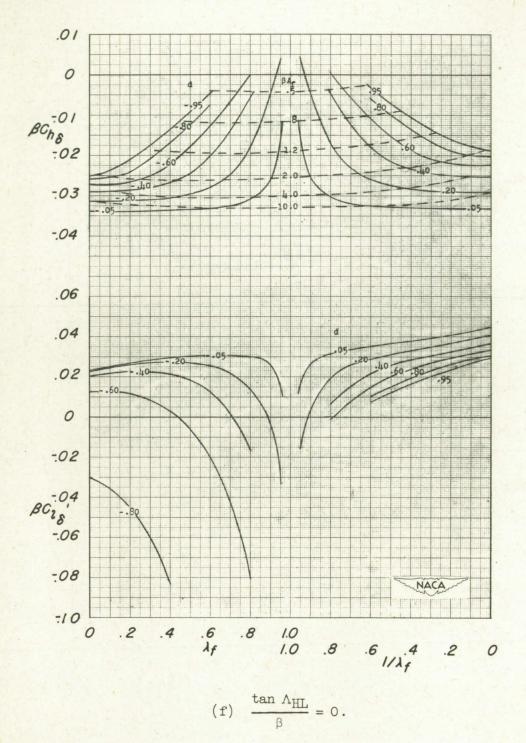
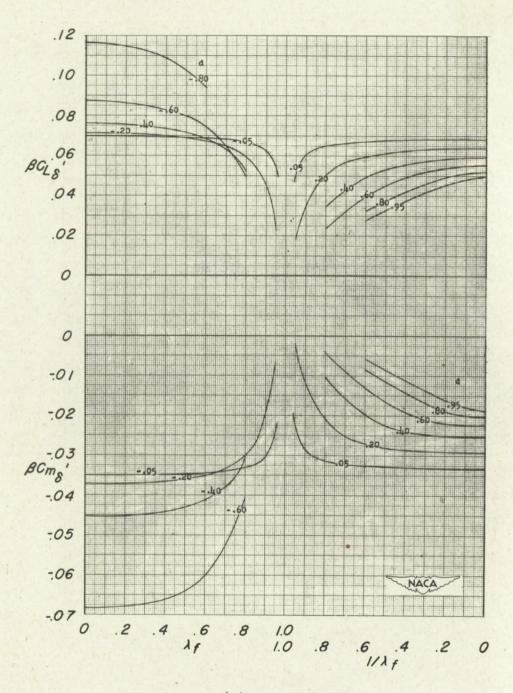


Figure 4. - Continued.



(f) Concluded.

Figure 4.- Continued.

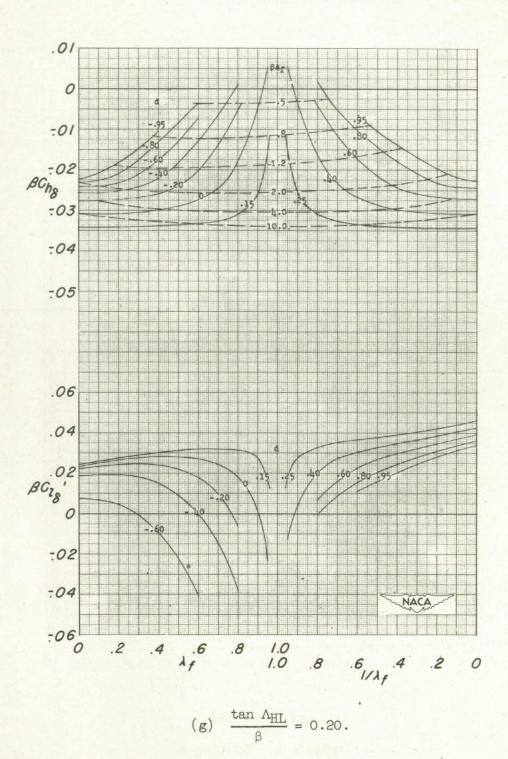
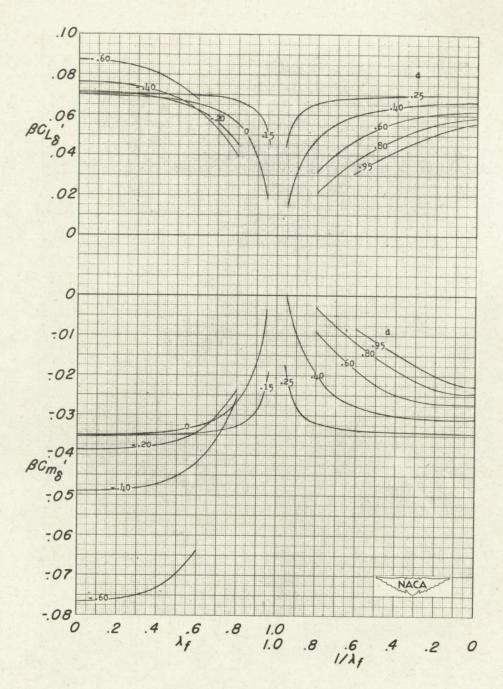


Figure 4. - Continued.



(g) Concluded.

Figure 4.- Continued.

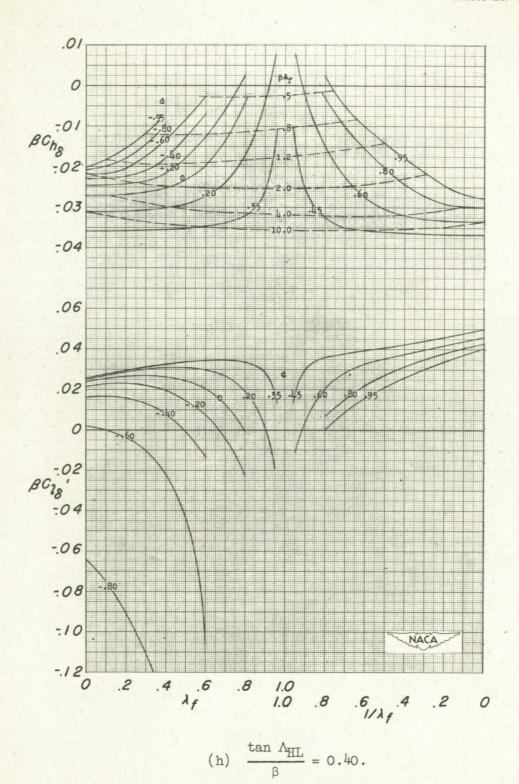
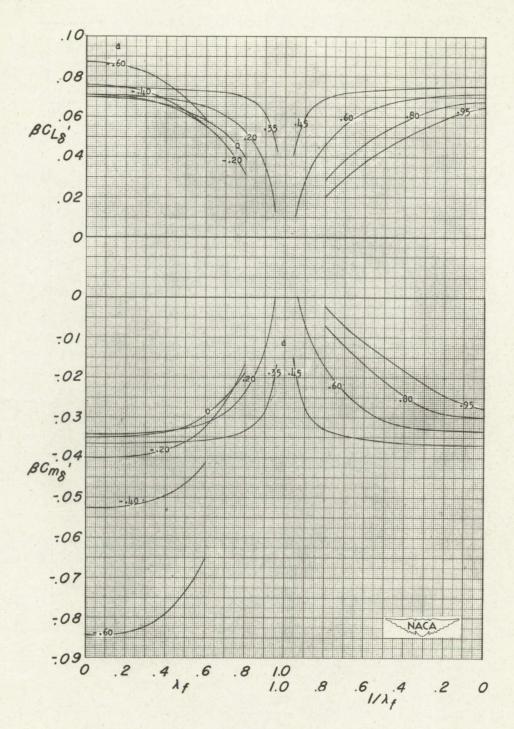
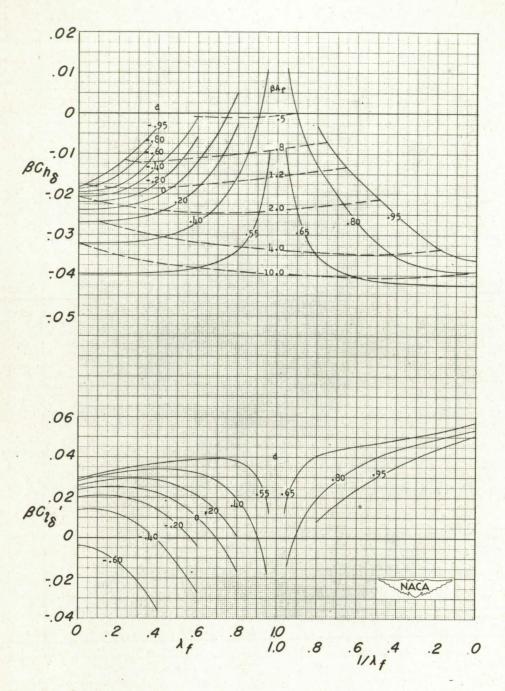


Figure 4.- Continued.



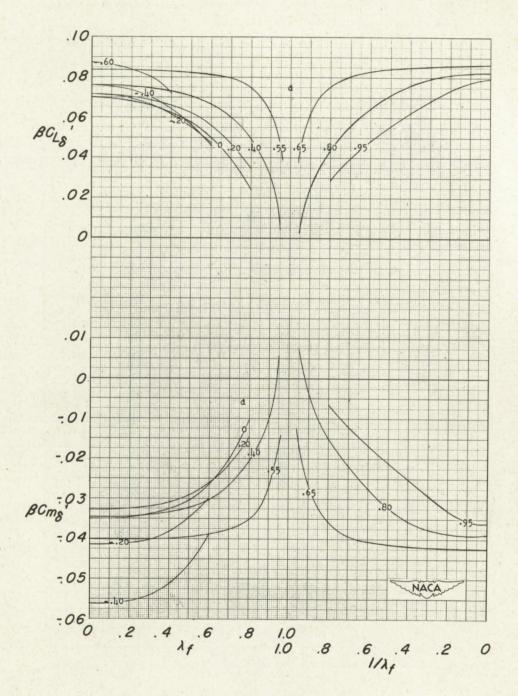
(h) Concluded.

Figure 4.- Continued.



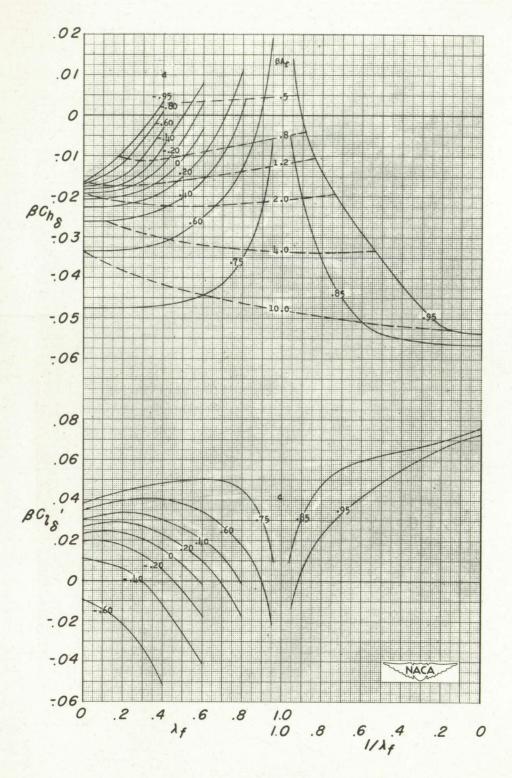
(i) $\frac{\tan \Lambda_{HL}}{\beta} = 0.60$.

Figure 4.- Continued.



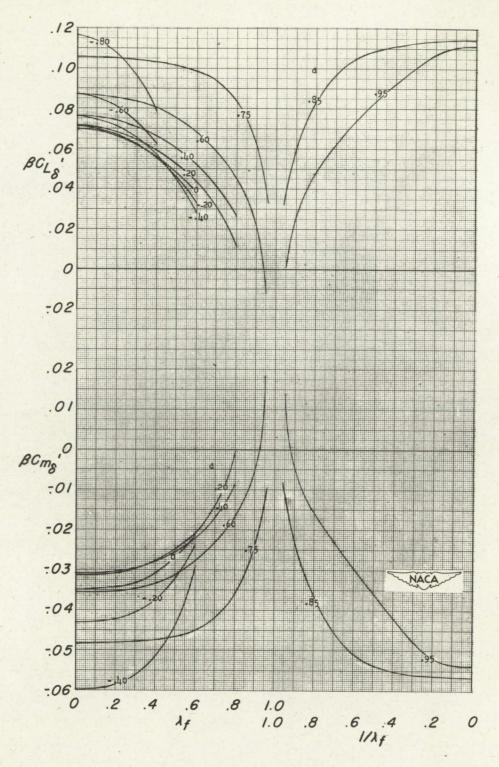
(i) Concluded.

Figure 4.- Continued.



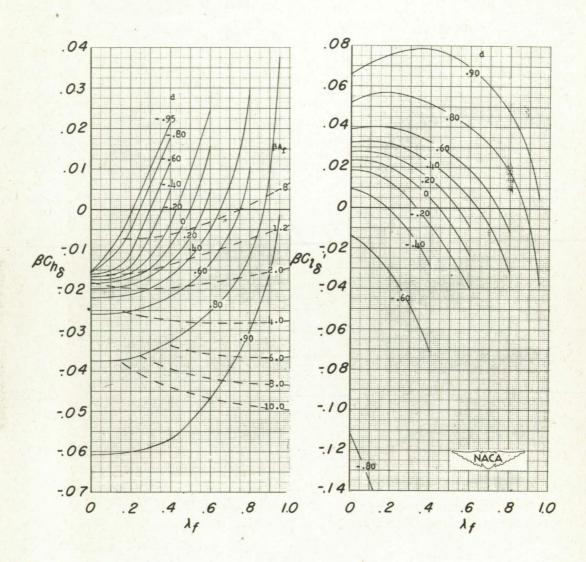
(j)
$$\frac{\tan \Lambda_{\text{HL}}}{\beta} = 0.80.$$

Figure 4.- Continued.



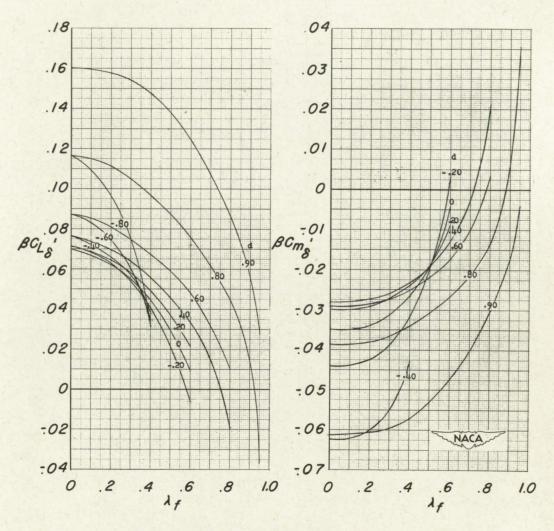
(j) Concluded.

Figure 4.- Continued.



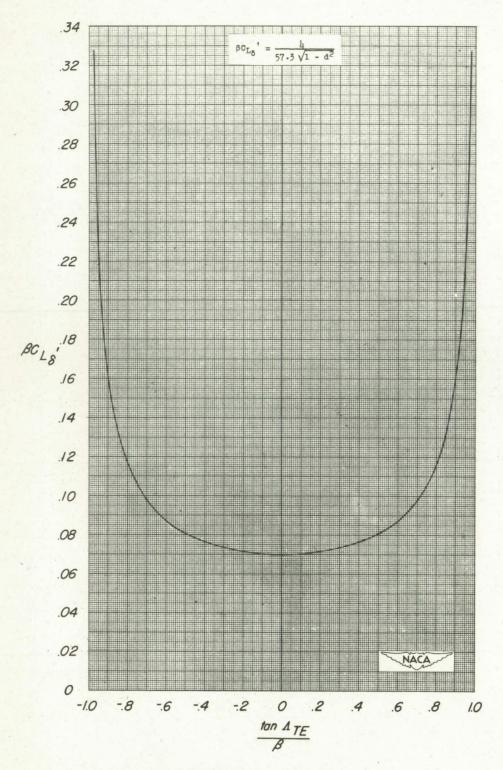
(k)
$$\frac{\tan \Lambda_{\text{HL}}}{\beta} = 0.95$$
.

Figure 4.- Continued.



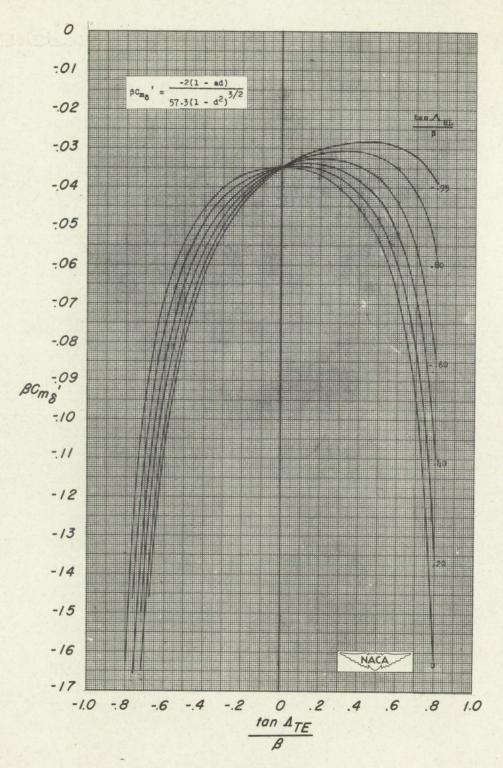
(k) Concluded.

Figure 4.- Concluded.



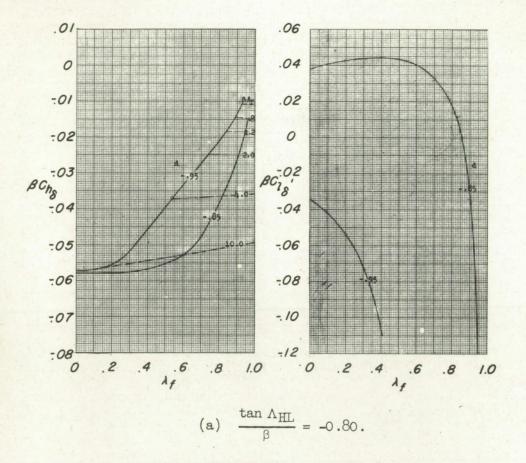
(a) Lift coefficient.

Figure 5.- Lift and pitching-moment parameters for deflected trailing-edge flaps located inboard from wing tip.



(b) Pitching-moment coefficient.

Figure 5.- Concluded.



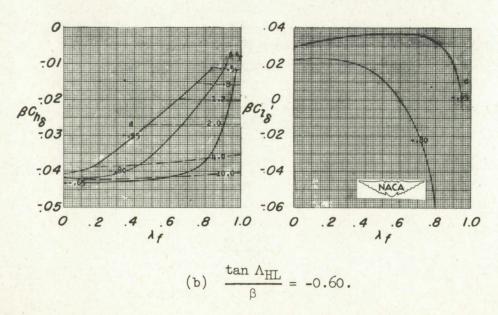
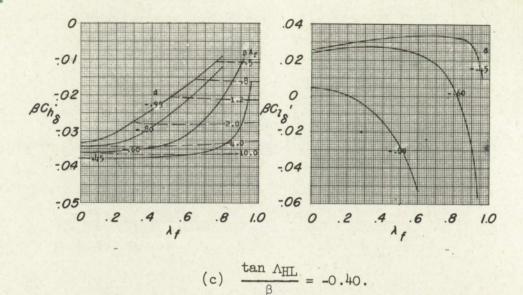


Figure 6.- Hinge-moment and rolling-moment parameters for control surfaces located inboard from wing tip.



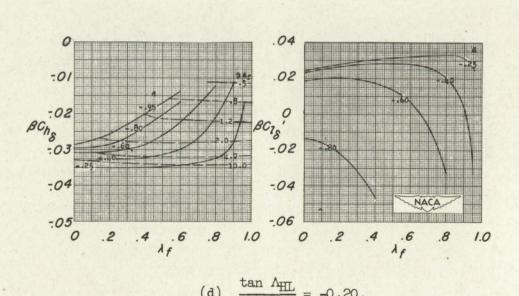
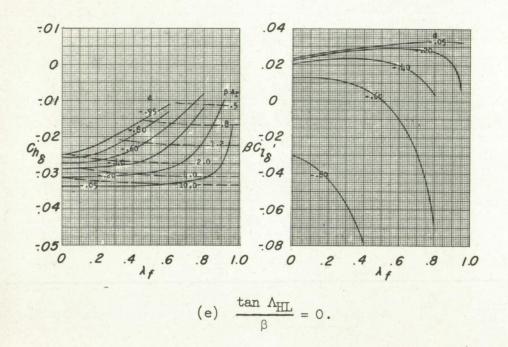
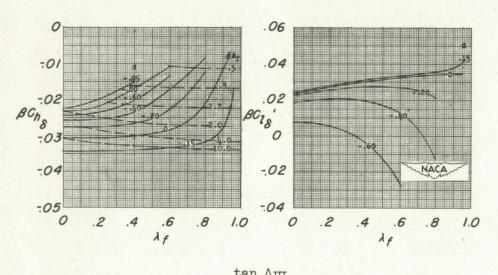


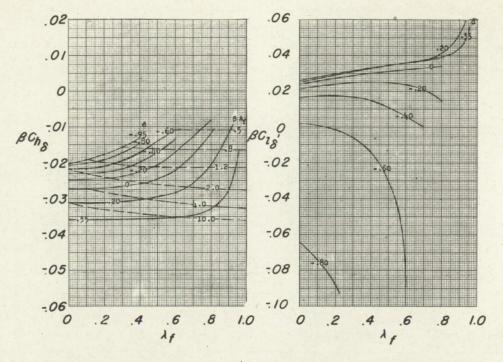
Figure 6.- Continued.



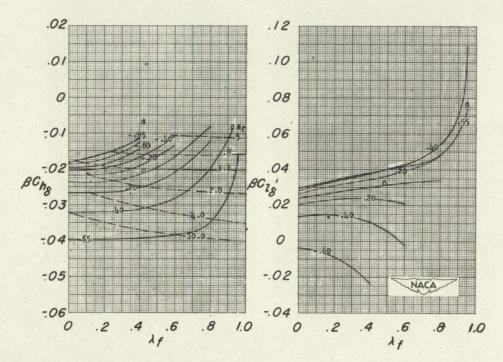


(f) $\frac{\tan \Lambda_{HL}}{\beta} = 0.20$.

Figure 6.- Continued.

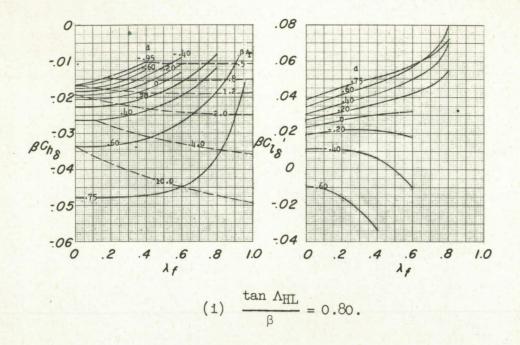


(g)
$$\frac{\tan \Lambda_{\text{HL}}}{\beta} = 0.40$$
.



(h)
$$\frac{\tan \Lambda_{HL}}{\beta} = 0.60$$
.

Figure 6.- Continued.



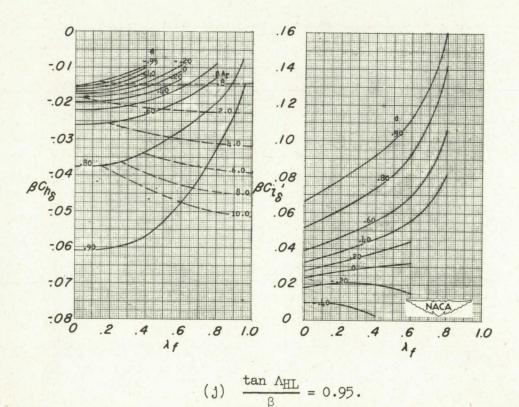


Figure 6.- Concluded.

(j)

NACA TN 2221

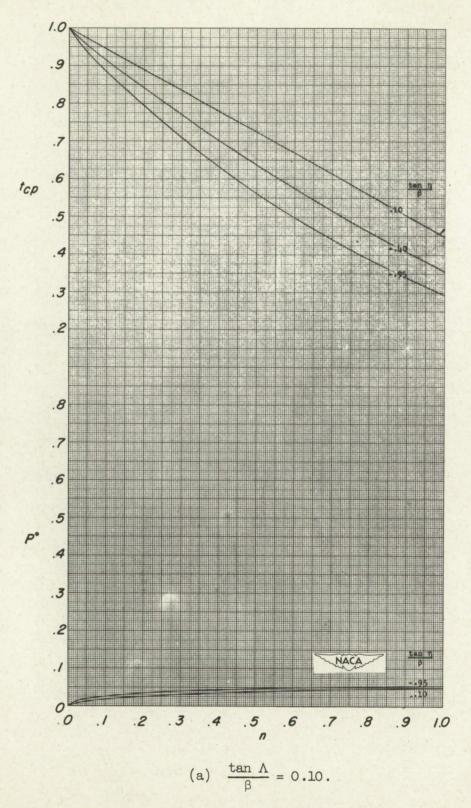


Figure 7.- Loading distribution along inclined sections intersecting the wing-root Mach cone.

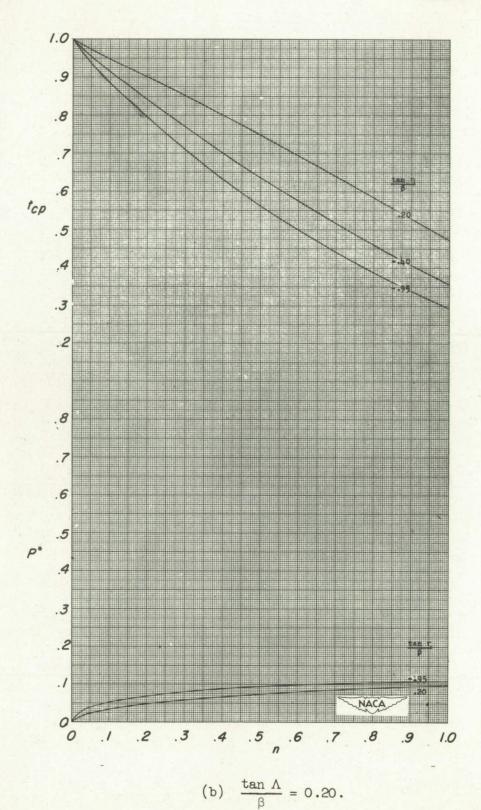


Figure 7.- Continued.

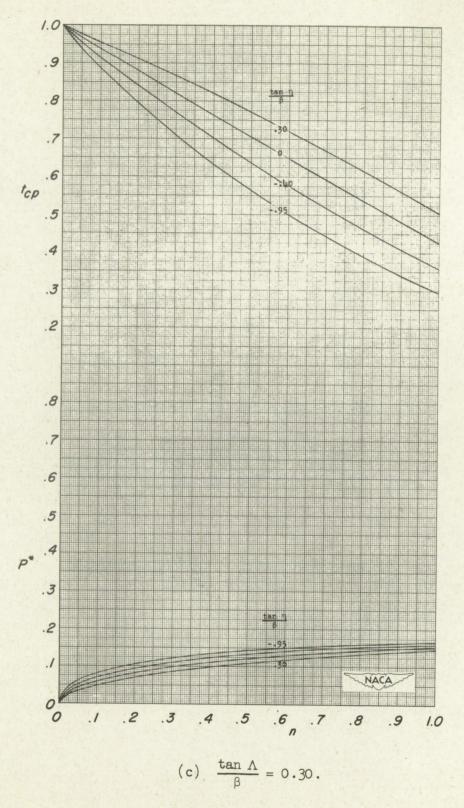


Figure 7.- Continued.

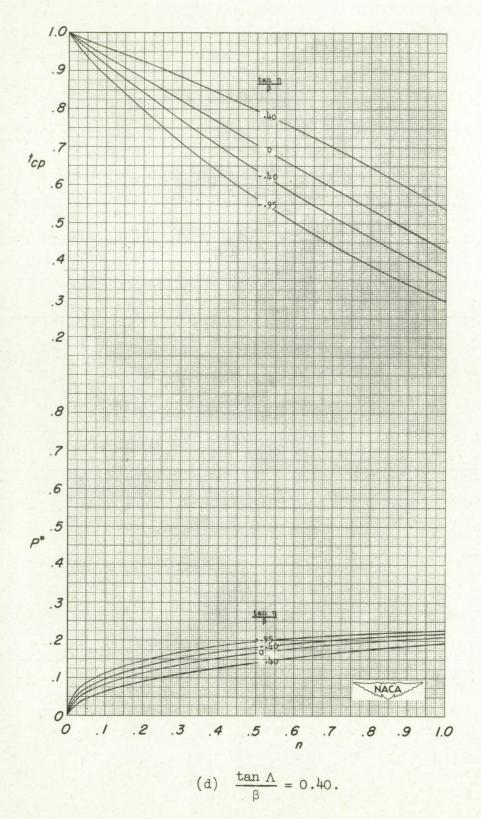


Figure 7.- Continued.

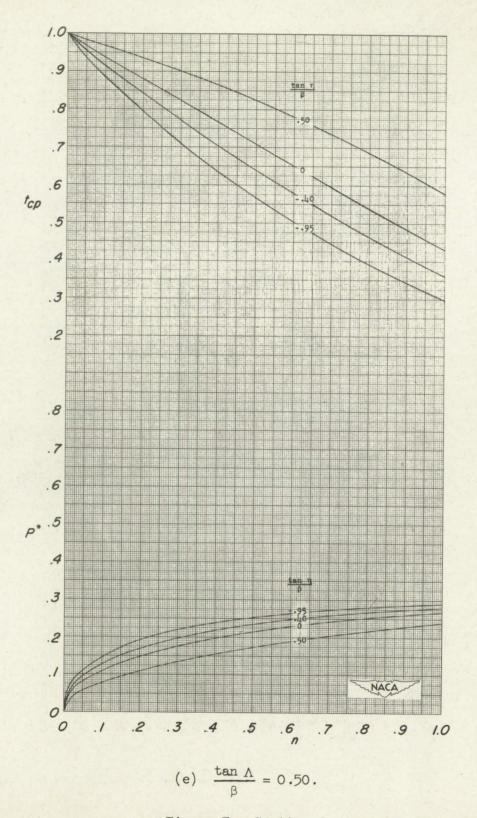


Figure 7.- Continued.

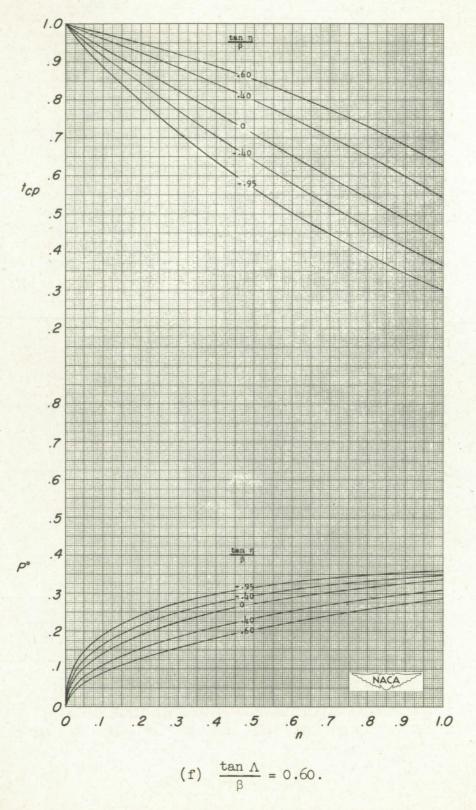


Figure 7.- Continued.

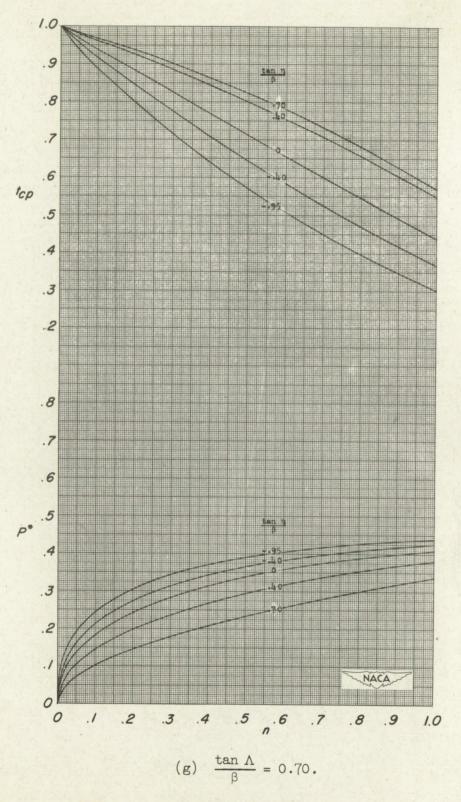


Figure 7.- Continued.

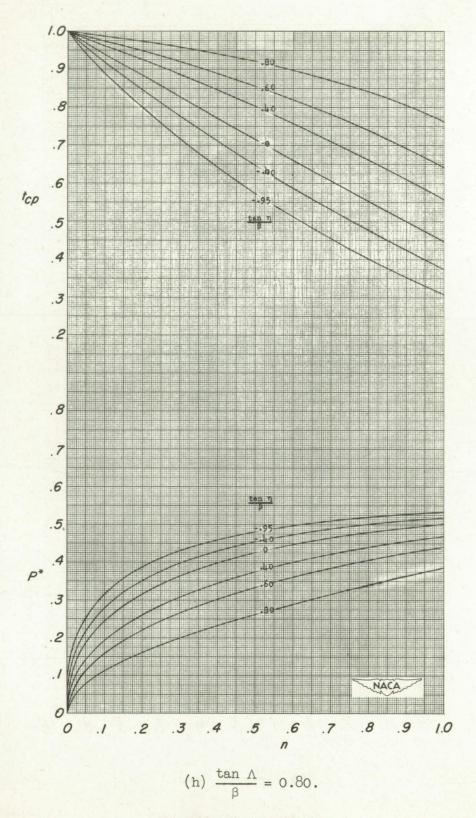


Figure 7 .- Continued.

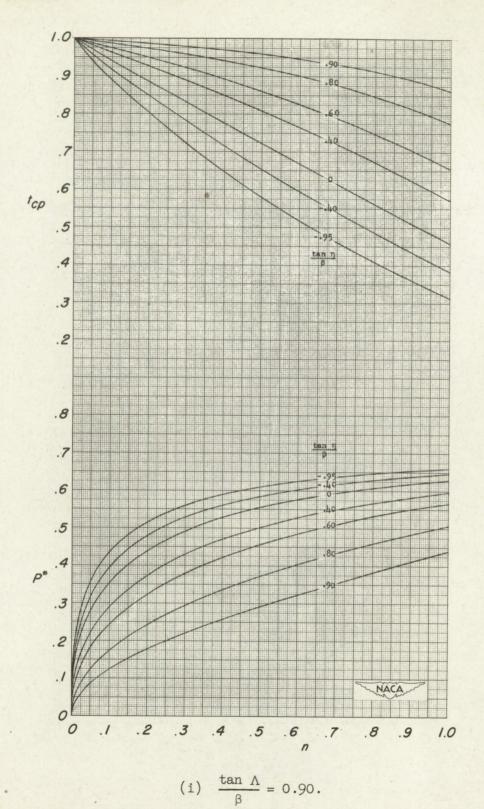


Figure 7.- Continued.

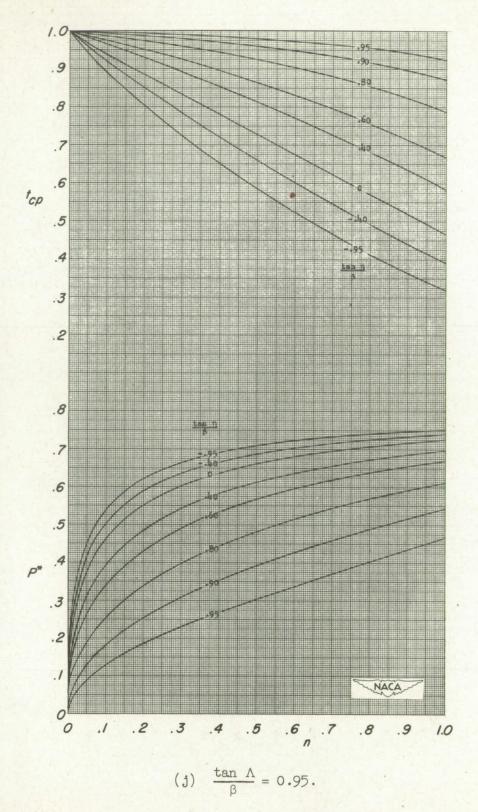


Figure 7.- Concluded.

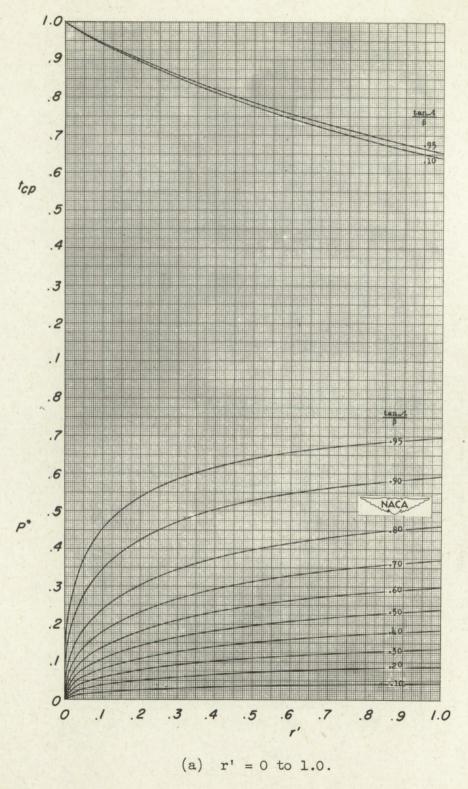
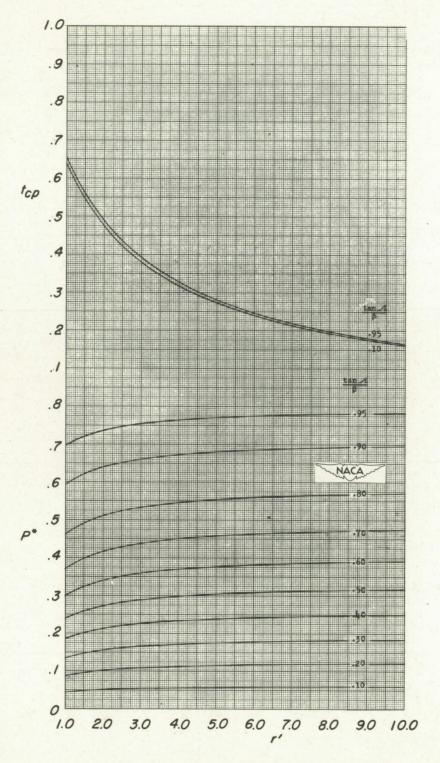


Figure 8.- Loading distribution along streamwise sections intersecting wing-root Mach cone.



(b) $r^{i} = 1.0$ to 10.0.

Figure 8.- Concluded.

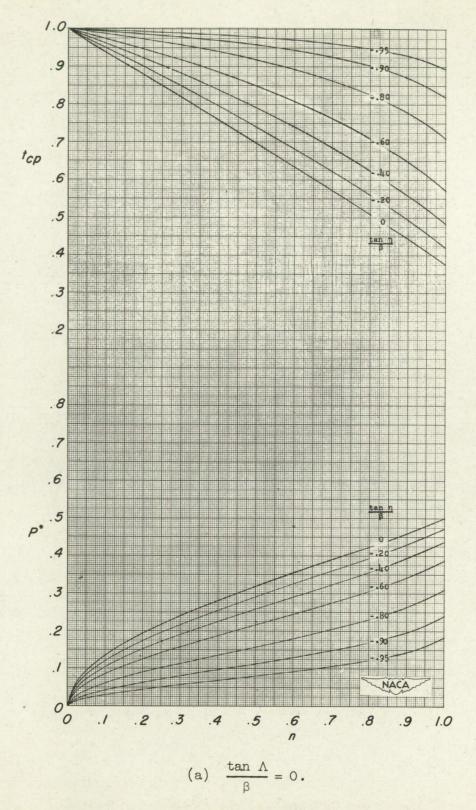


Figure 9.- Loading distribution along inclined sections intersecting wingtip Mach cone.

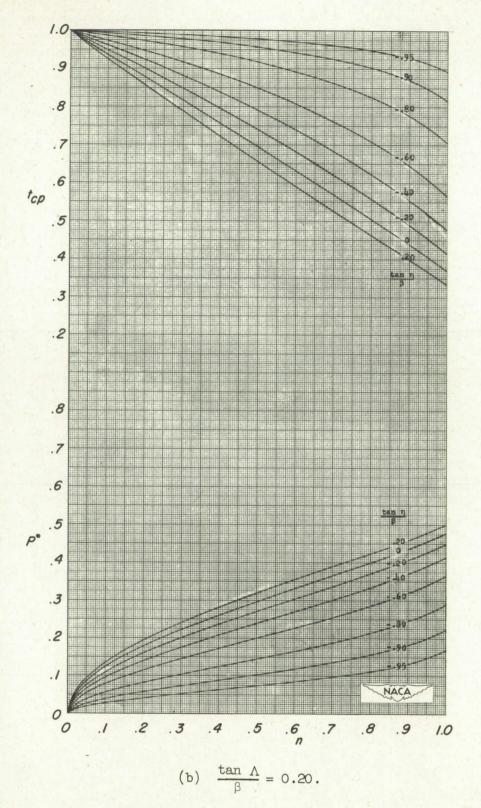


Figure 9.- Continued.

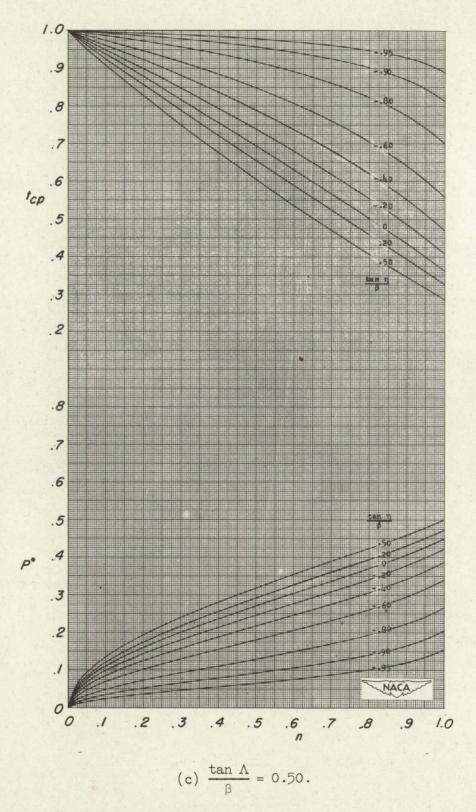


Figure 9.- Continued.

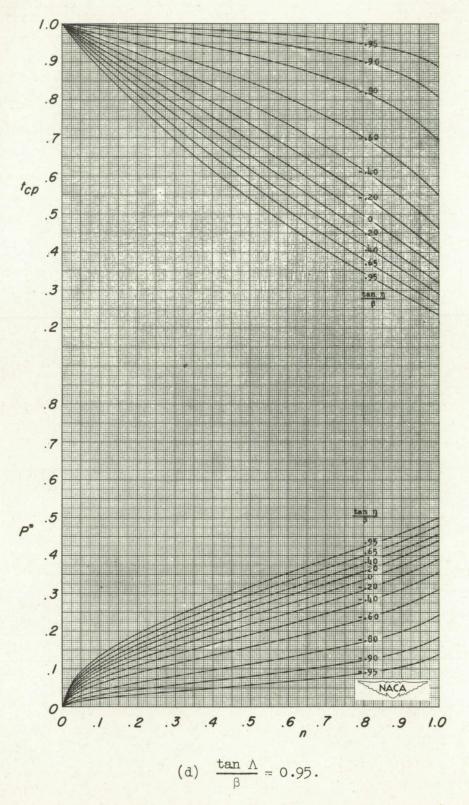


Figure 9.- Concluded.

NACA TN 2221

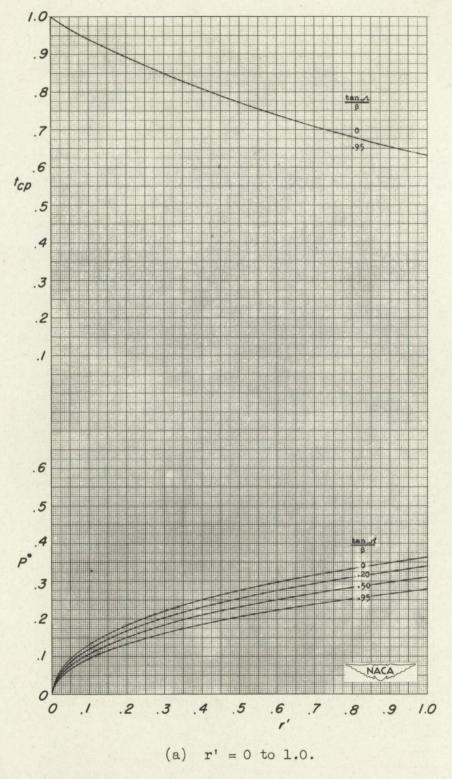
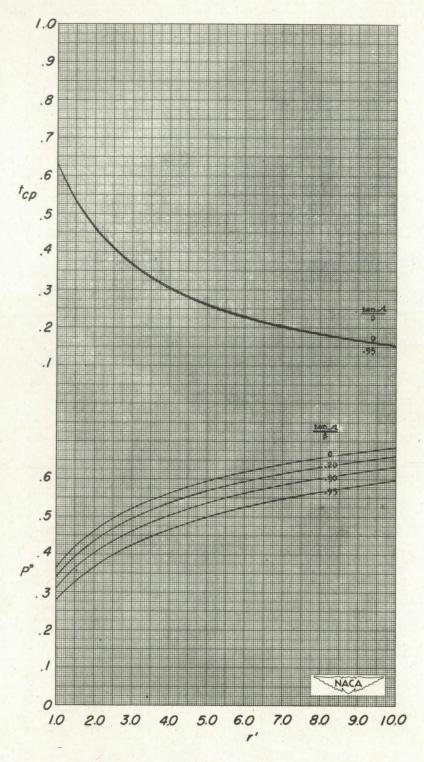


Figure 10.- Loading distribution along streamwise sections intersecting wing-tip Mach cone.



(b) r' = 1.0 to 10.0.

Figure 10.- Concluded.

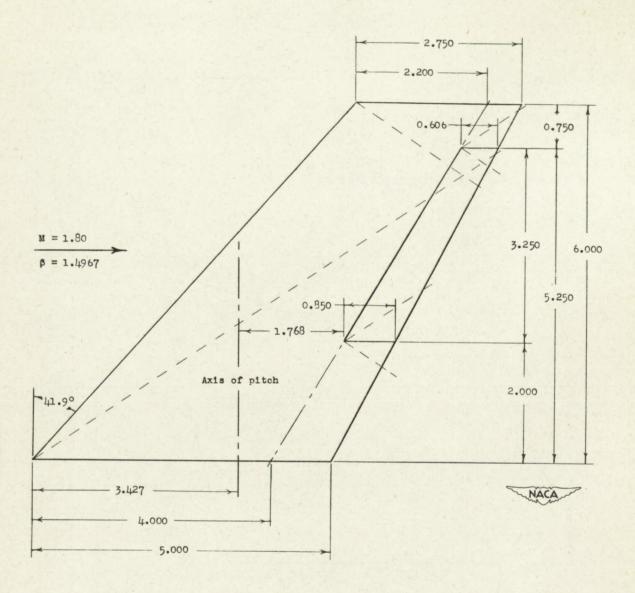


Figure 11.- Configuration used in sample calculation.
$$\left(\frac{\tan\Lambda}{\beta}=0.5995, \frac{\tan\Lambda_{HL}}{\beta}=0.3990, \frac{\tan\Lambda_{TE}}{\beta}=0.3489, S=23.250, \bar{c}=3.984, \lambda_{f}=0.713, S_{f}=2.366, 2M_{a}=1.490\right)$$

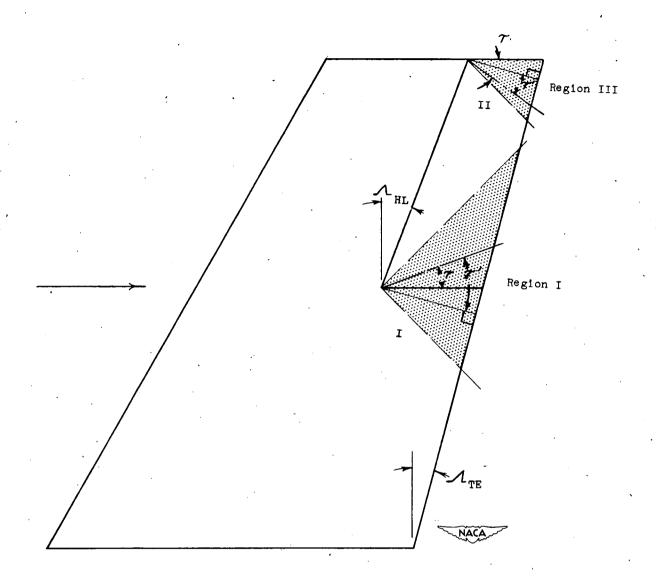
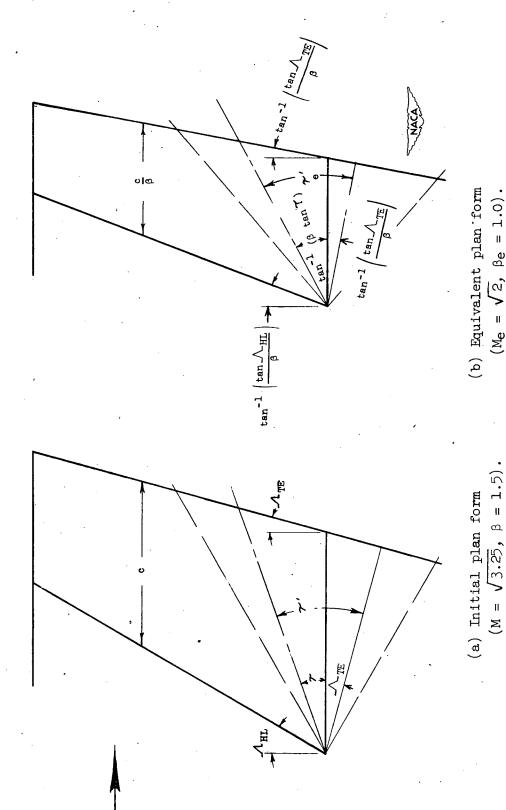
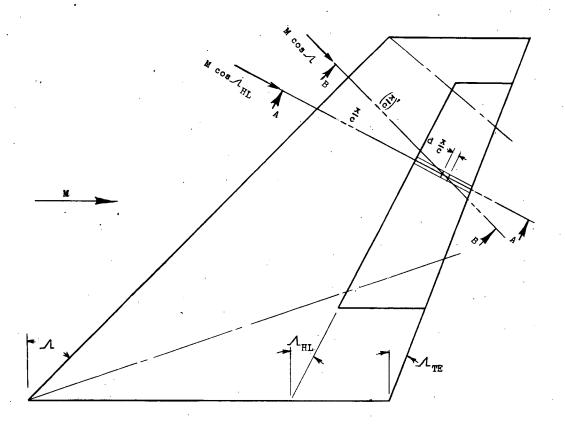


Figure 12.- Illustration of ordinates used in integrating pressures over conical regions of deflected controls.



 $(M_e = \sqrt{2}, \beta_e = 1.0)$.

Figure 13.- Example transformation from one plan-form Mach number configuration to an equivalent plan form at a Mach number of $\sqrt{2}$.



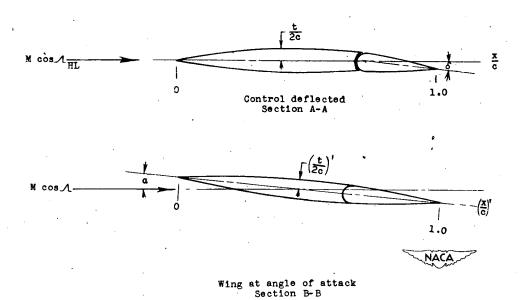


Figure 14.- Illustration of parameters used in determining the two-dimensional characteristics of trailing-edge controls having thickness.